Max-Planck-Institut für Mathematik
Bonn

The real Mordell-Weil group of rational elliptic surfaces and real lines on del Pezzo surfaces of degree $K^2 = 1$

by

Sergey Finashin
Viatcheslav Kharlamov

Max-Planck-Institut für Mathematik
Preprint Series 2024 (16)

Date of submission: July 24, 2024

The real Mordell-Weil group of rational elliptic surfaces and real lines on del Pezzo surfaces of degree $K^2 = 1$

by

Sergey Finashin
Viatcheslav Kharlamov

Max-Planck-Institut für Mathematik
Vivatsgasse 7
53111 Bonn
Germany

Middle East Technical University
Department of Mathematics
Ankara 06531
Turkey

Université de Strasbourg
et IRMA (CNRS)
7 rue René-Descartes
67084 Strasbourg Cedex
France

MPIM 24-16

THE REAL MORDELL-WEIL GROUP OF RATIONAL ELLIPTIC SURFACES AND REAL LINES ON DEL PEZZO SURFACES OF DEGREE $K^2 = 1$

S. FINASHIN, V. KHARLAMOV

ABSTRACT. We undertake a study of topological properties of the real Mordell-Weil group $\mathrm{MW}_{\mathbb{R}}$ of real rational elliptic surfaces X which we accompany by a related study of real lines on X and on the "subordinate" del Pezzo surfaces Y of degree 1. We give an explicit description of isotopy types of real lines on $Y_{\mathbb{R}}$ and an explicit presentation of $\mathrm{MW}_{\mathbb{R}}$ in the mapping class group $\mathrm{Mod}(X_{\mathbb{R}})$. Combining these results we establish an explicit formula for the action of $\mathrm{MW}_{\mathbb{R}}$ in $H_1(X_{\mathbb{R}})$.

> The most fascinating thing about algebra and geometry is the way they struggle to help each other to emerge from the chaos of non–being, from those dark depths of subconscious where all roots of intellectual creativity reside.
>
> Y. Iv. Manin "Von Zahlen und Figuren"

1. Introduction

1.1. **Prologue.** Our initial motivation came from a search how the wall-crossing invariant count of real rational curves on real del Pezzo surfaces introduced in [FK-3] can be extended to other real rational surfaces. This brought us to investigate one of the first cases, the case of lines on a real rational elliptic surface, and to study directly related questions arising in this setting: (1) how the real lines are arranged on real rational elliptic surfaces and on *subordinate* real del Pezzo surfaces of degree 1, that is on the surfaces obtained by contracting a line on the elliptic surface; (2) how the real Mordell-Weil group acts on the real lines and what is its presentation in the mapping class group of the real locus of the surface.

To respond to the first question, we introduce the division of real lines in 5 types, enumerate the lines of each type for every real deformation class of del Pezzo surfaces (of degree 1) and describe their position on the real locus of the surface up to isotopy. It is combining these results with a study of a topological analog of the real Mordell-Weil group that we respond to the second question.

1.2. **On del Pezzo side.** A standard model for a real del Pezzo surface Y of degree 1 is given by a double covering of a real quadratic cone Q branched along a transversal intersection C of Q with a real cubic surface. This reduces the study of real lines on Y to a study of the *positive tritangents*, that is the real hyperplane sections l of Q tritangent to C whose real part $l_{\mathbb{R}}$ is contained in the half $Q^+_{\mathbb{R}}$ of $Q_{\mathbb{R}} \smallsetminus C_{\mathbb{R}}$ which is the image of $Y_{\mathbb{R}}$.

2020 *Mathematics Subject Classification.* Primary: 14P25. Secondary: 14J27, 14J26.

The real deformation classes of sextics $C \subset Q$ that arise as branching loci for $Y \to Q$ are listed in Table 1 (see, for example, [DIK, Theorem A3.6.1]). There, the code $\langle|||\rangle$ refers to $C_{\mathbb{R}}$ having three "parallel" connected components *embracing the vertex* v of Q. The code $\langle p|q\rangle$, with $p \geqslant 0, q \geqslant 0$, means that $C_{\mathbb{R}}$ contains one component which embraces the vertex and $p+q$ components which bound disjoint discs and placed in $Q_{\mathbb{R}}$ so that: q of them bound disc components of $Q^+_{\mathbb{R}}$ and are called *negative ovals*; the other p bound disc components of the opposite half of $Q_{\mathbb{R}}$ and are called *positive ovals*. The components embracing the vertex are called *J-components*.

Our division of real lines on Y in 5 types is invariant under *Bertini involution* (that is the deck transformation of the covering $Y \to Q$) and can be translated into a division of positive tritangents to C in 5 types as follows. For a given tritangent, we let τ be the number of ovals with odd number of tangency points counted with multiplicities, and if $1 \leqslant \tau \leqslant 3$ assign to this tritangent type T_τ. If $\tau = 0$, we distinguish two types, T_0 and T_0^*. A tritangent of type T_0^* has two tangency points to the same oval separated by a tangency with the J-component as it is shown on Fig. 1, while other kind of tritangents with $\tau = 0$ belong to type T_0.

FIG. 1

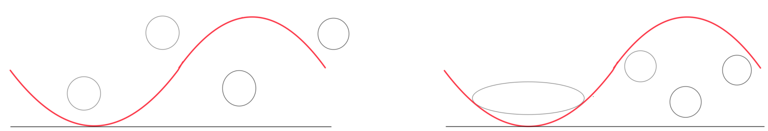

T_0 $\qquad\qquad$ T_0^*

The bottom segments depict the J-component. The curved lines represent a positive tritangent.

1.2.1. **Theorem.** *The number of positive tritangents of a given type depends on the topological type of $C_{\mathbb{R}} \subset Q_{\mathbb{R}}$, and the choice of a half $Q^+_{\mathbb{R}}$, as is indicated in Tab. 1.*

One of the main tools in the proof of this theorem is a certain *oval-bridge decomposition* (see Section 2.5) which allows to implement a lattice arithmetic approach for not only enumerating the tritangents but also to control their isotopy types. In what concerns the isotopy types, formulating the results requires a special encoding and therefore we refer the reader to Section 4 for precise statements.

TAB. 1. Number of positive tritangents of given types

$C_{\mathbb{R}}$	$\langle 4\|0\rangle$	$\langle 3\|0\rangle$	$\langle 2\|0\rangle$	$\langle 1\|0\rangle$	$\langle 0\|0\rangle$	$\langle 1\|1\rangle$	$\langle\|\|\|\rangle$	$\langle 0\|1\rangle$	$\langle 0\|2\rangle$	$\langle 0\|3\rangle$	$\langle 0\|4\rangle$
T_0	4	4	4	4	4	3	12	3	2	1	0
T_0^*	4	3	2	1	0	1	0	0	0	0	0
T_1	32	24	16	8	0	8	0	0	0	0	0
T_2	48	24	8	0	0	0	0	0	0	0	0
T_3	32	8	0	0	0	0	0	0	0	0	0

1.3. **On Mordell-Weil side.** The real Mordell-Weil group of a real elliptic surface has a simple lattice description. However, there is no "royal road" to extract from such a description a topological information on the action of the Mordell-Weil group on the real loci. In our study of rational elliptic surfaces, X, we overcome this difficulty by appealing systematically to subordinate del Pezzo surfaces, Y, for which we developed in the first part of the paper a good control on the real topology through the lattice arithmetic of $\Lambda_Y = \ker(1+\mathrm{conj}_*)\cap K_Y^\perp \subset H_2(Y)$ (see Tab. 2). The pullback map $H_2(Y)\to H_2(X)$ identifies Λ_Y with $\Lambda_X = \ker(1+\mathrm{conj}_*)\cap\langle K_X, L\rangle^\perp \subset H_2(X)$, and we use a shorten notation Λ for both of them, when it does not lead a confusion.

TAB. 2. Elliptic surface X and its subordinate del Pezzo surface Y

$C_{\mathbb{R}}$	$\langle 4\|0\rangle$	$\langle 3\|0\rangle$	$\langle 2\|0\rangle$	$\langle 1\|0\rangle$	$\langle 0\|0\rangle$	$\langle 1\|1\rangle$	$\langle\|\|\|\rangle$	$\langle 0\|q\rangle$, $q\leqslant 4$
$Y_{\mathbb{R}}$	$\mathbb{RP}^2\#4\mathbb{T}^2$	$\mathbb{RP}^2\#3\mathbb{T}^2$	$\mathbb{RP}^2\#2\mathbb{T}^2$	$\mathbb{RP}^2\#\mathbb{T}^2$	$\mathbb{RP}^2$	$\mathbb{RP}^2\#\mathbb{T}^2\amalg\mathbb{S}^2$	$\mathbb{RP}^2\amalg\mathbb{K}$	$\mathbb{RP}^2\amalg q\mathbb{S}^2$
$X_{\mathbb{R}}$	$\mathbb{K}\#4\mathbb{T}^2$	$\mathbb{K}\#3\mathbb{T}^2$	$\mathbb{K}\#2\mathbb{T}^2$	$\mathbb{K}\#\mathbb{T}^2$	$\mathbb{K}$	$\mathbb{K}\#\mathbb{T}^2\amalg\mathbb{S}^2$	$\mathbb{K}\amalg\mathbb{K}$	$\mathbb{K}\amalg q\mathbb{S}^2$
Λ	E_8	E_7	D_6	$D_4\oplus A_1$	$4A_1$	D_4	D_4	$(4-q)A_1$

In addition, we complete this approach by giving for all types of real rational elliptic surfaces an explicit presentation of the real Mordell-Weil group in the mapping class group of the real locus of the surface (see Sections 5.7 and 6.2).

In most of our results on elliptic surfaces $f: X\to\mathbb{P}^1$ we make the following assumption:

Assumption A. *X is a real non-singular relatively minimal rational elliptic surface that has only 1-nodal singular fibers and whose set of real lines is non-empty.*

As a first application of the above approach we observe the following infiniteness results for the integer homology classes realized in $H_1(X_{\mathbb{R}})$ by real lines and real vanishing cycles. In the below statement on real lines, we choose an orientation of $\mathbb{P}^1_{\mathbb{R}}$, orient the real lines $L_{\mathbb{R}}\subset X_{\mathbb{R}}$ so that the f-projection $L_{\mathbb{R}}\to\mathbb{P}^1_{\mathbb{R}}$ is orientation-preserving, and denote by $\mathcal{N}$ the number of classes $[L_{\mathbb{R}}]\in H_1(X_{\mathbb{R}})$ realized by real lines.

1.3.1. **Theorem.** *Under the assumption* **A***, the topology of $X_{\mathbb{R}}$ and the corresponding number $\mathcal{N}$ is as indicated in Tab. 3. In particular, the number of classes realized in $H_1(X_{\mathbb{R}})$ by real lines is infinite if and only if $X_{\mathbb{R}}$ contains a component $\mathbb{K}\#p\mathbb{T}^2$ with $p\geqslant 1$.*

TAB. 3. The number of homology classes realized by real lines

$X_{\mathbb{R}}$	$\mathbb{K}\#p\mathbb{T}^2, 0<p\leqslant 4$	$\mathbb{K}$	$\mathbb{K}\#\mathbb{T}^2\amalg\mathbb{S}^2$	$\mathbb{K}\amalg\mathbb{K}$	$\mathbb{K}\amalg q\mathbb{S}^2, 0<q<4$	$\mathbb{K}\amalg 4\mathbb{S}^2$
$\mathcal{N}$	∞	2	∞	4	2	1

1.3.2. **Theorem.** *If X satisfies assumption* **A** *and $X_{\mathbb{R}} = \mathbb{K}\#p\mathbb{T}^2\amalg q\mathbb{S}^2$ with $p\geqslant 1$, then $H_1(X_{\mathbb{R}})$ contains an infinite number of vanishing classes.*

For a better presentation of the results on topological properties of the action of the Mordell-Weil group, $\mathrm{MW}_{\mathbb{R}}(X)$, on the real locus $X_{\mathbb{R}}$ of a real elliptic surface X, we define a topological analog of $\mathrm{MW}_{\mathbb{R}}(X)$ as a subgroup $\mathrm{Mod}^s(X_{\mathbb{R}})$ of the mapping class group $\mathrm{Mod}(X_{\mathbb{R}})$ formed by isotopy classes of fiber-preserving diffeomorphisms

$X_{\mathbb{R}} \to X_{\mathbb{R}}$ acting by group-shifts in each non-singular real fiber. One of the objects of our study is the natural homomorphism $\Phi : \mathrm{MW}_{\mathbb{R}}(X) \to \mathrm{Mod}^s(X_{\mathbb{R}})$.

1.3.3. **Theorem.** *Under the assumption* **A**, *the homomorphism* $\Phi : \mathrm{MW}_{\mathbb{R}}(X) \to \mathrm{Mod}^s(X_{\mathbb{R}})$ *has image and kernel as is indicated in Tab. 4.*

TAB. 4. Image and kernel of $\Phi : \mathrm{MW}_{\mathbb{R}}(X) \to \mathrm{Mod}^s(X_{\mathbb{R}})$

$X_{\mathbb{R}}$	$\mathbb{K}\#4\mathbb{T}^2$	$\mathbb{K}\#3\mathbb{T}^2$	$\mathbb{K}\#2\mathbb{T}^2$	$\mathbb{K}\#\mathbb{T}^2$	$\mathbb{K}$	$\mathbb{K}\#\mathbb{T}^2\amalg\mathbb{S}^2$	$\mathbb{K}\amalg\mathbb{K}$	$\mathbb{K}\amalg q\mathbb{S}^2$
$\mathrm{MW}_{\mathbb{R}} = \Lambda$	E_8	E_7	D_6	$D_4 \oplus A_1$	$4A_1$	D_4	D_4	$(4-q)A_1$
$\mathrm{Mod}^s(X_{\mathbb{R}})$	$\mathbb{Z}^8 \oplus \mathbb{Z}/2$	$\mathbb{Z}^6 \oplus \mathbb{Z}/2$	$\mathbb{Z}^4 \oplus \mathbb{Z}/2$	$\mathbb{Z}^2 \oplus \mathbb{Z}/2$	$\mathbb{Z}/2$	$\mathbb{Z}^2 \oplus \mathbb{Z}/2$	$\mathbb{Z}/2 \oplus \mathbb{Z}/2$	$\mathbb{Z}/2$
$\mathrm{Im}(\Phi)$	$\mathbb{Z}^8$	$\mathbb{Z}^6 \oplus \mathbb{Z}/2$	$\mathbb{Z}^4 \oplus \mathbb{Z}/2$	$\mathbb{Z}^2 \oplus \mathbb{Z}/2$	$\mathbb{Z}/2$	$\mathbb{Z} \oplus \mathbb{Z}/2$	$\mathbb{Z}/2 \oplus \mathbb{Z}/2$	$\begin{cases} \mathbb{Z}/2, q<4 \\ 0, \quad q=4 \end{cases}$
$\mathrm{Ker}(\Phi)$	0	$\mathbb{Z}$	$\mathbb{Z}^2$	$\mathbb{Z}^3$	$\mathbb{Z}^4$	$\mathbb{Z}^3$	$\mathbb{Z}^4$	$\mathbb{Z}^{4-q}$

For an explicit presentation of the subgroup $\mathrm{Mod}^s(X_{\mathbb{R}}) \subset \mathrm{Mod}(X_{\mathbb{R}})$ and that of $\Phi(\mathrm{MW}_{\mathbb{R}}(X))$, we address the reader to Sections 5.7 and 6.2.

According to Theorem 1.3.3, for all types of $X_{\mathbb{R}}$ except $\mathbb{K}\#4\mathbb{T}^2$, $\mathbb{K}\#\mathbb{T}^2\amalg\mathbb{S}^2$, and $\mathbb{K}\amalg 4\mathbb{S}^2$, all isotopy classes of smooth sections of $f_{\mathbb{R}} : X_{\mathbb{R}} \to \mathbb{P}^1_{\mathbb{R}}$ are realized by real lines $L_{\mathbb{R}} \subset X_{\mathbb{R}}$. If $X_{\mathbb{R}} = \mathbb{K}\amalg 4\mathbb{S}^2$ then only one isotopy classes of sections is realized by real lines. An explicit $\mathbb{Z}/2$-valued obstruction for the case $\mathbb{K}\#4\mathbb{T}^2$, and an explicit $\mathbb{Z}$-valued obstruction for the case $\mathbb{K}\#\mathbb{T}^2\amalg\mathbb{S}^2$, are given in Theorems 7.3.2 and 7.3.3, respectively.

Under the assumptions of Theorem 1.3.2, we fix a direct sum decomposition of $H_1(X_{\mathbb{R}}) = H_1(\mathbb{K}\#p\mathbb{T}^2)$ determined by fixing a real line $L_{\mathbb{R}} \subset X_{\mathbb{R}}$ and a non-singular connected real fiber $F_{\mathbb{R}} \subset X_{\mathbb{R}}$. In addition to the classes $[F_{\mathbb{R}}]$ (of order 2) and $[L_{\mathbb{R}}]$, the group $H_1(X_{\mathbb{R}})$ contains the classes of positive ovals o_i, $i = 1, \dots, p$ (as we identify $C_{\mathbb{R}}$ in $Q_{\mathbb{R}}$ with its lifting in $X_{\mathbb{R}}$). Furthemore, for each oval o_i we pick a real non-singular elliptic fiber intersecting it. Such a fiber has 2 connected components among which we denote by a_i the one intersecting $L_{\mathbb{R}}$ and by b_i the other one (see details in Sec. 8.1 including the orientation conventions for the classes involved). The classes $[F_{\mathbb{R}}], b_1, o_1, \dots, b_p, o_p, [L_{\mathbb{R}}]$ form a basis giving a direct sum

FIG. 2

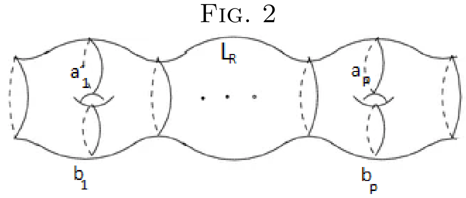

decomposition

$$H_1(X_{\mathbb{R}}) = \mathbb{Z}/2 \oplus \Big[\bigoplus_{i=1}^{p} (\mathbb{Z} \oplus \mathbb{Z}) \Big] \oplus \mathbb{Z}. \tag{1.3.1}$$

With respect to this basis, the class of any real line has a unique coordinate expression of the form $[L_{\mathbb{R}}]+\kappa[F_{\mathbb{R}}]+\sum_{i=1}^{p}(m_i b_i+\varkappa_i o_i)$ with $\kappa \in \mathbb{Z}/2,\ m_i \in \mathbb{Z},\ \varkappa_i \in \{0,1\}$.

1.3.4. **Theorem.** *Let X satisfy the assumption* $\mathbf{A}$, $X_{\mathbb{R}} = \mathbb{K}\#p\mathbb{T}^2 \amalg q\mathbb{S}^2$ *and* $g \in \mathrm{MW}_{\mathbb{R}}$ *send a real line L to a real line L'. Then the action of g in $H_1(X_{\mathbb{R}})$ is described by the following matrix with respect to the basis* $[F_{\mathbb{R}}], b_1, o_1, \dots, b_p, o_p, [L_{\mathbb{R}}]$:

$[1]$	$[\varkappa_1]$	$[m_1]$	$\dots$	$[\varkappa_p]$	$[m_p]$	κ
0	$(-1)^{\varkappa_1}$	$-2m_1$	$\dots$	0	0	m_1
0	0	$(-1)^{\varkappa_1}$	$\dots$	0	0	$\varkappa_1$
$\dots$	$\dots$	$\dots$	$\dots$	$\dots$	$\dots$	$\dots$
0	0	0	$\dots$	$(-1)^{\varkappa_p}$	$-2m_p$	m_p
0	0	0	$\dots$	0	$(-1)^{\varkappa_p}$	$\varkappa_p$
0	0	0	$\dots$	0	0	1

Here, $\kappa \in \mathbb{Z}/2,\ m_i \in \mathbb{Z},\ \varkappa_i \in \{0,1\}$ *are the coefficients in the decomposition*

$$[L'_{\mathbb{R}}] - [L_{\mathbb{R}}] = \kappa[F_{\mathbb{R}}] + \sum_{i=1}^{p} m_i b_i + \sum_{i=1}^{p} \varkappa_i o_i \in H_1(X_{\mathbb{R}}).$$

1.3.5. **Theorem.** *Under the assumptions of Theorem 1.3.4, consider a pair of real lines $L', L'' \subset X$ with coordinate expressions*

$$\begin{aligned} [L'_{\mathbb{R}}] - [L_{\mathbb{R}}] &= \kappa_1[F_{\mathbb{R}}] + \sum_{j=1}^{p}(m_{1j}b_j + \varkappa_{1j}o_j) \\ [L''_{\mathbb{R}}] - [L_{\mathbb{R}}] &= \kappa_2[F_{\mathbb{R}}] + \sum_{j=1}^{p}(m_{2j}b_j + \varkappa_{2j}o_j) \end{aligned} \qquad \kappa_{ij} \in \mathbb{Z}/2,\ m_{ij} \in \mathbb{Z},\ \varkappa_{ij} \in \{0,1\},$$

and the element $g \in \mathrm{MW}_{\mathbb{R}}$ sending L to L'. Then the class $[g(L'')_{\mathbb{R}}] \in H_1(X_{\mathbb{R}})$ of the line $g(L'')$ has a coordinate expression

$$[g(L'')_{\mathbb{R}}] - [L_{\mathbb{R}}] = \kappa[F_{\mathbb{R}}] + \sum_{j=1}^{p}(m_j b_j + \varkappa_j o_i)$$

where $\kappa = \kappa_1 + \kappa_2 + \sum_{j=1}^{p}(\varkappa_{1j}m_{2j} + \varkappa_{2j}m_{1j}) \bmod 2$ *and*

$$\begin{bmatrix} (-1)^{\varkappa_{1j}} & m_{1j} \\ 0 & (-1)^{\varkappa_{1j}} \end{bmatrix} \begin{bmatrix} (-1)^{\varkappa_{2j}} & m_{2j} \\ 0 & (-1)^{\varkappa_{2j}} \end{bmatrix} = \begin{bmatrix} (-1)^{\varkappa_j} & m_j \\ 0 & (-1)^{\varkappa_j} \end{bmatrix}.$$

1.4. **Plan of the paper.** We start Section 2 by recalling the deformation classification of the sextic curves on a quadric cone, the del Pezzo surfaces of degree 1 and the real rational elliptic surfaces. We remind also a lattice arithmetic description of lines, and apply it to introduce the notion of oval- and bridge-classes and determine their mutual intersections. In Section 3 we develop a certain mod 2 arithmetic of roots, and based on it introduce our principal tool for enumerating the positive tritangents, an *oval-bridge decomposition*. By a systematic use of this tool we not only prove Theorem 1.2.1 but moreover supply the enumeration of positive tritangents with an information on their position with respect to the ovals. It is this information that we use in Section 4 for giving an explicite description of isotopy types of positive tritangents and that of isotopy types of real lines on real rational elliptic surfaces, see Theorem 4.7.1 and Tab. 8. In Section 5 we introduce and evaluate the groups $\mathrm{Mod}^s(X_{\mathbb{R}})$ and $\mathrm{MW}_{\mathbb{R}}(X)$. Section 6 is devoted to the proof of Theorem 1.3.3 and a lattice description of $\operatorname{Ker}\Phi$, see Theorem 6.3.1. Section 7 is devoted to proving Theorems 1.3.1, 1.3.2, 7.3.2, and 7.3.3. In Section 8 we perform a matrix description of the action of $\mathrm{Mod}^s(X_{\mathbb{R}})$ in $H_1(X_{\mathbb{R}})$ and apply it to proving Theorems 1.3.4 and 1.3.5.

In the concluding remarks we discuss a few related topics. We start with Proposition 9.1.1, which describes the MW-action in $H_2(X)$ in the complex setting. Being an analogue of our Theorem 1.3.4, it demonstrates however, a significant difference. Namely, the MW-action on $H_2(X)$ restricts to identity on $K^{\perp}/K$, while the action of $\mathrm{MW}_{\mathbb{R}}$ is not identical on $K_{\mathbb{R}}^{\perp}/K_{\mathbb{R}}$ (although is identity modulo 2). In Section 9.2 we give a coordinate expression for a $\mathbb{Z}/2$-obstruction for realizability of classes in $H_1(X_{\mathbb{R}})$ by real lines. In Section 9.3 we give an application of our count of tritangents to a count of real conics tangent to a pair of real lines and a real cubic. In Section 9.4 we discuss a relation between 5 types of tritangents and θ-characteristics. In Section 9.5 we address a question on non-rational real elliptic surfaces. Finally, in Section 9.6 we indicate a puzzling persistence phenomenon in counting real vanishing cycles on del Pezzo surfaces.

1.5. **Notation and conventions.** For complex algebraic varieties we denote by the same letter the variety itself and its complex point set. If a complex variety Z is defined over $\mathbb{R}$, then $\mathrm{conj} : Z \to Z$ denotes the complex conjugation and $Z_{\mathbb{R}}$ its *real locus*. The same convention is applied to conj-invariant subsets $V \subset Z$ (complex algebraic cycles, etc.).

By a *line on an algebraic surface* Z we mean a rational non-singular curve $L \subset Z$ with $L^2 = -1$. Recall that lines on relatively minimal rational elliptic surfaces are just its sections.

Given a nonsingular relatively minimal rational elliptic surface $f_X : X \to \mathbb{P}^1$ with a fixed section $L \subset X$, the blow down of L gives rise to a nonsingular del Pezzo surface Y of degree 1 which we call the *subordinate* del Pezzo surface. Conversely the blow up of the fixed point of $|-K_Y|$ provides a relatively minimal rational elliptic surface. This establishes a canonical correspondence between pairs (X, L) and del Pezzo surfaces Y as above. Under this correspondence the linear system $|-K_X|$ and the map $f_X : X \to \mathbb{P}^1$ turn into, respectively, a proper transform of the linear system $|-K_Y|$ and a proper transform of the map $f_Y : Y \dashrightarrow \mathbb{P}^1$.

The anti-bicanonical linear system gives rise to a standard model of Y as a double covering $\pi : Y \to Q$ of a quadratic cone $Q \subset \mathbb{P}^3$ branched at the vertex $v \in Q$ and along a transversal intersection C of Q with a cubic surface. This establishes a canonical correspondence between surfaces Y and pairs (Q, C). Under this correspondence the linear system $|-K_Y|$ and the map $f_Y : Y \dashrightarrow \mathbb{P}^1$ turn into, respectively, a pull-back of the system of generators of Q and a pull-back of the projection map $f_Q : Q \dashrightarrow \mathbb{P}^1$ from v. The deck transformation of the covering $\pi : Y \to Q$ is called *Bertini involution* and denoted by β.

For a compact (oriented) surface S, we denote by $\mathrm{Mod}(S)$ the mapping class group of orientation-preserving diffeomorphisms of S fixing the boundary ∂S pointwise.

1.6. **Acknowledgements.** An essential part of this work was accomplished during our Research in Residence visits at the Centre International de Rencontres Mathématiques in Luminy in 2022-2023. It took its final shape during our stay at the Max-Planck Institute for Mathematics in Bonn in summer 2024. We thank the both institutions for hospitality and excellent working conditions.

2. Preliminaries

2.1. **Swept cone $Q_{\mathbb{R}}$.** On figures, we think of the quadratic cone $Q_{\mathbb{R}} \subset \mathbb{P}^3_{\mathbb{R}}$ as a vertically directed cylinder in an affine chart $\mathbb{R}^3 \subset \mathbb{P}^3_{\mathbb{R}}$ (placing the vertex v of Q at infinity), pick a real generator $\mathcal{F}^\infty \subset Q$, and then sweep $Q_{\mathbb{R}} \smallsetminus \mathcal{F}^\infty_{\mathbb{R}}$ on a real plane $\mathbb{R}^2$. In particular, this allows us to make "flat" sketches of the sextic $C_{\mathbb{R}} \subset Q_{\mathbb{R}}$ (*cf.* Fig. 1). We assume that this development of $Q_{\mathbb{R}}$ is agreed with the projection map $f_Q : Q \dashrightarrow \mathbb{P}^1$ in such a way that the map f_Q reads in coordinates as $(x, y) \mapsto x$. We suppose also that $\mathcal{F}^\infty$ does not intersect the ovals, so that they can be numerated consecutively $o_1, \dots, o_r$ along the positive direction of axis x.

2.2. **Real loci of C, Y and X.** To fix a correspondence between real sextics C on a real quadratic cone Q with a fixed orientation of real generators, real del Pezzo surfaces $\pi : Y \to Q$ of degree 1, and real elliptic surfaces $f_X : X \to \mathbb{P}^1$ with a fixed real line, we use the following convention.

A real non-singular relatively minimal rational elliptic surface X equipped with a marked real line is identified with a real del Pezzo surface Y blown up at the fixed point of the anti-canonical pencil $-K_Y$. Next, like in Introduction, we assume that the real structure $\mathrm{conj}_Y : Y \to Y$ covers the standard complex conjugation involution $\mathrm{conj}_Q : Q \to Q$ and $\pi(Y_{\mathbb{R}}) = Q^+_{\mathbb{R}}$. Accordingly, we equip the line-generators of $Q_{\mathbb{R}}$ with an orientation that is coherent with passing at the vertex v from $Q^+_{\mathbb{R}}$ to $Q^-_{\mathbb{R}} = Q_{\mathbb{R}} \smallsetminus Q^+_{\mathbb{R}}$. In the opposite direction, a real sextic C and an orientation of the line-generators of $Q_{\mathbb{R}}$ determine uniquely the half $Q^+_{\mathbb{R}}$ of $Q_{\mathbb{R}}$.

The deformation classifications stated below are well known (see [DIK][Theorem A3.6.1, Theorem 17.3] for the first two; the third one is a straightforward consequence of the second).

2.2.1. **Theorem.** *There exist 11 deformation classes of non-singular real sextics $C \subset Q \smallsetminus \{v\}$ on a real quadratic cone Q with a fixed orientation of the line-generators. Each of the deformation classes is determined by the isotopy class of the embedding $C_{\mathbb{R}} \subset Q_{\mathbb{R}} \smallsetminus \{v\}$. These isotopy classes have the following codes:*

$$\boxed{\langle p \,|\, 0\rangle,\ 0 \leqslant p \leqslant 4 \quad \bullet \quad \langle 1 \,|\, 1\rangle \quad \bullet \quad \langle \,|\,|\,|\, \rangle \quad \bullet \quad \langle 0 \,|\, q\rangle,\ 1 \leqslant q \leqslant 4} \qquad \square$$

2.2.2. **Theorem.** *There exist 11 deformation classes of real del Pezzo surfaces Y of degree 1. These classes are distinguished by the topological types of $Y_{\mathbb{R}}$, which are as indicated in the second row of Tab. 2.* $\square$

2.2.3. **Corollary.** *There exist 11 deformation classes of real rational elliptic surfaces X satisfying the assumption A. Each of the deformation classes is determined by the topological type of $X_{\mathbb{R}}$. These topological types are listed in the third row of Tab. 2.* $\square$

2.3. **Lines and positive tritangents via roots of E_8.** As is known, the orthogonal complement of K_Y in $H_2(Y)$ is $K_Y^\perp = E_8$. Let us underline as well that the adjunction formula implies $L \cdot K_Y = -1$ for any line $L \subset Y$. The following is also well known (see [FK-1, Theorem 2.1.1] and references therein).

2.3.1. **Proposition.** *Assume that Y is a real del Pezzo surface of degree 1 with the canonical divisor class K_Y. Then:*

1. *Every homology class $h \in H_2(Y)$ with $h^2 = -1$, $h \cdot K_Y = -1$ is realized by a line $L \subset Y$. This establishes a one-to-one correspondence between the set of lines in Y and the set $\{h \in H_2(Y) \,|\, h^2 = h \cdot K_Y = -1\}$.*

(2) *For every root $e \in E_8$ there exists a unique line L_e that realizes the homology class $-K_Y - e$. This establishes a one-to-one correspondence between the set of lines in Y and the set of roots in E_8.*
(3) *If Y is real, then a line L_e is real if and only if $e \in \Lambda = K_Y^\perp \cap \ker(1+\mathrm{conj}_*)$.* □

Since the Bertini involution acts on $K_Y^\perp \subset H_2(Y)$ as multiplication by (-1), we have also an analogous correspondence for positive tritangents.

2.3.2. **Proposition.** *For each root $e \in E_8$, the Bertini involution interchanges the lines*

$$L_e = -K_Y - e, \quad L_{-e} = -K_Y + e,$$

while the projection $\pi : Y \to Q$ maps them to a tritangent. When Y and $L_{\pm e}$ are real, $\pi(L_{\pm e})$ is a positive tritangent. Conversely, each tritangent (resp. positive tritangent) is covered by a pair of lines (resp. real lines), which are permuted by the Bertini involution. This gives a one-to-one correspondence between the set of pairs of opposite roots $\{\pm e\} \subset E_8$ (resp., the set of pairs of opposite roots $\{\pm e\} \subset \Lambda$) and the set of tritangents (resp., the set of positive tritangents). □

Note that each real tritangent ℓ of $C \subset Q$, like any real hyperplane section of Q not passing through the vertex $v \in Q$, divides $Q_\mathbb{R}$ into 2 half-cones. The half-cone which contains the germ of $Q^+_\mathbb{R}$ at $v \in Q$ will be denoted by $\hat{\ell}$.

2.4. **Positivity of intersection for totally real conj-anti-invariant 2-cycles.** By an *anti-invariant 2-cycle* in a nonsingular complex surface Y with a real structure $\mathrm{conj} : Y \to Y$ we mean an embedded orientable smooth 2-submanifold $Z \subset Y$ such that $Z = \mathrm{conj}\, Z$ and $\mathrm{conj}\,|_Z$ is orientation-reversing. We say that Z is *totally real*, if the tangent space T_pZ is not complex (equivalently, if $T_pY = T_pZ + JT_pZ$ where J stands for the multiplication by $\sqrt{-1}$) for each $p \in Z$.

If Z is a totally real anti-invariant 2-cycle Z and $p \in Z_\mathbb{R}$, then there exists a real basis $v, w \in T_pY_\mathbb{R}$ such that v and $J\,w$ is a basis of T_pZ. Moreover, such vectors v and w are unique up to rescaling. The local orientation of $Y_\mathbb{R}$ at p given by $v \wedge w$ and the local orientation of Z given by $v \wedge J\,w$ are said to be *coherent*.

2.4.1. **Proposition.** *Assume that $p \in Y_\mathbb{R}$ is a point of transversal intersection of totally real anti-invariant 2-cycles Z_1 and Z_2. Choose some local orientation of $Y_\mathbb{R}$ at $p \in Y_\mathbb{R}$ and coherent with it local orientations of Z_1 and Z_2. Assume that there exists a smooth real algebraic curve $C \subset Y$ intersecting Z_1 along a smooth* conj*-invariant arc containing p and intersecting Z_2 along a smooth* conj*-anti-invariant arc passing through p. Then the local intersection index of these cycles, $\mathrm{ind}_p(Z_1, Z_2)$, is equal to 1.*

Proof. Let v_1, w_1 be a pair of vectors providing coherent orientations, $v_1 \wedge w_1$ of $T_pY_\mathbb{R}$ and $v_1 \wedge Jw_1$ of T_pZ_1. For a similar pair v_2, w_2 for Z_2, transversality of Z_2 with Z_1 implies $v_2 = w_1 + \lambda v_1$, $\lambda \in \mathbb{R}$. From the conditions imposed on C we have $Jv_1 \in T_pZ_2$, which together with coherence of the orientations implies $w_2 = -v_1$. Now, the result follows from $v_1 \wedge Jw_1 \wedge (w_1 + \lambda v_1) \wedge J(-v_1) = v_1 \wedge Jv_1 \wedge w_1 \wedge Jw_1$. □

2.5. **Oval and bridge classes.** Let $C_0 \subset Q$ be a 6-nodal sextic which splits into 3 real hyperplane sections. Select once and for all the 5 perturbations constructed as is shown on Figure 3. This yields non-singular real sextics, $C_\varepsilon \subset Q$, of types $\langle p \,|\, 0 \rangle$, $1 \leqslant p \leqslant 4$ and $\langle 1 \,|\, 1 \rangle$, which we call *smart*.

Fig. 3. Construction of smart sextics

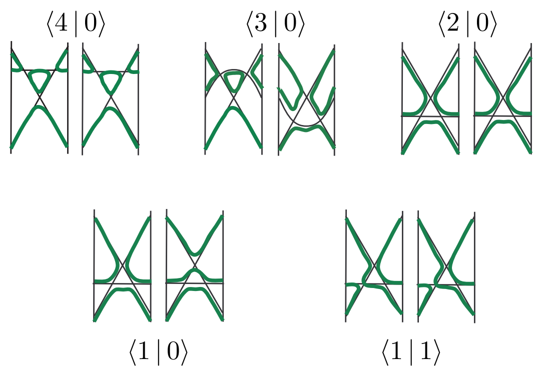

The cone $Q_{\mathbb{R}}$ is depicted as a pair of bands with the left-to-left and right-to-right identification of sides in each pair.

By passing to the double covering we get a small real perturbation $Y_\varepsilon \to Q$ of a 6-nodal surface Y_0. Each of the 6 nodes in the case of types $\langle p\,|\,0\rangle$, $p = 4, 3, 2$, and 5 nodes in the cases $\langle 1\,|\,0\rangle$ and $\langle 1\,|\,1\rangle$ (see Fig. 3), provides a conj-anti-invariant totally real vanishing cycle $B \subset Y_\varepsilon$ (well-defined up to isotopy preserving conj-anti-invariance and total reality) called a *bridge-cycle*. Its class in $\Lambda \subset H_2(X)$ is denoted also by B and called a *bridge-class*.

On the other hand, each of the p positive ovals of C_ε bounds a disc $D \subset Q^-_{\mathbb{R}}$, whose pull-back to Y_ε is a 2-sphere which represents a totally real conj-anti-invariant cycle called an *oval-cycle* and denoted by O. It realizes a class in $\Lambda \subset H_2(Y_\varepsilon)$ (also denoted by O) called an *oval-class*.

Note that the real loci, $B_{\mathbb{R}}$ and $O_{\mathbb{R}}$, represent in $H_1(Y_{\varepsilon\mathbb{R}}; \mathbb{Z}/2)$ the image of the bridge-class B and the oval-class O under the Viro homomorphism (see [FK-1, Section 2.2])

$$\Upsilon : H_2^-(Y_\varepsilon) \to H_1(Y_{\varepsilon\mathbb{R}}; \mathbb{Z}/2), \quad H_2^-(Y_\varepsilon) = \ker(1 + \mathrm{conj}_*) \subset H_2(Y_\varepsilon).$$

By construction, each bridge-class is incident to two connected components of $C_{\varepsilon\mathbb{R}}$, which may coincide. When the positive ovals of C_ε are numerated consecutively, the oval-class corresponding to the i-th oval is denoted by O_i, a bridge-class incident to the J-component and O_i is denoted by B_i, and a bridge-class incident to O_i and O_j, $j = i + 1$, by B_{ij}.

Fig. 4 shows the incidence relations between the bridge- and oval-classes. In the rightmost column the oval-classes $O_i \in \Lambda$ are depicted as circles and bridge-classes as line segments which either join two ovals, or join an oval with a J-component of $C_{\mathbb{R}}$ and depicted as pendant line segments attached to ovals.

In the middle column we present the graphs, where both oval- and bridge-cycles are taken as vertices, while edges show the incidences between ovals and bridges. More precisely, we indicate only a part of edges, to obtain Coxeter's graph of the corresponding lattice Λ. In the last three rows representing $\Lambda = D_6$, D_4, and $D_4 + A_1$, there are several pending bridges incident to O_i and we use beyond B_i also notation B'_i, B''_i (without a particular rule, just to distinguish).

2.6. **Orientation of oval- and bridge-cycles.** There exists a natural way to orient oval- and bridge-cycles. It is determined after fixing a real generator $\mathcal{F}^\infty \subset Q$

FIG. 4. Oval- and bridge-classes in the root-graph of Λ

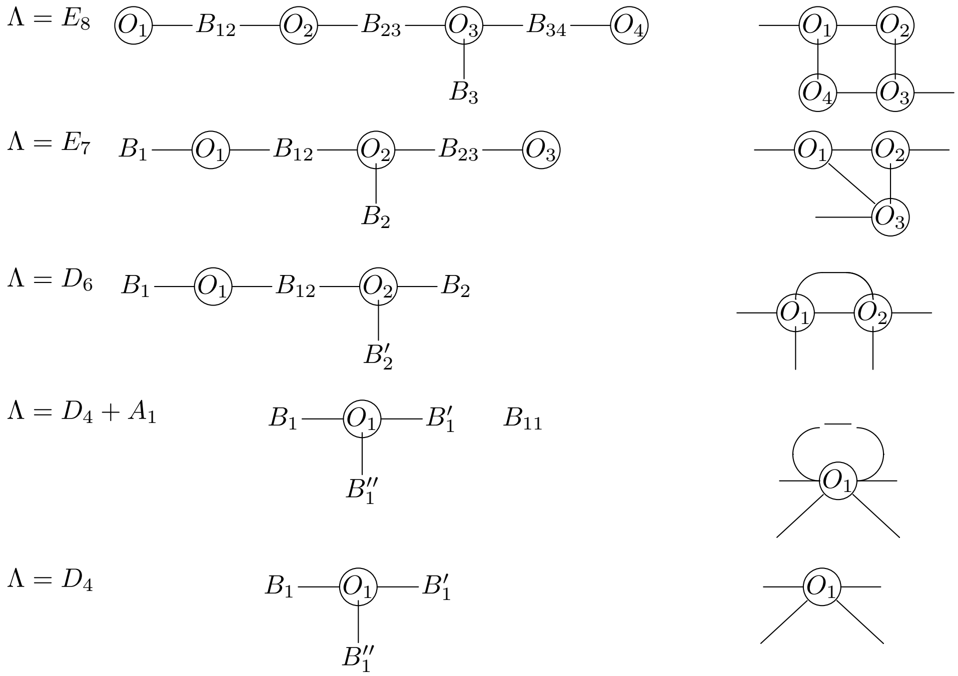

as in Section 2.1 (so that it does not intersect the ovals) and an orientation of the real part $Y^0_{\mathbb{R}}$ of $Y^0 = \pi^{-1}(Q \smallsetminus \mathcal{F}^\infty)$. The orientation of the oval- and bridge-cycles contained in Y^0 are chosen coherently with the orientation of $Y^0_{\mathbb{R}}$ in the sense of Section 2.4.

2.6.1. **Proposition.** *With the orientations of oval- and bridge-cycles specified above, their intersection index is* $+1$ *if they represent adjacent vertices in graphs of Fig. 4 and* 0 *otherwise.*

Proof. This positivity property is a direct consequence of Proposition 2.4.1 when the bridge-cycle does not intersect $\pi^{-1}(\mathcal{F}^\infty_{\mathbb{R}})$.

The only case to consider in addition is when $C_{\mathbb{R}}$ is of type $\langle 1 \,|\, 0\rangle$, since the bridge-cycle B_{11} representing a single vertex on the graph is intersected by $\pi^{-1}(\mathcal{F}^\infty_{\mathbb{R}})$. This cycle is depicted by a loop in the rightmost column of Figure 4 and contrary to all other chosen cycles, its intersection points with O_1 have intersection indices of opposite sign, as it follows from Proposition 2.4.1. Therefore, this bridge-class is orthogonal to O_1. □

2.7. **Lower and upper ovals.** Assume that $C_{\mathbb{R}}$ has type $\langle p \,|\, 0\rangle$, $1 \leqslant p \leqslant 4$, and consider the ovals $o_i = O_{i\mathbb{R}}$, $i = 1, \dots p$ with consecutive numeration. If $p = 4$ we suppose that o_1 and o_3 have bridges to the J-component and call o_1, o_3 the *lower* and o_2, o_4 the *upper ovals.*

2.7.1. **Proposition.** *The distinction between lower and upper ovals in the case* $p = 4$ *is well defined.*

Proof. Since existence of a bridge is a property preserved by deformation, it is sufficient to check such an uniqueness for the sextic C_0 constructed in Section 2.5.

There, we have already observed that under appropriate numeration the ovals o_1 and o_3 do have bridges to the J-component. Now, it remains to trace a hyperplane intersecting o_1, o_3, and o_2 (respectively, o_4) and to observe that such a hyperplane separates o_4 (respectively, o_2) from the J-component, so that by Bézout no nodal degeneration connecting o_4 (respectively, o_2) with the J-component is possible. $\square$

2.8. **Intersecting oval-classes by lines.** Let a real line $L \subset Y$ be transversal to an oval-cycle $O \subset Y$ at a point q, or equivalently let the positive tritangent $\ell = \pi(L)$ meet the positive oval $O_{\mathbb{R}} \subset Q_{\mathbb{R}}$ at the point $p = \pi(q)$ with simple tangency.

Our aim is to evaluate the intersection index $\operatorname{ind}_q(L, O)$, where O is oriented coherently with a chosen local orientation of $Y_{\mathbb{R}}$ along o as described in Section 2.4. Note that there is unique up to rescaling a nonzero real vector field w tangent to $Y_{\mathbb{R}}$ along $O_{\mathbb{R}}$ such that Jw together with a nonzero real vector field v of vectors tangent to $O_{\mathbb{R}}$ generates the tangent spaces of O along $O_{\mathbb{R}}$. In particular, due to transversality between L and O the vector $w(q)$ can not be tangent to L. For simplicity, let us choose the field v so that $v \wedge w$ defines the chosen local orientation of $Y_{\mathbb{R}}$.

When drawing a piece of $Y_{\mathbb{R}}$ (as on Fig. 5) we imagine it in a form of two sheets, permuted by Bertini involution, and choose as the front sheet the one whose orientation coincides with the right-hand (positive) orientation.

2.8.1. **Lemma.** *If the oval-cycle O is oriented coherently with respect to a pair of vector fields v, w and $L_{\mathbb{R}}$ is directed at the point q by $av + bw$ with $ab > 0$ (respectively, $ab < 0$), then $\operatorname{ind}_q(L, O) = -1$ (respectively, $\operatorname{ind}_q(L, O) = 1$).*

Proof. It follows from $v \wedge Jw \wedge (av + bw) \wedge (aJv + bJw) = -ab\, v \wedge Jv \wedge w \wedge Jw$. $\square$

Fig. 5. Detecting the intersection index of lines with oval-cycles

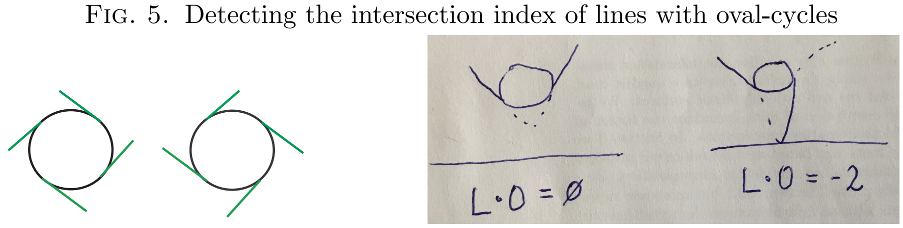

$\operatorname{ind}_q(L, O) = 1$ $\quad$ $\operatorname{ind}_q(L, O) = -1$

Here, the lines are shown on the front sheet.

The following two corollaries are straightforward consequences of Lemma 2.8.1.

2.8.2. **Corollary.** *Under the assumptions of Lemma 2.8.1 (and the above surface-drawing convention), the intersection index $\operatorname{ind}_q(L, O)$ depends on the direction of $L_{\mathbb{R}}$ at q as it is indicated on Fig. 5.* $\square$

2.8.3. **Corollary.** *Let a real line $L \subset Y$ cover a positive tritangent ℓ, and let $O \subset Y$ be a vanishing oval-cycle. Assume that $\ell_{\mathbb{R}}$ meets the oval $O_{\mathbb{R}} \subset Q_{\mathbb{R}}$ at a pair of points, and with simple tangency. Then $L \cdot O = 0$ if these tangency points are consecutive on $\ell_{\mathbb{R}}$ and $L \cdot O = \pm 2$ if these points are separated on $\ell_{\mathbb{R}}$ by a tangency with J-component of C (see Fig. 5).* $\square$

3. Arithmetic of real lines on del Pezzo surfaces

3.1. **Modulo 2 arithmetic of roots.** In this subsection we start with considering an arbitrary even negative definite lattice, which we denote by Λ, and put $V = \Lambda/2\Lambda$. For any $e \in \Lambda$, we denote by $[e]$ its image in V under the quotient map.

3.1.1. **Lemma.** *For any $e_1, e_2 \in \Lambda$, if $[e_1] = [e_2]$ and $e_1^2 = e_2^2 = -2$ then $e_2 = \pm e_1$.*

Proof. According the triangle inequality, $|\frac{e_1-e_2}{2}| \leqslant \frac{|e_1|+|e_2|}{2} = \sqrt{2}$. So, since $v = \frac{e_1-e_2}{2}$ belongs to Λ and the lattice Λ is even, in the case of $v \neq 0$ this inequality should be identity and thus, e_2 is collinear with e_1. $\square$

Reducing the lattice product modulo 2 we obtain a $\mathbb{Z}/2$-valued bilinear form $V \times V \to \mathbb{Z}/2$ and denote by R its radical $R = \{v \in V \mid v \cdot V = 0\}$. We consider also a $\mathbb{Z}/2$-valued quadratic form

$$\mathfrak{q}_0 : V \to \mathbb{Z}/2, \mathfrak{q}_0([v]) = \frac{v^2}{2} \mod 2$$

associated with this bilinear form. In R we introduce another $\mathbb{Z}/2$-valued bilinear form $b : R \times R \to \mathbb{Z}/2, b([v_1],[v_2]) = \frac{v_1 \cdot v_2}{2} \mod 2$, and an associated with it $\mathbb{Z}/4$-valued quadratic form

$$\mathfrak{q} : R \to \mathbb{Z}/4, \mathfrak{q}([v]) = \frac{v^2}{2} \mod 4.$$

Then, we put

$$V_i = \mathfrak{q}_0^{-1}(i), i \in \mathbb{Z}/2, \quad \text{and} \quad R_i = \mathfrak{q}^{-1}(i), i \in \mathbb{Z}/4.$$

In the same time, we let $\Lambda^* = \{x \in \Lambda \otimes \mathbb{Q} : x \cdot L \subset \mathbb{Z}\}$ and consider the discriminant group $\mathcal{D} = \Lambda^*/\Lambda$ of Λ.

The following two lemmas are well known and straightforward from definitions.

3.1.2. **Lemma.** *If the discriminant group $\mathcal{D}$ of Λ is 2-periodic, then $\mathcal{D} = \Lambda^*/\Lambda \to V = \Lambda/2\Lambda$ sending $x + \Lambda \in \Lambda^*/\Lambda$ to $2(x + \Lambda) \in \Lambda/2\Lambda$ is a well-defined monomorphism whose image is R and which identifies the quadratic form q with the discriminant form of Λ. In particular, $\mathfrak{q}$ is given by a matrix $[-1]$ for $\Lambda = A_1$, $\mathfrak{q} = [1]$ for $\Lambda = E_7$, and $\begin{bmatrix} 2 & 1 \\ 1 & -k \end{bmatrix}$ for $\Lambda = D_{2k}$.* $\square$

3.1.3. **Lemma.** *For any $e \in \Lambda$, $e^2 = -2$, we have $[e] \in V_1 \smallsetminus R_1$.* $\square$

A kind of opposite property, stated in the next proposition, does not hold for arbitrary even lattice Λ (for example, does not hold for $\Lambda = nA_1$ with $n \geqslant 5$) but it holds for each of the lattices we need.

3.1.4. **Proposition.** *Any element of $V_1 \smallsetminus R_1$ is realized by some root $e \in \Lambda$ as soon as Λ is one of the lattices Λ from Tab. 5.*

Now, when we consider real sextics $C \subset Q$, we can, following Proposition 3.1.4 and Proposition 2.3.2, associate with each $v \in V_1 \smallsetminus R_1$ a unique positive tritangent $l_v = \pi(L_e)$ where e is a (unique up to sign) root in Λ with $[e] = v$.

3.1.5. **Lemma.** *Consider a positive tritangent ℓ_v, $v \in V_1 \smallsetminus R_1$, and one of the geometric vanishing classes, an oval-cycle O or a bridge-cycle B.*

(1) *$v \cdot [O] = 1$ if and only if ℓ_v has odd tangency with the oval.*

TAB. 5. Lattices $\Lambda = \Lambda(Y)$ versus the type of C

$C_\mathbb{R}$	$\langle 4\,|\,0\rangle$	$\langle 3\,|\,0\rangle$	$\langle 2\,|\,0\rangle$	$\langle 1\,|\,0\rangle$	$\langle 1\,|\,1\rangle$	$\langle\,|\,|\,|\,\rangle$	$\langle 0\,|\,q\rangle, 0 \leqslant q \leqslant 4$
Λ	E_8	E_7	D_6	$D_4 + A_1$	D_4	D_4	$(4-q)A_1$
$\|V\| = 2^{\operatorname{rk}\Lambda}$	256	128	64	32	16	16	2^{4-q}
$\|R\| = 2^{\operatorname{rk}R}$	1	2	4	8	4	4	2^{4-q}
$\|V_1\|$	120	64	32	16	12	12	2^{3-q}
$\|R_1\|$	0	1	2	3	0	0	$\binom{4-q}{3}$
$\|V_1 \smallsetminus R_1\|$	120	63	30	13	12	12	$2^{3-q} - \binom{4-q}{3} = 4-q$

(2) $v \cdot [B] = 1$ *if and only if* ℓ_v *separates the components of* $C_\mathbb{R}$ *incident to the bridge.*

Proof. By definition, the tritangent ℓ_v is covered by a line L_e where e is a root in Λ with residue $[e] = v$. Note also that an oval of C has an odd tangency with ℓ_v if and only if in $Y_\mathbb{R}$ the oval has an odd intersection with $L_{e\mathbb{R}}$. Since in $Y_\mathbb{R}$ the oval represents the image $O_\mathbb{R} \in H_1(Y_\mathbb{R};\mathbb{Z}/2)$ of $O \in H_2(Y)$ by Viro homomorphism, we have $v \cdot [O] = L_e \cdot O \bmod 2 = L_{e\mathbb{R}} \cdot O_\mathbb{R}$, which gives the claim (1). Analogously, a separation of two components of $C_\mathbb{R}$, incident to a given bridge-class B, by ℓ_v is equivalent to an odd intersection of $L_{e\mathbb{R}}$ with $B_\mathbb{R} \in H_1(Y_\mathbb{R};\mathbb{Z}/2)$, which gives the claim (2), since $L_{e\mathbb{R}} \cdot B_\mathbb{R} = e \cdot B \mod 2 = v \cdot [B]$. □

3.1.6. **Lemma.** *For lattices* $\Lambda = \Lambda(Y)$ *associated with real sextics* $C \subset Q$, *the following holds:*

(1) *The cardinalities* $|V_1|$, $|R_1|$, *and* $|V_1 \smallsetminus R_1|$ *depend on the type of a sextic* C *as it is indicated in Tab. 5.*
(2) *In the cases* $\langle r\,|\,0\rangle$ *and* $\langle 0\,|\,r\rangle$, $0 \leqslant r \leqslant 3$ *we have* $|R_1|+|R_3| = |R_0|+|R_2| = \frac{1}{2}|R| = 2^{3-r}$.

Proof. To count $|V_1|$ we apply the rule saying that a quadratic function on a non-degenerate quadratic space (case $R = 0$) takes value one $2^{g-1}(2^g + (-1)^{\mathrm{Arf}+1})$ times where Arf is its Arf-invariant and g its symplectic rank (half dimension of the underlying vector space), and that in the case $R \neq 0$ a quadratic function takes value 1 the same number of times as value 0, if the function does not vanish on R. For computing Arf-invariants we use explicit symplectic bases. To check vanishing/nonvanishing of $\mathfrak{q}_0$ on R we use the congruence $\mathfrak{q}_0|_R = q \bmod 2$ and Lemma 3.1.2. The computations of R_i are also straightforward from Lemma 3.1.2 and give, for $i = 0,1,2,3$, the following values of $|R_i|$:

$$|R_i| = \begin{cases} \binom{4-r}{i} + \binom{4-r}{i+4}, & \text{for types } \langle r\,|\,0\rangle \\ \binom{4-r}{4-i} + \binom{4-r}{8-i}, & \text{for types } \langle 0\,|\,r\rangle \end{cases}$$

$$|R_0| = 1,\ R_2 = 3,\ R_1 = R_3 = 0 \quad \text{for type } \langle 1\,|\,1\rangle$$ □

Proof of Proposition 3.1.4. Since the half of the number of roots in Λ is equal to the number of elements in $V_1 \smallsetminus R_1$ found in Lemma 3.1.6 and shown in Tab. 5, the result stated follows from Lemmas 3.1.1 and 3.1.3. □

3.2. **Oval/bridge classes decomposition.** Here, we develop an approach for describing the real lines on a del Pezzo surface via reduction modulo 2 of the geometric root bases formed by oval- and bridge-classes that are specified, for a smart sextic C_ε, in Section 2.5. The crucial role here is playing by a direct sum decomposition $V = V^o + V^b$ where V^o is generated by residues of the vanishing oval-classes and V^b by the residues of the bridge-classes that are shown at the rightmost column of Fig. 4. Verification and principal properties of this decomposition are discussed in the next proposition.

3.2.1. **Proposition.** *Assume that C_ε is a smart real sextic of type $\langle p|q\rangle$ where either $p = q = 1$ or $q = 0, 1 \leqslant p \leqslant 4$. Then:*

(1) *$V = V^o + V^b$ is a direct sum decomposition.*
(2) *$\dim V^o = p$ and the residues $[O_1], \dots, [O_p] \in V$ of the oval-classes form a basis of V^o.*
(3) *$\dim V^b = 4 - q$ and the residues of the bridge-classes that take part of the Coxeter-Dynkin diagrams in Fig. 4 form a basis of V^b.*
(4) *The radical $R \subset V$ has dimension $4 - p - q$ and is contained in V^b.*
(5) *Subspaces V^o and V^b are isotropic with respect to the $\mathbb{Z}/2$-pairing in V inherited from Λ, and the induced pairing $V^o \times (V^b/R)$ is non-degenerate.*

Proof. The classes taking part of the Coxeter-Dynkin diagrams in Fig. 4 form a basis of Λ. This implies claims (1), (2), and (3). Since oval- and bridge-classes alternates in the Coxeter-Dynking graphs, the subspaces V^o and V^b are isotropic. To prove claims (4) and (5), it is sufficient to notice that for any collection of oval-classes there exists a bridge-class in the Coxeter-Dynkin diagrams which has odd number of incidences with the chosen collection of oval-classes. □

According Proposition 3.2.1, the spaces V^o and V^b have specific bases formed respectively by the residues $\mathfrak{o}_i$ of oval-classes $[O_i]$, $i = 1, \dots, p$ and by the residues of $4 - q$ bridge-classes which are indicated on Fig. 4 and which we will denote $\mathfrak{b}_1, \dots, \mathfrak{b}_{4-q}$ (with random enumeration). These bases of V^o and V^b will be called *geometric bases.*

Any vector $v \in V$ is decomposed as $v = v^o + v^b$ in accord with the direct sum decomposition $V = V^o + V^b$. By o-length $|v|_o$ and b-length $|v|_b$ of v we mean the number of non-zero coordinates of v^o and v^b in the geometric bases $\mathfrak{o}_1, \dots, \mathfrak{o}_p, \mathfrak{b}_1, \dots, \mathfrak{b}_{4-q}$ fixed above.

3.2.2. **Lemma.** *For any $v \in V$, $\mathfrak{q}_0(v) = |v|_o + |v|_b + v^o \cdot v^b \mod 2$.*

Proof. Since $\mathfrak{q}_0$ takes value 1 on each of the basic elements $\mathfrak{o}_1, \dots, \mathfrak{o}_p, \mathfrak{b}_1, \dots, \mathfrak{b}_{4-q}$, the relations $\mathfrak{q}_0(v^o) = |v|_o$ and $\mathfrak{q}_0(v^b) = |v|_b$ follow from the linearity of the restrictions $\mathfrak{q}_0|_{V^o}$ and $\mathfrak{q}_0|_{V^b}$ (*cf.* Proposition 3.2.1(5)). Applying quadraticity of $\mathfrak{q}_0$ to $v = v^o + v^b$, we obtain the required relation. □

3.3. **Internal and tangent ovals with respect to a tritangent.** With each positive tritangent ℓ we associate two index sets $S_{in}, S_{tan} \subset \{1, \dots, p\}$. Namely, $i \in S_{in}$ if and only if the oval with number i is contained in $\hat{\ell}$ (defined in Subsection 2.3), and $i \in S_{tan}$ if and only if ℓ has odd tangency with this oval.

Consider also a *boundary homomorphism* $\delta : V^b \to V^o$ that sends a basic class $\mathfrak{b}_j \in V^b$ to the sum of the residues $\mathfrak{o}_i = [O_i]$ of those oval-classes $O_i \in \Lambda \subset H_2(Y)$ that are incident to the bridge underlying the class $\mathfrak{b}_j$. More precisely, we put, by definition,

$$\delta(\mathfrak{b}_j) = \sum_{i=1,\dots,p} (\mathfrak{o}_i \cdot \mathfrak{b}_j)\mathfrak{o}_i. \tag{3.3.1}$$

Note, that

$$\ker \delta = R \tag{3.3.2}$$

as it follows immediately from Proposition 3.2.1.

3.3.1. **Proposition.** *Assume that C_ε is a smart real sextic of type $\langle p|0\rangle$ with $p \geqslant 1$ and $l_v, v \in V_1 \smallsetminus R_1$, is a positive tritangent with the associated index sets $S_{in}, S_{tan} \subset \{1,\dots,p\}$. Then:*

(1) *$v^o = \sum_{i\in S_{in}} \mathfrak{o}_i$ and in particular $|v|_o = |S_{in}|$.*
(2) *$\delta v^b = \sum_{i\in S_{tan}} \mathfrak{o}_i$ and in particular $\mathfrak{o}_i$-class in V is a summand in δv^b if and only if $\mathfrak{o}_i$ has odd tangency with ℓ_v.*
(3) *$v^o \cdot v^b = |S_{in} \cap S_{tan}| \mod 2$.*

Proof. Due to non-degeneracy of the pairing $V^o \times (V^b/R) \to \mathbb{Z}/2$ (see Proposition 3.2.1), the component v^o of v is determined by the intersection indices $v^o \cdot \mathfrak{b}_j = v \cdot \mathfrak{b}_j$ with $j = 1,\dots,4-q$. On the other hand, by Lemma 3.1.5, $v \cdot \mathfrak{b}_j \in \mathbb{Z}/2$ does not vanish if and only if the bridge-class with number j is incident to one and only one oval lying in $\hat\ell_{v\mathbb{R}}$. Since the same non-vanishing property holds for $(\sum_{i\in S_{in}} \mathfrak{o}_i)\cdot \mathfrak{b}_j$, we obtain the claim (1).

Due to (6.3.2) and linearity of δ, we have $\delta v^b = \sum_{i=1,\dots,p} (\mathfrak{o}_i \cdot v)\mathfrak{o}_i$. Thus, to get claim (2) there remains to notice that, due to Lemma 3.1.5, $o_i \cdot v = 1$ if and only if ℓ_v is tangent to the oval with number i.

Finally, we deduce from claim (1) and Lemma 3.1.5 that $v^o \cdot v^b = \sum_{i\in S_{in}} \mathfrak{o}_i \cdot v$ counts the number of $i \in S_{in}$ for which the oval with number i is tangent to ℓ_v, that is the number of elements in $S_{in} \cap S_{tan}$. □

3.4. Pairs (S_{in}, S_{tan}) for sextics of type $\langle 4\,|\,0\rangle$.

3.4.1. **Lemma.** *If a smart sexic $C = C_\varepsilon$ is of type $\langle 4\,|\,0\rangle$, then, for any positive tritangent ℓ_v*

$$|v|_b = |S_{tan} \cap \{1,3\}| \mod 2.$$

Proof. Each bridge is incident either to o_1 or to o_3 (but not to both). Therefore, $|v|_b$ has the same parity as $v\cdot\mathfrak{o}_1 + v\cdot\mathfrak{o}_3$, which, due to Lemme 3.1.5, has the same parity as the total number of tangencies of ℓ_v with o_1 and o_3. □

3.4.2. **Lemma.** *For any sextic $C \subset Q$ of type $\langle 4\,|\,0\rangle$ and any positive tritangent ℓ,*

$$|S_{in} \smallsetminus S_{tan}| + |S_{tan} \cap \{1,3\}| \qquad \textit{is odd.}$$

Conversely, for any pair of sets $S_1, S_2 \subset \{1,2,3,4\}$ with odd sum $|S_1 \smallsetminus S_2| + |S_2 \cap \{1,3\}|$, there exists a positive tritangent ℓ for which $S_1 = S_{in}$ and $S_2 = S_{tan}$.

Proof. The number and type of positive tritangents are preserved under deformation of C. So, it is enough to prove the statement for a smart sextic $C = C_\varepsilon$ of type $\langle 4\,|\,0\rangle$.

For any tritangent ℓ_v, $v \in V_1 \smallsetminus R_1$, we have $\mathfrak{q}_0(v) = 1$, while Proposition 3.3.1 with Lemmas 3.4.1 and 3.2.2 imply that

$$\begin{aligned}\mathfrak{q}_0(v) =& \mathfrak{q}_0(v^o) + \mathfrak{q}_0(v^b) + v^o\cdot v^b = |S_{in}| + |S_{tan}\cap\{1,3\}| + |S_{in}\cap S_{tan}| = \\ & |S_{in} \smallsetminus S_{tan}| + |S_{tan}\cap\{1,3\}| \mod 2.\end{aligned} \tag{3.4.1}$$

To prove the converse statement, we put $v = v^o + v^b$, $v^o = \sum_{i\in S_1} \mathfrak{o}_i$ and $v^b = \delta^{-1}(\sum_{i\in S_2} \mathfrak{o}_i)$, where the inverse map δ^{-1} is well defined, since in the case of type

$\langle 4\,|\,0\rangle$ the homomorphism $\delta : V^b \to V^o$ is an isomorphism, as it follows from $\ker\delta = R$ (see (3.3.2)) and $R = 0$, $\dim V^b = \dim V^o$ (see Proposition 3.2.1). With such a choice, we have $q(v^0) = |S_1| \bmod 2$, while due to $\sum_{i\in S_2}\mathfrak{o}_i = \delta(v^\delta) = \sum_i(\mathfrak{o}_i\cdot v^b)\mathfrak{o}_i$ (see (6.3.2) we get $\mathfrak{q}(v^b) = (v^b, \mathfrak{o}_1+\mathfrak{o}_3) = |S_2\cap\{1,3\}|$ and $v^o\cdot v^b = \sum_{i\in S_1}\cdot v^b = |S_1\cap S_2|$. Therefore, $\mathfrak{q}(v) = |S_1|+|S_2\cap\{1,3\}|+|S_1\cap S_2| = |S_1\smallsetminus S_2|+|S_2\cap\{1,3\}| = 1$. Propositions 3.1.4 and 2.3.2, now, imply existence of a tritangent ℓ_v. Proposition oval-bridge-components shows finally that $S_{in} = S_1$ and $S_{tan} = S_2$ for this ℓ_v. $\square$

3.4.3. **Proposition.** *Assume that C is a sextic of type $\langle 4\,|\,0\rangle$. Then:*

1. *A subset $S\subset\{1,2,3,4\}$ can be realized as S_{tan} of a positive tritangent ℓ if and only if $S\neq\{1,2,3,4\}$.*
2. *For each of the 15 subsets $S_2\subsetneq\{1,2,3,4\}$ there are precisely 8 subsets $S_1\subset\{1,2,3,4\}$ for which there exists a positive tritangent ℓ with $S_{in} = S_1, S_{tan} = S_2$, and this positive tritangent is uniquely determined by (S_1, S_2).*

Proof. Like in the proof of Lemma 3.4.1, we may suppose that $C = C_\varepsilon$ is smart. Consider elements $b_{ij}\in V^b$, $j = i+1$, represented by the bridge-classes $B_{ij}\in\Lambda$ (see Fig. 4). The sum $v^b = b_{12}+b_{34}$ is the only element of V^b with $\delta v^b = \mathfrak{o}_1+\dots+\mathfrak{o}_4$, which by Proposition 3.3.1 means that $S_{tan} = \{1,2,3,4\}$, but tangency of a tritangent to 4 ovals is impossible. This proves "only if" in part (1).

The "if"-part of (1) follows from (2), so let us prove the latter claim. According to Proposition 3.3.1, a choice of S_{tan} is equivalent to a choice of v^b, while a choice of S_{in} to a choice of v^a. In its turn, according to Propositions 3.1.4 and 2.3.2, v defines a line if and only if $\mathfrak{q}_0(v) = 1$, and such a line is unique, when it exists. The condition $\mathfrak{q}(v) = 1$ reads: $\mathfrak{q}_0(v^o)+\mathfrak{q}_0(v^b)+v^o\cdot v^b = 1$. Finally, there remain to notice that $\dim V^0 = 4$ and $\mathfrak{q}_0(v^o)+v^o\cdot v^b$ is a linear function of v^o, which is identically zero if and only if $v^b = b_{12}+b_{34}$. $\square$

3.4.4. **Corollary.** *For every M-sextic C of type $\langle 4\,|\,0\rangle$, a pair (S_1, S_2) of subsets $S_1, S_2\subset\{1,\dots,4\}$ is realized as (S_{in}, S_{tan}) of some positive tritangent if and only if $|S_1|\leqslant 3$ and $S_2\smallsetminus S_1$ satisfies the criteria for $|S_{in}\smallsetminus S_{tan}|$ pointed in the table below.* $\square$

	T_0	T_0^*	T_1	T_2	T_3
$\lvert S_{in}\smallsetminus S_{tan}\rvert =$	3	1	$\lvert S_{tan}\cap\{1,3\}\rvert+1 \bmod 2$	$\lvert S_{tan}\cap\{1,3\}\rvert \bmod 2$	$\begin{cases}0, & \text{if } \{2,4\}\subset S_{tan}\\ 1, & \text{if } \{1,3\}\subset S_{tan}\end{cases}$

3.5. Pairs (S_{in}, S_{tan}) for sextics of type $\langle p\,|\,0\rangle$ with $p\leqslant 3$.

3.5.1. **Proposition.** *Assume that C is a sextic of type $\langle p\,|\,0\rangle$, $0\leqslant p\leqslant 3$. Then:*

1. *For any pair of subsets $S_1, S_2\subset\{1,\dots,p\}$, except $S_1 = S_2 = \varnothing$ for $p\in\{2,3\}$, there exists a positive tritangent with $S_1 = S_{in}$ and $S_2 = S_{tan}$.*
2. *If $S_1 = S_2 = \varnothing$, then there exist precisely $2^{3-p}-(4-p)$* (that is four for $p = 0$, one for $p = 1$, and zero for $p\in\{2,3\}$) such realizations.

Any other pair (S_1, S_2) is realized by precisely 2^{3-p} positive tritangents.

Proof. Once more we refer to invariance of positive tritangents under deformation of C, pick a smart sextic C_ε of type $\langle 4\,|\,0\rangle$, and prove the statement for $C = C_\varepsilon$.

According to Proposition 3.3.1, for every positive tritangent ℓ_v with given $S_{in} = S_1, S_{tan} = S_2$ we should have $v = v^o+v^b$ with $v^o = \sum_{i\in S_1}\mathfrak{o}_i$ and $v^b\in\delta^{-1}(\sum_{i\in S_2}\mathfrak{o}_i)$. Thus, the component v^o is determined uniquely, while v^b varies in a given R-coset and thus can be chosen in $|\ker\delta| = |R| = 2^{4-p}$ ways (see Proposition 3.2.1). In the opposite direction, according to Lemma 3.1.3 and Proposition 3.1.4, $v = v^o + v^b$ does correspond to a positive tritangent if and only if $v \in V_1 - R_1$, and such a tritangent is unique, if exists.

Since $\mathfrak{q}(v) = \mathfrak{q}(v^a) + \mathfrak{q}(v^b) + v^a \cdot v^b = |S_1| + \mathfrak{q}(v^b) + |S_1 \cap S_2| = \mathfrak{q}(v^b) + |S_1 - S_2|$ mod 2 (*cf.* Proof of Proposition 3.4.3), to achieve $v \in V_1$ we need to achieve $q(v^b) = 1 + |S_1 - S_2|$ mod 2. Now, note that, for $\Lambda = E_7, D_6, D_4 + A_1, 4A_4$ corresponding to $p = 3, 2, 1, 0$ (see Fig. 4), precisely half of elements v^b of R have $\mathfrak{q}(v^b) = 0$ and half have $\mathfrak{q}(v^b) = 1$, which follows from linearity of $\mathfrak{q}$ on R and existence in R of elements with $\mathfrak{q} = 1$. This proves that the number of tritangents representing $(S_{in} = S_1, S_{tan} = S_2)$ is $\frac{1}{2}|R| = 2^{3-p}$ as soon as $S_1 \neq \varnothing$ or $S_2 \neq \varnothing$. Indeed, if $S_1 \neq \varnothing$ then $v^o \neq 0$ and thus $v \notin R_1$, while if $S_2 \neq \varnothing$ then v^b belongs to a R-coset distinct from $R = \ker\delta$, and thus never belongs to R_1.

If both S_1 and S_2 are empty, then we have deal with $v^o = 0$ and $v^b \in R$. In cases $p \in \{2, 3\}$, we have $\Lambda = D_6$ and $\Lambda = E_7$. Since for these lattices $R \cap V_1 \subset R_1$, Proposition 3.1.4 implies that no positive tritangent exists in these cases. In cases $p = 0, 1$, we have $\Lambda = 4A_4$ and $\Lambda = D_4 + A_1$, where $(R \cap V_1) \smallsetminus R_1$ is nonempty and consists of, respectively, 4 and 1 elements. ☐

3.6. **Pairs** (S_{in}, S_{tan}) **for sextics of type** $\langle 1 \,|\, 1\rangle$.

3.6.1. **Proposition.** *Assume that C is a sextic of type $\langle 1 \,|\, 1\rangle$. Then, for a pair of subsets $S_1, S_2 \subset \{1\}$ there exists a positive tritangent with $S_{in} = S_1$ and $S_{tan} = S_2$ if and only if $(S_1, S_2) \neq (\varnothing, \varnothing)$. Each of the remaining 3 pairs $(S_1, S_2) \neq (\varnothing, \varnothing)$ is realized precisely by 4 positive tritangents.*

Proof. The proof is analogous to that of Proposition 3.5.1. Here, $\Lambda = D_4$, the radical R is or dimension 2, and $\mathfrak{q}_0$ is identically zero on R, so that $V_1 = \varnothing$. The emptyness of V_1 exclude the case $v^o = 0, v^b \in R, \mathfrak{q}(v) = 1$ (which is equivalent to $(S_1, S_2) = (\varnothing, \varnothing)$). In its turn, from $\dim R = 2$ and $\mathfrak{q}_0|_R = 0$ it follows that in each of the cases $(S_1, S_2) \neq (\varnothing, \varnothing)$ there are precisely 4 choices of v^b in the R-coset $\delta^{-1}(\sum_{i \in S_{tan}} \mathfrak{o}_i)$ for which $\mathfrak{q}_0(v) = 1$. ☐

3.7. **Proof of Theorem 1.2.1.**

3.7.1. *The case of C of type $\langle 4 \,|\, 0\rangle$.* By definition, for the type T_k, $0 \leqslant k \leqslant 3$ and T_0^* the cardinality $|S_{tan}|$ is k and 0 respectively. Thus, applying Proposition 3.4.3 we conclude that the number of tritangents is

- $\binom{4}{0} \times 8 = 8$ for the types T_0 and T_0^* counted together,
- $\binom{4}{k} \times 8$ for the type T_k, that is 32, 48 and 32 for $k = 1, 2, 3$ respectively,

where $\binom{4}{k}$ indicates a choice of a subset $S_{tan} \subset \{1, \dots, 4\}$.

To finish the proof we separate the types T_0 and T_0^* by means of the following criterium.

3.7.1. **Proposition.** *The 4 cases with $|S_{in}| = 3, S_{tan} = \varnothing$ and 4 cases with $|S_{in}| = 1, S_{tan} = \varnothing$ represent the tritangents ℓ of type T_0 and T_0^*, respectively.*

Proof. According to Proposition 3.3.1, a positive tritangent l_v has $S_{in} = \{i\}, S_{tan} = \varnothing$, if an only if $v = \mathfrak{o}_i$. In such a case, it is the vanishing oval-class O_i that lifts v to $\Lambda = E_8$. Thus, by Proposition 2.3.2 $|L_v \cdot O_i| = |(-K \pm O_i) \cdot O_i| = |O_i^2| = 2$, and by Corollary 2.8.3 L_v should have two tangency points with oval O_i separated by tangency with the J-component.

Similarly, a positive tritangent l_v has $S_{in} = \{i, j, k\}, S_{tan} = \varnothing$ if and only if $v = \mathfrak{o}_i + \mathfrak{o}_j + \mathfrak{o}_k$. The corresponding roots $e \in E_8$ are given by the following linear combinations of the basic geometric vanishing classes indicated in Fig. 4 (to point the position of the oval-classes, we encircle their multiplicities).

$$\begin{smallmatrix} 0&0&1&2&3&2&1\\ &&&&2&& \end{smallmatrix} \qquad \begin{smallmatrix} 1&2&3&4&4&2&1\\ &&&&2&& \end{smallmatrix} \qquad \begin{smallmatrix} 1&2&2&2&3&2&1\\ &&&&2&& \end{smallmatrix} \qquad \begin{smallmatrix} 1&2&3&4&4&2&1\\ &&&&2&& \end{smallmatrix}$$

For each of these 4 roots e, the product $e \cdot O_i$ with each of the oval-classes O_i vanishes.

□

3.7.2. *The case of C of type $\langle p \,|\, 0\rangle$, $0 \leqslant p \leqslant 3$.* In the case of tritangents of types T_k, $k = 1, 2, 3$, Proposition 3.5.1 gives $8\binom{p}{k}$, tritangents, where 8 appears as the product of 2^{3-p} with the number 2^p of subsets S_{in}. If we count together tritangents of types

Tab. 6

p	Λ	root	root	root	root
3	E_7	$\begin{smallmatrix} 1&1&1&1&0&0\\ &&&1&& \end{smallmatrix}$	$\begin{smallmatrix} 0&1&2&3&2&1\\ &&&2&& \end{smallmatrix}$	$\begin{smallmatrix} 1&2&3&3&2&1\\ &&&1&& \end{smallmatrix}$	$\begin{smallmatrix} 1&1&1&2&2&1\\ &&&1&& \end{smallmatrix}$
2	D_6	$\begin{smallmatrix} 1&1&1&1&0\\ &&&1& \end{smallmatrix}$	$\begin{smallmatrix} 1&1&1&1&1\\ &&&0& \end{smallmatrix}$	$\begin{smallmatrix} 0&0&0&1&1\\ &&&1& \end{smallmatrix}$	$\begin{smallmatrix} 0&1&2&2&1\\ &&&1& \end{smallmatrix}$
1	$D_4 + A_1$	$\begin{smallmatrix} 1&1&0&&0\\ &1&&& \end{smallmatrix}$	$\begin{smallmatrix} 1&1&1&&0\\ &0&&& \end{smallmatrix}$	$\begin{smallmatrix} 0&1&1&&0\\ &1&&& \end{smallmatrix}$	$\begin{smallmatrix} 0&0&0&&1\\ &0&&& \end{smallmatrix}$
0	$4A_1$	1 0 0 0	0 1 0 0	0 0 1 0	0 0 0 1

T_0 and T_0^*, Proposition 3.5.1 gives $2^{3-p} \cdot 2^p - (4-p) = 4+p$ tritangents, among which p corresponding to $|S_{in}| = 1$ represent case T_0^* as it follows from by Corollary 2.8.3 as above, and the remaining 4 tritangents represent T_0-case. The corresponding 4 roots are described in Tab. 6. In Tab. 6, the 4 positive roots $e \in \Lambda$ representing the 4 tritangents ℓ_v, $v = [e]$ of type T_0 for C of type $\langle p \,|\, 0\rangle$. For each of these roots e we have $e \cdot O_i = 0$ for each (encircled) oval-root. An oval o_i lies above ℓ_v if the corresponding (encircled) coefficient is odd.

3.7.3. *The case of C of type $\langle 1 \,|\, 1\rangle$.* By Proposition 3.6.1 the type T_1 is represented by $8 \times \binom{1}{1} = 8$ tritangents, among which 4 correspond to $S_{in} = \varnothing$ and 4 to $S_{in} = \{1\}$, while the types T_0 and T_0^* together are represented by 4 tritangents corresponding to $S_{tan} = \varnothing$ and $S_{in} = \{1\}$. Among the latter four, only one represents type T_0^*, since there is only one oval above the J-component (which follows again from Corollary 2.8.3 applied in a similar way). The roots indicating the corresponding pairs (S_{in}, S_{tan}) are shown in Tab. 7.

The types T_3 and T_2 are not represented by tritangents since $\binom{1}{3} = \binom{1}{2} = 0$.

3.7.4. *The case of C of type $\langle | \, | \, | \rangle$.* Absence of ovals implies that all tritangents are of type T_0. Their number is the half of the number of roots in $\Lambda = D_4$, that is 12.

3.7.5. *The case of type $\langle 0 \,|\, q\rangle$, $q \geqslant 1$.* In this case, $\Lambda = qA_1$. Such a lattice has precisely q pairs of opposite roots. So, according to Proposition 2.3.2, in this case we have precisely q positive tritangents. Since all ovals of $C_{\mathbb{R}}$ bound disc-components of $Q^+_{\mathbb{R}}$, all these tritangents are of type T_0.

Tab. 7

root e in $\Lambda = D_4$				type of $\ell_{[e]}$	$(\lvert S_{in}\rvert, \lvert S_{tan}\rvert)$	# roots
$\begin{smallmatrix} 0 & 1 & 0 \\ & 0 & \end{smallmatrix}$				T_0^*	(1,0)	1
$\begin{smallmatrix} 1 & 1 & 1 \\ & 0 & \end{smallmatrix}$	$\begin{smallmatrix} 1 & 1 & 0 \\ & 1 & \end{smallmatrix}$	$\begin{smallmatrix} 0 & 1 & 1 \\ & 1 & \end{smallmatrix}$		T_0	(1,0)	3
$\begin{smallmatrix} 1 & 1 & 0 \\ & 0 & \end{smallmatrix}$	$\begin{smallmatrix} 0 & 1 & 1 \\ & 0 & \end{smallmatrix}$	$\begin{smallmatrix} 0 & 1 & 0 \\ & 1 & \end{smallmatrix}$	$\begin{smallmatrix} 1 & 1 & 1 \\ & 1 & \end{smallmatrix}$	T_1	(1,1)	4
$\begin{smallmatrix} 1 & 0 & 0 \\ & 0 & \end{smallmatrix}$	$\begin{smallmatrix} 0 & 0 & 1 \\ & 0 & \end{smallmatrix}$	$\begin{smallmatrix} 0 & 0 & 0 \\ & 1 & \end{smallmatrix}$	$\begin{smallmatrix} 1 & 2 & 1 \\ & 1 & \end{smallmatrix}$	T_1	(0,1)	4

4. Descriptive topology of positive tritangents to sextics and of real lines on del Pezzo surfaces

As before, we consider a real sextic $C \subset Q$ and a real del Pezzo surface Y obtained as the double covering $\pi : Y \to Q$ branched along C and the vertex $v \in Q$. Our goal here is to describe the isotopy types of positive real tritangents to $C_{\mathbb{R}} \subset Q_{\mathbb{R}}$, which gives an isotopy classification of real lines on $Y_{\mathbb{R}}$.

4.1. **Removable pairs of tangencies.** It will be convenient to consider a more flexible, topological, version of tritangents in $Q^+_{\mathbb{R}}$ and lines in $Y_{\mathbb{R}}$. Namely, by a *loose section* we will mean a smoothly embedded circle $r \subset Q^+_{\mathbb{R}}$ which:

- meets each real generator of $Q_{\mathbb{R}}$ transversely at one point,
- has intersection $r \cap C_{\mathbb{R}}$ at one or three simple tangency points.

In its turn, by a *pseudo-line* we will mean a smoothly embedded circle $R \subset Y_{\mathbb{R}}$ which meets the real locus $F_{\mathbb{R}}$ of each real anti-canonical effective divisor $F \in |-K|$ transversely at one point (such divisors F are nothing but pullbacks of the generators of Q).

4.1.1. **Lemma.** *For any loose section $r \subset Q^+_{\mathbb{R}}$ its pull-back $\pi^{-1}(r) \subset Y_{\mathbb{R}}$ splits into a union $R \cup R'$ of pseudo-lines $R' = \tau(R)$. These pseudo-lines intersect each other transversally over the tangency points of r, and both $\pi|_R$ and $\pi|_{R'}$ are diffeomorphisms.* □

The J-component is said to have a *zig-zag* over an interval $[a, b] \subset \mathbb{P}^1_{\mathbb{R}}$ if a, b are critical points of the projection $J \to \mathbb{P}^1_{\mathbb{R}}$ and over intermediate points $a < t < b$ the projection preimages are 3-point subsets of J, as is shown on Fig. 6. Respectively, we say that a real del Pezzo surface Y contains a zig-zag, if there exists a zig-zag on the J-component of the associated sextic $C_{\mathbb{R}} \subset Q_{\mathbb{R}}$.

A *strong isotopy* of loose sections, r_t, is defined as an isotopy formed by loose sections which moves the tangency point set $r_t \cap C_{\mathbb{R}}$ by an isotopy on $C_{\mathbb{R}}$. By a *fiberwise isotopy* of pseudo-lines, R_t, we mean an isotopy in $Y_{\mathbb{R}}$ formed by pseudo-lines.

By an *ambient isotopy* of a loose section we understand an isotopy induced by a continuous family of diffeomorphisms $Q^+_{\mathbb{R}} \to Q^+_{\mathbb{R}}$. Such isotopies allow to perform *zigzag moves* of loose sections like the one shown on Fig. 6.

For loose sections r having several tangency points with the same connected component γ of $C_{\mathbb{R}}$, we define also a *simplification move*. Namely, such a move can

FIG. 6. Zigzag move

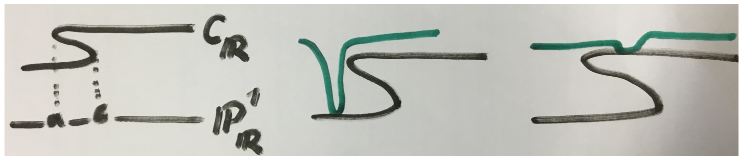

be performed if a pair of points $a, b \in r \cap \gamma$ is *removable*, which means that there exists a topological disc $D \subset Q^+_{\mathbb{R}}$ whose boundary is formed by two arcs, $D \cap r$ and $D \cap \gamma$, connecting a and b. Then, a *simplification move of r guided by D and supported near $\delta = D \cap r$* slightly pushes the arc $\delta = D \cap r$ out of D and preserves r unchanged outside a small neighborhood of this arc. As a result, we obtain a loose section $\widetilde{r} \subset Q^+_R \smallsetminus D$, whose number of tangencies with $C_{\mathbb{R}}$ is dropped by 2.

FIG. 7. Removable and not removable pairs of tangent points

removable   not removable

4.1.2. **Lemma.** *Assume that a positive real tritangent ℓ to a real non-singular sextic $C \subset Q$ of type different from T^*_0 has more than one tangency point with a connected component of C. Then at least one pair of these tangency points is removable.*

Proof. By Bézout, every real generator of Q intersects $\ell_{\mathbb{R}}$ at a unique real point and meets each oval of C in at most 2 real points. Therefore, if a and b are two consecutive points of tangency of $\ell_{\mathbb{R}}$ with an oval O, we consider that arc ab of $\ell_{\mathbb{R}}$ which does not contain the third tangency point. If ℓ is not of type T^*_0, the real generators of Q passing through the points of this arc trace on O two arcs. One of them has a, b as extremities and forms together with ab a circle bounding in Q^+ a disc formed by intervals of the above real generators (see on the left of Fig. 8). This proves the statement in the case of tangencies with an oval.

Next, assume that ℓ has 3 tangency points with the J-component: a, b, and c. Then, $\ell_{\mathbb{R}} \cup J$ form 3 topological circles and, if neither of them bounds a disc in Q^+, inside each of these circles there is an oval. Now intersecting l with a real tritangent ℓ' of type T_3 tangent to these 3 ovals we observe at least $6 > 2$ intersection points (see at the center of Fig. 8), which is in contradiction with Bézout theorem.

Finally, assume that a and b are 2 tangency points of ℓ with the J-component, and c is a tangency point of ℓ with an oval O. Then, $\ell_{\mathbb{R}} \cup J$ form 2 topological circles. One of them contains c. If the other circle does not bound a disc in Q^+, then inside it there is an oval, O'. Now, intersecting ℓ with a real tritangent ℓ' of type T_2 tangent to the ovals O and O' and passing below O, we observe at least $4 > 2$ intersection points (see at the right of Fig. 8), which is in contradiction with the Bézout theorem. □

We say that a loose section (and in particular, a tritangent) is *simple* if either it is tangent to each connected component of $C_{\mathbb{R}}$ not more than once or it is of type T^*_0.

FIG. 8. To the proof of Lemma 4.1.2

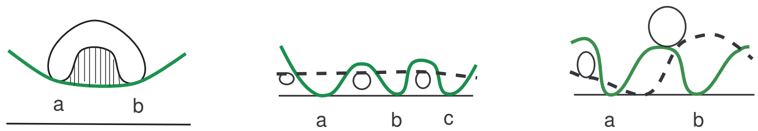

4.1.3. **Proposition.** *Every positive tritangent either is simple itself, or can be made simple by a simplification move.*

The Bertini-pair of pseudo-lines covering a loose section obtained by a simplification move are isotopic to the Bertini-pair of lines covering the initial tritangent. If the arc δ supporting the simplification move is a part of an oval, or if δ is a part of a J-component with no zig-zag in δ, the isotopy can be made fiberwise.

Proof. The first part follows directly from Lemma 4.1.2. For the second part, consider a loose section r_2 obtained by a simplification move of r_0 and note that, due to a disk D guiding the move, r_2 can be obtained by a continuous family r_t, $t \in [0, 2]$, such that:

- it performs a an isotopy for $t \in [0, 1)$ so that the removable tangency points $a, b \in r_0 \cap \gamma$ move towards each other along γ and merge into a double tangency point of $r_1 \cap \gamma$;
- while for $t \in [1, 2]$, it performs shifting of this double tangency from γ to obtain r_2.

If γ is an oval, or a J-component with the arc $\gamma \cap D$ not containing zig-zag, then the disc D is sliced in intervals by the generators of Q (see the leftmost sketch on Fig. 8), and by this reason in such a case the above isotopies can be made fiberwise.

For every $t \in [0, 2]$, the pull-back $\pi^{-1}(r_t) \subset Y_{\mathbb{R}}$ splits into a Bertini-pair of pseudo-lines R_t and R'_t. Each of these two families of pseudo-lines forms an isotopy (at moment $t = 1$ these pseudo-lines are just tangent to each other, see Fig. 9). $\square$

FIG. 9. A family r_t connecting a tritangent r_0 with its simplification r_2 (upper row) and the covering isotopy of Bertini pairs (lower row)

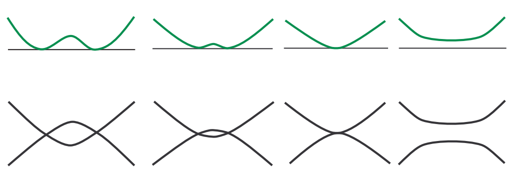

In what follows by a *simplified tritangent* we mean a tritangent itself if it is simple, or a loose section obtained from the tritangent by a simplification move.

4.2. **The simplest case: Sextics C of type $\langle 0 \,|\, q \rangle$.** Absence of positive ovals implies that all positive tritangents in this case are of type T_0. By Theorem 1.2.1, their number is $4 - q$, and in particular, there are no positive tritangents if $q = 4$ and no real lines on the corresponding $Y_{\mathbb{R}} = \mathbb{RP}^2 \amalg 4\mathbb{S}^2$.

If $q \leqslant 3$, each positive tritangent is isotopic to the J-component, and each real line on the corresponding $Y_{\mathbb{R}} = \mathbb{RP}^2 \amalg q\mathbb{S}^2$ is isotopic to the (unique) lift of the

J-component to $Y_{\mathbb{R}}$, and, in particular, all real lines are isotopic to each other. If the J-component contains no zig-zag, then the isotopies between the real lines can be performed fiberwise, while the tritangents becomes strongly isotopic after simplification moves.

4.3. **Sextics C of type $\langle|||\rangle$.** In this case $C_{\mathbb{R}}$ has three J-components and $Q^+_{\mathbb{R}}$ has two connected components: a disc containing the vertex of Q and a band, which are covered in $Y_{\mathbb{R}}$ by $\mathbb{RP}^2$ and $\mathbb{K}$, respectively. The components of $C_{\mathbb{R}}$ will be denoted by J_1, J_2, J_3 so that J_1 bounds the disc-component of $Q^+_{\mathbb{R}}$, while J_2 and J_3 bound the band-component and J_2 lies between J_1 and J_3 on $Q_{\mathbb{R}}$.

For the same reason as in the previous case, all positive tritangents are of type T_0, each of the tritangents is isotopic either to J_1, or to J_2, or to J_3, and each real line on $X_{\mathbb{R}} = \mathbb{RP}^2 \amalg \mathbb{K}$ is isotopic to the lift of a corresponding J-component.

4.3.1. **Lemma.** *There exist 4 geometric bridge classes $B_1, \dots, B_4$ between components J_2 and J_3, and any 3 of these four classes together with the class $B_0 = -\frac{1}{2}(B_1 + \cdots + B_4)$ form a root basis of the D_4-lattice Λ, wherein B_0 represents the central vertex of the D_4-graph and the 3 other chosen classes the pendant vertices.*

FIG. 10. A sextic C of type $\langle|||\rangle$ with 4 geometric bridge-classes

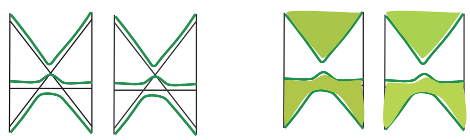

Proof. For existence of 4 bridge classes, see Fig. 10, where the sextic is obtained by a small real perturbation of 3 real hyperplane sections. A divisibility of their sum by 2 follows from comparison of the discriminants of D_4 and $4A_1$. □

4.3.2. **Proposition.** *If $C \subset Q$ is of type $\langle|||\rangle$, then, for each of the components J_i, $i = 1, 2, 3$, there exist precisely 4 positive tritangents having odd tangency with it.*

Proof. By Theorem 1.2.1, the total number of positive tritangents is 12. Among them there are 4 corresponding to the geometric bridge classes $B_1, \dots, B_4$ and 8 to the 8 pairs of opposite roots $\frac{1}{2}(\pm B_1 \pm \cdots \pm B_4)$. The tritangents $\pi(L_{B_i})$ $(i = 1, \dots, 4)$ are contained in the disc-component, while the tritangents $\pi(L_e)$ with $e = \frac{1}{2}(\pm B_1 \pm \cdots \pm B_4)$ belong to the band-component, as it follows from $L_{B_i} \cdot B_j = -B_i \cdot B_j = 0 \mod 2$ and $L_e \cdot B_j = -e \cdot B_j = \mp\frac{1}{2} B_j^2 = 1 \mod 2$, for every $1 \leqslant i, j \leqslant 4$.

To conclude, we notice that according to Theorem 4.2.2 in [FK-1] the positive tritangents tangent to J_1 and J_3 are hyperbolic, while those tangent to J_2 are elliptic, and that according to Theorem 1.1.2 in [FK-2] the number of hyperbolic tritangents minus the number of elliptic is equal to 4. □

4.3.3. **Proposition.** *If $C \subset Q$ is of type $\langle|||\rangle$, then the 12 positive tritangents split in 3 groups by 4 tritangents isotopic to the same J-component. For each of the 3 groups, the 4 covering Bertini pairs of real lines are fiberwise isotopic to each other, while the 4 tritangents themselves becomes strongly isotopic after simplification moves.*

Proof. Existence of fiberwise isotopies for lines, as well as that of strong isotopies for tritangents, follows from absence of zig-zags on sextics of type $\langle|||\rangle$. $\square$

4.4. **Sextics C of type $\langle 1 \,|\, 1\rangle$.** Proposition 4.1.3 together with Table 7, which lists possible combinations of (S_{in}, S_{tan}), and Theorem 1.2.1, which provides the number of positive tritangent of each type, can be summarized in the following description.

4.4.1. **Proposition.** *For any nonsingular sextic C of type $\langle 1 \,|\, 1\rangle$, up to ambient isotopy in Q_+ the simplified positive tritangents are as shown on Fig. 11. The*

FIG. 11

Type T_0 *Type T_0^** *Type T_1*

leftmost type, T_0, is represented by 3 distinct tritagents, the next type, T_0^*, by 1, and each of the remaining ones (both T_1) by 4. The Bertini pairs of real lines covering the tritangents of the same type are isotopic. If C has no zig-zags, then the isotopies between the Bertini pairs can be performed fiberwise, while the simplified tritangents become strongly isotopic. $\square$

4.5. **Encoding of the isotopy types.** If a simplified tritangent, $r \subset Q^+_{\mathbb{R}}$, goes below (resp., above) a positive oval without tangency, we say that r *underpasses* (resp., *overpasses*) this oval, and use the symbol $\underline{\bigcirc}$ (resp., $\overline{\bigcirc}$) to encode such mutual position. If r goes below (resp. above) an oval with one simple tangency we use the symbol $\underline{\bigcirc}$ (resp., $\overline{\bigcirc}$) and say that r is an *undertangent* (resp., *overtangent*). When we wish to underline that both, undertangent and overtangent, positions are realizable, we put the symbol $\overline{\underline{\bigcirc}}$. In the case of a tritangent of type T_0^* we introduce an additional symbol $\mathcal{O}$ for an oval having a pair of tangencies separated by an J-tangency.

Note that the fiber $f_Q^{-1}(t) \subset Q_{\mathbb{R}}$, $t \in \mathbb{P}^1_{\mathbb{R}}$, containing a J-tangency point cannot intersect an overpassed or overtangent oval of $C_{\mathbb{R}}$. It follows that t belongs to the complement $I_r^\circ \subset \mathbb{P}^1_{\mathbb{R}}$ of the projection of the union of such ovals with the set of undertangent tangency points. We let $I_r \subset I_r^\circ$ be obtained by removing from I_r° the projection of the undertangent ovals and put $J_r = f_Q^{-1}(I_r) \cap J$.

4.5.1. **Lemma.** *Assume that r is a simple loose section with a J-tangency point. Then:*

(1) *A strong isotopy of r does not change the sets I_r and J_r.*
(2) *If r is not of type T_0^*, then it can be moved by a strong isotopy so that the fiber $f_Q^{-1}(t), t \in \mathbb{P}^1_{\mathbb{R}}$ that contains the J-tangency point will not intersect the ovals of $C_{\mathbb{R}}$.*
(3) *The connected component of I_r containing the point t obtained after a strong isotopy in (2) as well as the component of J_r containing the J-tangency point do not depend on such isotopy.*

Proof. (1) is straightforward. For proving (2) we just need to move to I_r the J-tangency point which may occur under the undertangent ovals, which can be obviously done by a strong isotopy. Presence of an undertangency point shows that the direction of this moving is uniquely defined, which implies (3). □

The codes to be used in Tab. 8 in addition to the information about tangency of a simplified tritangent r with ovals, its over- and underpassing, contains also information about the location of a J-tangency point (if any). Namely, after we push it using Lemma 4.5.1 to I_r, one should specify the connected component of I_r containing the J-tangency.

It turns out however, that such information is required only if r has type T_2, while in the other cases the question about J-tangency does not rise. For T_0-type, it is because the interval I_r is connected. For T_0^*-type, the position of the J-tangency is prescribed by the definition of T_0^*. For T_1-type, the simplification procedure allows to remove the J-tangencies due to Lemma 4.1.2, and for T_3-type, there is no J-tangencies at all.

In the case of T_2-type, we distinguish the component of I_r containing the J-tangency by means of delimiters $\langle$ and $\rangle$ that mark the endpoints of this component. Note that some number of symbols $\bigcirc$ may be enclosed by the delimiters.

For example, the code $\underline{\bigcirc}\langle\, \underline{\underline{\bigcirc}}\, \underline{\underline{\bigcirc}}\,\rangle\, \underline{\bigcirc}$ refers to $C_{\mathbb{R}}$ with 4 ovals and a tritangent r underpassing the second and the third ovals and undertangent the first and the fourth ovals. The brackets indicate presence of a J-tangency between the first and the fourth ovals. For more examples, the 4 tritangents shown on Fig. 11 can be encoded respectively as $\overline{\overline{\bigcirc}}$, $\bigcup\!\!\!\bigcirc$, $\underline{\bigcirc}$, and $\overline{\bigcirc}$.

4.5.2. **Lemma.** *The code of a simple loose section r determines it uniquely up to an ambient isotopy in Q_+.*

Proof. Like in the cases of $\langle 0|q\rangle$ in Subsection 4.2, if J-component contains no zigzags, then loose sections with the same code can be connected by a strong isotopy.

To connect loose sections in presence of zigzags it is enogh to perform zigzag moves. □

4.6. **Restrictions on the position of J-tangencies.** These restrictions concern the tritangents of type T_2, and only in the cases $\langle 4\,|\,0\rangle$ and $\langle 3\,|\,0\rangle$.

4.6.1. **Proposition.** *Let ℓ be a positive tritangent of type T_2 to a real sextic C of type $\langle 4\,|\,0\rangle$ or $\langle 3\,|\,0\rangle$.*

(1) *If C is of type $\langle 4\,|\,0\rangle$ and the pair of tangent to $\ell_{\mathbb{R}}$ ovals include precisely one of the ovals O_1 and O_3, then the non-tangent ovals lie both above or both below $\ell_{\mathbb{R}}$ while the J-tangency point belongs to that interval of ℓ delimited by projections of the tangency points with ovals which contains the projection of non-tangent ovals in the first (above) case and does not contain the projection of non-tangent ovals in the second (below) case.*
(2) *If C is of type $\langle 4\,|\,0\rangle$ and the two tangent ovals are either O_1 and O_3 or O_2 and O_4, then one of the non-tangent ovals lie above and one lie below $\ell_{\mathbb{R}}$, while the J-tangency point belongs to that interval of ℓ delimited by projections of the tangency points with ovals which contains the projection of the non-tangent oval lying above $\ell_{\mathbb{R}}$.*
(3) *If C is of type $\langle 3\,|\,0\rangle$, then the J-tangency point belongs to that interval of ℓ delimited by projections of the tangency points with ovals which contains the projection of the non-tangent oval if the latter one lies above $\ell_{\mathbb{R}}$, and does not contain the projection of the non-tangent oval otherwise.*

Proof. To justify each of the above restrictions on the position of J-tangency points on the J-component we assume the contrary and trace an auxiliary tritangent ℓ' of type T_3, which contradicts to the Bezout theorem applied to $\ell' \cap \ell$. Typical examples are shown on Fig. 12. The upper row shows the location of the J-tangency in each of the 4 chosen examples. In the bottom row we demonstrate why another location of a J-tangency is forbidden. For that, in each example we indicate an auxilliary tritangent of type T_3 (dotted curve) whose intersection with the given tritangent contradicts to the Bezout theorem. Existence of such auxiliary tritangents follows from Theorem 1.2.1 and Lemma 4.6.2. $\square$

FIG. 12. Examples of realizable, and not realizable, J-tangencies

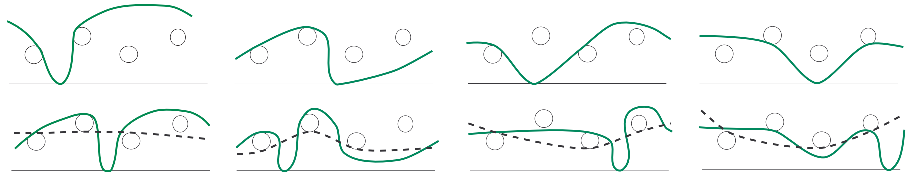

4.6.2. **Lemma.** *A real del Pezzo surface contains a Bertini pair of real lines of isotopy type* $x\underline{\bigcirc}y$ *if and only if it contains a Bertini pair of real lines of isotopy type* $x\overline{\bigcirc}y$.

Proof. Switching from one to another is equivalent to adding the oval-class e to v^o in the oval/bridge decomposition, as it follows from Proposition 3.3.1. $\square$

4.7. **Sextics of type $\langle p \,|\, 0\rangle$.** We say that the code of a sextic of type $\langle p \,|\, 0\rangle$, $p < 4$, is a derivative of a code of type $\langle 4 \,|\, 0\rangle$, if the first is obtained from the second by dropping $4 - p$ symbols of type $\underline{\bigcirc}$ and $\overline{\bigcirc}$.

4.7.1. **Theorem.** *The 120 positive tritangents to a real sextic $C \subset Q$ of type $\langle 4 \,|\, 0\rangle$ in their simplified forms (as loose sections) have the codes listed in Table 8. For sextics of type $\langle p \,|\, 0\rangle$ with $p < 4$, the codes are exactly the derivatives of the above ones. Respectively, on every real del Pezzo surface Y with $Y_{\mathbb{R}} = \mathbb{RP}^2 \# p\mathbb{T}^2$, $p \leqslant 4$, the real lines are isotopic to the pseudo-lines covering the simplified loose sections given by the codes from Table 8 and their derivatives.*

Proof. Passage to a simplified form for positive tritangents to C, and to a pseudo-line for real lines on Y, is justified by Proposition 4.1.3. Corollary 3.4.4 and Proposition 3.5.1 give us the list of pairs (S_{in}, S_{tan}) for sextics of type $\langle 4 \,|\, 0\rangle$ and those of type $\langle p \,|\, 0\rangle$, $0 \leqslant p \leqslant 3$, respectively. Proposition 4.6.1 determines, for sextics of type $\langle 4 \,|\, 0\rangle$ and $\langle 3 \,|\, 0\rangle$, the positions of the J-tangency point in the case of type T_2 (for simplifications of positive tritangents of other types, changing position of the J-tangency point does not change the loose section isotopy type of a simplification). $\square$

5. Preliminaries on rational elliptic surfaces

Here we assume that $f : X \to \mathbb{P}^1$ is an elliptic surface satisfying assumption **A**.

Tab. 8. The codes of 120 positive simplified tritangents. The first oval is chosen among the two lower ones.

T_0	$\underline{\bigcirc}\ \underline{\bigcirc}\ \underline{\bigcirc}\ \overline{\bigcirc}$	$\underline{\bigcirc}\ \underline{\bigcirc}\ \overline{\bigcirc}\ \underline{\bigcirc}$	$\underline{\bigcirc}\ \overline{\bigcirc}\ \underline{\bigcirc}\ \underline{\bigcirc}$	$\overline{\bigcirc}\ \underline{\bigcirc}\ \underline{\bigcirc}\ \underline{\bigcirc}$	4
T_0^*	$\bigcirc\!\!\!\!\!\cup\ \overline{\bigcirc}\ \overline{\bigcirc}\ \overline{\bigcirc}$	$\overline{\bigcirc}\ \bigcirc\!\!\!\!\!\cup\ \overline{\bigcirc}\ \overline{\bigcirc}$	$\overline{\bigcirc}\ \overline{\bigcirc}\ \bigcirc\!\!\!\!\!\cup\ \overline{\bigcirc}$	$\overline{\bigcirc}\ \overline{\bigcirc}\ \overline{\bigcirc}\ \bigcirc\!\!\!\!\!\cup$	4
T_1	$\overline{\underline{\bigcirc}}\ \underline{\bigcirc}\ \underline{\bigcirc}\ \overline{\bigcirc}$	$\overline{\underline{\bigcirc}}\ \underline{\bigcirc}\ \overline{\bigcirc}\ \underline{\bigcirc}$	$\overline{\underline{\bigcirc}}\ \overline{\bigcirc}\ \underline{\bigcirc}\ \underline{\bigcirc}$	$\overline{\underline{\bigcirc}}\ \overline{\bigcirc}\ \overline{\bigcirc}\ \overline{\bigcirc}$	8
T_1	$\underline{\bigcirc}\ \underline{\bigcirc}\ \overline{\underline{\bigcirc}}\ \overline{\bigcirc}$	$\underline{\bigcirc}\ \overline{\bigcirc}\ \overline{\underline{\bigcirc}}\ \underline{\bigcirc}$	$\overline{\bigcirc}\ \underline{\bigcirc}\ \overline{\underline{\bigcirc}}\ \underline{\bigcirc}$	$\overline{\bigcirc}\ \overline{\bigcirc}\ \overline{\underline{\bigcirc}}\ \overline{\bigcirc}$	8
T_1	$\underline{\bigcirc}\ \overline{\underline{\bigcirc}}\ \overline{\bigcirc}\ \overline{\bigcirc}$	$\overline{\bigcirc}\ \overline{\underline{\bigcirc}}\ \overline{\bigcirc}\ \underline{\bigcirc}$	$\overline{\bigcirc}\ \overline{\underline{\bigcirc}}\ \overline{\bigcirc}\ \underline{\bigcirc}$	$\underline{\bigcirc}\ \overline{\underline{\bigcirc}}\ \underline{\bigcirc}\ \underline{\bigcirc}$	8
T_1	$\underline{\bigcirc}\ \overline{\bigcirc}\ \overline{\bigcirc}\ \overline{\underline{\bigcirc}}$	$\overline{\bigcirc}\ \overline{\bigcirc}\ \underline{\bigcirc}\ \overline{\underline{\bigcirc}}$	$\overline{\bigcirc}\ \underline{\bigcirc}\ \overline{\bigcirc},\overline{\underline{\bigcirc}}$	$\underline{\bigcirc}\ \underline{\bigcirc}\ \underline{\bigcirc}\ \overline{\underline{\bigcirc}}$	8
T_2	$\overline{\underline{\bigcirc}}\ \overline{\underline{\bigcirc}}\langle\underline{\bigcirc}\ \underline{\bigcirc}\rangle$	$\overline{\underline{\bigcirc}}\langle\rangle\overline{\underline{\bigcirc}}\ \overline{\bigcirc}\ \overline{\bigcirc}$	$\underline{\bigcirc}\ \rangle\overline{\underline{\bigcirc}}\ \overline{\underline{\bigcirc}}\langle\underline{\bigcirc}$	$\overline{\bigcirc}\ \overline{\underline{\bigcirc}}\langle\rangle\overline{\underline{\bigcirc}}\ \overline{\bigcirc}$	16
T_2	$\langle\underline{\bigcirc}\ \underline{\bigcirc}\rangle\overline{\underline{\bigcirc}}\ \overline{\underline{\bigcirc}}$	$\overline{\bigcirc}\ \overline{\bigcirc}\ \overline{\underline{\bigcirc}}\langle\rangle\overline{\underline{\bigcirc}}$	$\overline{\underline{\bigcirc}}\langle\underline{\bigcirc}\ \underline{\bigcirc}\rangle\overline{\underline{\bigcirc}}$	$\rangle\overline{\underline{\bigcirc}}\ \overline{\bigcirc}\ \overline{\bigcirc}\ \overline{\underline{\bigcirc}}\langle$	16
T_2	$\overline{\underline{\bigcirc}}\langle\underline{\bigcirc}\rangle\overline{\underline{\bigcirc}}\ \overline{\bigcirc}$	$\overline{\underline{\bigcirc}}\ \overline{\bigcirc}\ \overline{\underline{\bigcirc}}\langle\underline{\bigcirc}\rangle$	$\langle\underline{\bigcirc}\rangle\overline{\underline{\bigcirc}}\ \overline{\bigcirc}\ \overline{\underline{\bigcirc}}$	$\overline{\bigcirc}\ \overline{\underline{\bigcirc}}\langle\underline{\bigcirc}\rangle\overline{\underline{\bigcirc}}$	16
T_3	$\overline{\underline{\bigcirc}}\ \overline{\underline{\bigcirc}}\ \overline{\underline{\bigcirc}}\ \underline{\bigcirc}$	$\overline{\underline{\bigcirc}}\ \overline{\underline{\bigcirc}}\ \overline{\bigcirc}\ \overline{\underline{\bigcirc}}$	$\overline{\underline{\bigcirc}}\ \underline{\bigcirc}\ \overline{\underline{\bigcirc}}\ \overline{\underline{\bigcirc}}$	$\overline{\bigcirc}\ \overline{\underline{\bigcirc}}\ \overline{\underline{\bigcirc}}\ \overline{\underline{\bigcirc}}$	32

The numbers indicated in the last column vary, since the symbol $\overline{\underline{\bigcirc}}$ represents two cases. Intervals $\langle\ \rangle$ of J-tangency are shown only for the T_2-type.

5.1. **Lines on a rational elliptic surface.** Recall, that, since the fibers of f belongs to the anti-canonical divisor class $-K$ of X, the set of lines in X coincide with the set of sections of f. As is also well-known, the lines in X can be distinguished by their homology classes in $H_2(X)$ as follows.

5.1.1. **Proposition.** *Assume that X is a relatively minimal rational elliptic surface with a fixed line $L \subset X$ and the canonical divisor class K. Then:*

(1) *$\langle K, L\rangle^\perp \subset H_2(X)$ is isomorphic to E_8.*

(2) *If f has only 1-nodal singular fibers, then there is a natural 1–1 correspondence between the lines in X and elements of $E_8 = \langle K, L\rangle^\perp$ that associates with each $v \in E_8$ the line which is uniquely determined by its divisor class $L_v = L + \frac{v^2}{2}K + v$.*

(3) *If f has only 1-nodal singular fibers and X is real, then a line L_v is real if and only if $v \in \Lambda = E_8 \cap \ker(1 + \mathrm{conj}_*)$.*

Proof. For items (1)–(2) see [SS], while (3) follows from functoriality of the correspondence in (2). □

Contraction of a line $L \subset X$ gives a del Pezzo surface $Y = X/L$ of degree $K_Y^2 = 1$. The following relation between lines on $Y = X/L$ and lines on X is straightforward from the definition of lines given in Section 1.5.

5.1.2. **Proposition.** *Each of the lines in $Y = X/L$ lifts to one and only one line in X, which establishes a bijection between the set of lines in Y and the set of lines in X disjoint from L. If X and L are real, then this induces a bijection between the set of real lines in Y and the set of real lines in X disjoint from L.* □

Note also that the homomorphism $\phi_* : H_2(X) \to H_2(Y)$ induced by the contraction $\phi : X \to Y = X/L$ establishes an isomorphism between $E_8 = \langle K, L\rangle^\perp$, $K = K_X$, and $E_8 = K_Y^\perp \subset H_2(Y)$. Using this canonical isomorphism, we will omit ϕ_* and ϕ_*^{-1}, as soon as it does not lead to a confusion.

5.2. **Fibers of a real elliptic fibration.** In subsections 5.2 — 5.6 we restrict ourselves with the connected case $X_\mathbb{R} = \mathbb{K}\#p\mathbb{T}^2$, and later on apply the same conventions to the component $\mathbb{K}\#p\mathbb{T}^2$ if $X_\mathbb{R} = \mathbb{K}\#p\mathbb{T}^2 \amalg q\mathbb{S}^2$.

5.2.1. **Lemma.** (1) *The mapping $f_\mathbb{R} : X_\mathbb{R} = \mathbb{K}\#p\mathbb{T}^2 \to \mathbb{P}^1_\mathbb{R}$ has an even number, $2r \geqslant 0$, of critical points and the same number of singular fibers.*

(2) *Non-singular fibers $f_\mathbb{R}^{-1}(x)$, $x \in \mathbb{P}^1_\mathbb{R}$, have either 1 or 2 connected components, and these numbers alternate as x overpass critical values. More precisely, we can cyclically in $\mathbb{P}^1_\mathbb{R}$ enumerate the critical values as $x_1, \dots, x_{2r}$ so that the non-singular fibers $f_\mathbb{R}^{-1}(x)$, have 2 components on intervals $[x_{2i-1}, x_{2i}]$, $1 \leqslant i \leqslant r$, and 1 component on the other intervals between consecutive critical points.*

(3) *If $p = r = 0$, then all fibers are connected.*

Proof. Due to Assumption **A**, the fibration $f : X \to \mathbb{P}^1$ has 12 singular fibers and all the singular fibers are 1-nodal. This implies Claim (1). The number of connected components of $f_\mathbb{R}^{-1}(x)$ is > 0 due to existence of a real section and $\leqslant 2 = \frac{1}{2} b_*(\mathbb{T}^2)$ due to Harnack's inequality. Alternation follows from orientability of a real fiber neighborhood. This implies Claim (2). Claim (3) holds due to connectedness of $X_\mathbb{R}$ and existence of a real section. □

5.2.2. **Lemma.** *Under the same assumptions on $X_\mathbb{R}$ as in Lemma 5.2.1 we have:*

(1) *The complement $X_\mathbb{R} \smallsetminus f_\mathbb{R}^{-1}(x)$ of any connected fiber is a connected orientable surface of genus p with 2 holes.*

(2) *If the critical values $x_1, \dots, x_{2r}$ are enumerated as in Lemma 5.2.1, then there exist precisely p pairs x_{2i-1}, x_{2i} with the Morse indices 1 for each value.*

(3) *For each of the above pairs x_{2i-1}, x_{2i} and every $0 < \varepsilon \ll 1$, the part $f_\mathbb{R}^{-1}[x_{2i-1} - \varepsilon, x_{2i} + \varepsilon]$ of $X_\mathbb{R}$ is a torus with two holes bounded by circles $f_\mathbb{R}^{-1}(x_{2i-1} - \varepsilon)$ and $f_\mathbb{R}^{-1}(x_{2i} + \varepsilon)$.*

Proof. Connectedness in (1) is due to connectedness of $X_\mathbb{R}$ and existence of a section, while orientability is due to that $w_1(X_\mathbb{R})$ is dual to a fiber.

It follows from Lemma 5.2.1(1-2) that a fragment $f_\mathbb{R}^{-1}[x_{2i-1} - \varepsilon, x_{2i} + \varepsilon] \subset X_\mathbb{R}$ is a torus with 2 holes if both x_{2i-1} and x_{2i} have index 1. Moreover, otherwise the indices differ by 1 and form a removable pair of critical points. This implies (2) and (3). □

5.3. **A system of cuts.** Let us denote by N_j, $j = 1, \dots k$, the tori with holes from Lemma 5.2.2(3), consecutively numerated, and denote by $I_{N_j} = [y_j, z_j] \subset \mathbb{P}^1_\mathbb{R}$ the interval for which $N_j = f_\mathbb{R}^{-1}(I_{N_j})$. Denote also by $f_{N_j} : N_j \to I_j$ the restriction of $f_\mathbb{R}$ and introduce notation $c_i = f_N^{-1}(y_j)$ and $d_i = f_N^{-1}(z_j)$ for the boundary components of N_j.

Next, we cut $X_{\mathbb{R}}$ along a 1-component fiber $\mathcal{F}^{\infty}_{\mathbb{R}}$ (which exists by Lemma 5.2.1). In the case $k>0$, we choose a particular fiber $\mathcal{F}^{\infty}_{\mathbb{R}} = f_{\mathbb{R}}^{-1}(y_1)$.

After cutting $X_{\mathbb{R}}$ along $\mathcal{F}^{\infty}_{\mathbb{R}}$ we obtain a compact surface N (compactification of $X_{\mathbb{R}} \smallsetminus \mathcal{F}^{\infty}$) and its projection to the interval obtained by cutting $\mathbb{P}^1_{\mathbb{R}}$ will be denoted $f_N : N \to I_N$. By Lemma 5.2.2(1), the surface N is connected and orientable, and we fix any of its two orientations. Its boundary ∂N consists of two copies of $\mathcal{F}^{\infty}_{\mathbb{R}}$, denoted $\partial_- N$ and $\partial_+ N$, which are the fibers $\partial_- N = f_{\mathbb{R}}^{-1}(y_1)$ and $\partial_+ N = f_{\mathbb{R}}^{-1}(y_{p+1})$ over the endpoints of $I_N = [y_1, y_{p+1}]$.

The fragment of N between N_j and N_{j+1} is denoted by A_j, $j = 1, \dots, p-1$, and the fragment after N_p by A_p. It follows that A_j is diffeomorphic to $S^1 \times [0,1]$ for all $j = 1, \dots p$, and it is bounded by the fibers d_j and c_{j+1}, $j = 1, \dots, k$, where $c_{p+1} = \partial_+ N$. By $f_{A_j} : A_j \to I_{A_j}$ with $I_{A_j} = [z_j, y_{j+1}]$ will be denoted the restriction of f_N.

FIG. 13. A system of cuts: N_i, A_i, c_i, d_i, a_i, b_i

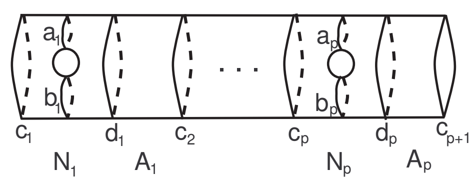

In each N_i we choose a non-singular fiber in between the singular ones and denote its two components by a_i and b_i. By cutting of N_i along the fiber $a_i \cup b_i$ we obtain a pair-of-pants decomposition of N_i (where *a pair-of-pants* is an elementary Morse cobordism with one critical point of index 1).

The orientation of N being fixed determines uniquely the Dehn twists $t_x \in \mathrm{Mod}(N_i) \subset \mathrm{Mod}(N)$ about $x = c_i, d_i, a_i, b_i$ (for injectivity of $\mathrm{Mod}(N_i) \to \mathrm{Mod}(N)$ see, for example, [FM, Theorem 3.18]). Here, t_{c_i} and t_{d_i} are the *boundary Dehn twists*, that is the Dehn twists about curves obtained by a shift of c_i, d_i inside N_i.

5.3.1. **Lemma.** *For $p \geqslant 0$, the Dehn twists $t_{c_i}, t_{a_i}, t_{b_i} \in \mathrm{Mod}(N)$, $1 \leqslant i \leqslant p$ and $t_{c_{p+1}}$ form a basis of a free abelian subgroup of rank $3p+1$ in $\mathrm{Mod}(N)$. The image of this group in $\mathrm{Mod}(X_{\mathbb{R}})$ is obtained by adding one relation $t_{c_1} t_{c_{p+1}} = 1$. In particular, for $k > 0$ this image is a free abelian group of rank $3p$, while for $p = 0$ this image is $\mathbb{Z}/2$ generated by the image of t_{c_1}.*

Proof. This is a straightforward consequence of [FM, Lemma 3.17] in what concerns $\mathrm{Mod}(N)$ and [S, Theorem 3.6] in what concerns $\mathrm{Mod}(X_{\mathbb{R}})$. □

5.4. **Fiberwise mapping class groups.** If $F \to I_F$ is a fragment of $f : X_{\mathbb{R}} \to \mathbb{P}^1_{\mathbb{R}}$ fibered over some projective line segment $I_F = [x_-, x_+] \subset I_N$ (like N_i, A_i, and N itself), we denote by $\widetilde{G}(F)$ the group formed by fiberwise diffeomorphisms $F \to F$ that act as a group shift in each fiber of $F \to I_F$. The subgroup $G(F) \subset \widetilde{G}(F)$ is formed by the diffeomorphisms whose restriction to ∂F is the identity. The image of the natural projection, $\pi_0(G(F)) \to \mathrm{Mod}(F)$, will be denoted by $\mathrm{Mod}^s(F)$ and the image in $\mathrm{Mod}^s(F)$ of elements $g \in G(F)$ by $[g] \in \mathrm{Mod}^s(F)$.

We include the whole fibration $f : X_{\mathbb{R}} \to \mathbb{P}^1_{\mathbb{R}}$ in the list of fragments, and apply to it the same definitions and notation as above (with replacement F by $X_{\mathbb{R}}$).

5.4.1. **Proposition.** *For any fragment F, the groups $\widetilde{G}(F), G(F)$, and $\mathrm{Mod}^s(F)$ are abelian.*

Proof. It is an immediate consequence of the commutativity of group shifts. $\square$

5.4.2. **Lemma.** *For $i = 1, \dots, p$, $\mathrm{Mod}^s(A_i) \cong \mathbb{Z}$ with a generator $t_{c_{i+1}}$.*

Proof. It is straightforward from $\mathrm{Mod}(A_i) \cong \mathrm{Mod}(S^1 \times [0,1]) = \mathbb{Z}$ and realizability of boundary Dehn twists $t_{c_{i+1}}$ by fiberwise group-shift diffeomorphisms identical on ∂A_i. $\square$

Given two sections $\lambda_i : I \to F$, $i = 1, 2$, let $\langle \lambda_2 - \lambda_1 \rangle \in \widetilde{G}(F)$ denote the uniquely defined element of $\widetilde{G}(F)$ that sends λ_1 to λ_2. If we assume in addition that λ_1 coincides with λ_2 at the endpoints of I, then $\langle \lambda_2 - \lambda_1 \rangle \in G(F)$.

A smooth section $\lambda_0 : I_F \to F$ being fixed, we define $\mathrm{Sec}(F))$ to be the space of smooth sections $\lambda : I \to F$ satisfying the boundary condition $\lambda(x_\pm) = \lambda_0(x_\pm)$. By $\mathrm{Sec}(X_\mathbb{R})$ we denote the space of all smooth sections $\lambda : \mathbb{P}^1_\mathbb{R} \to X_\mathbb{R}$.

5.4.3. **Lemma.** *For any fixed smooth section $\lambda_0 : I_F \to F$, the mapping $\mathrm{Sec}(F) \to G(F)$ assigning to $\lambda \in \mathrm{Sec}(F)$ the diffeomorphism $\langle \lambda - \lambda_0 \rangle \in G(F)$, is a homeomorphism with respect to the natural topology. In particular, the set of isotopy classes of sections with the boundary condition $\lambda(x_\pm) = \lambda_0(x_\pm)$ (i.e., the set of path-connected components in $\mathrm{Sec}(F)$) as a group is identified with $\pi_0(G(F))$ and $\mathrm{Mod}^s(F)$. Similarly, for a fixed smooth section $\lambda_0 : \mathbb{P}^1_\mathbb{R} \to X_\mathbb{R}$, the mapping $\lambda \mapsto \langle \lambda - \lambda_0 \rangle$ yields a group isomorphism between the groups $\mathrm{Sec}(X_\mathbb{R}) = \pi_0(G(X_\mathbb{R}))$ and $\mathrm{Mod}^s(X_\mathbb{R})$.* $\square$

5.4.4. **Lemma.** *Assume that $F \to I$ is a connected fragment, and one of its boundary fibers, $\partial_- F$ or $\partial_+ F$, has two connected components, a and b. Then a diffeomorphism $t_a^m t_b^n$, $m, n \in \mathbb{Z}$, belongs to $\mathrm{Mod}^s(F)$ if and only if $m = n$.*

Proof. Without loss of generality we may suppose that $\partial_+ F = a \cup b$. Since F is connected, there exist sections λ_0 and λ_1 of F intersecting the fiber $\partial_+ F$ at some points of a and b respectively, and the fiber $\partial_- F$ both at the same point. Then the diffeomorphism $h = \langle \lambda_1 - \lambda_0 \rangle \in \widetilde{G}$ interchanges a and b and preserves (any chosen) orientation of F.

If $g = t_a^m t_b^n$ belongs to $\mathrm{Mod}^s(F)$, then, by Lemma 5.4.3, there exists a section λ_2 such that $g = \langle \lambda_2 - \lambda_0 \rangle$, while due to Lemma 5.4.1 we have $h^{-1} g h = g$. On the other hand, $h^{-1} g h = t_a^n t_b^m$, since a and b are permuted and orientation of F is preserved. This implies $m = n$.

To complete the proof, it remains to notice that, for λ_0, λ_2 shown on Fig. 14, $g = \langle \lambda_2 - \lambda_0 \rangle$ is equal either to $t_a t_b$ or $t_a t_b^{-1}$, while the latter option is excluded by the previous argument. $\square$

FIG. 14. Pair of sections representing $t_a t_b$.

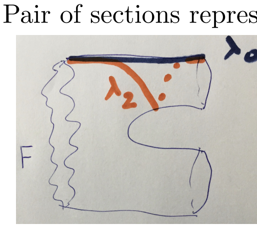

By a *pair-of-pants fragment* $f_F : F \to I_F$ we mean a fragment diffeomorphic to a pair-of-pants for which f_F is a Morse function with only one critical point.

5.4.5. **Lemma.** $\mathrm{Mod}^s(F) = \langle t_a t_b, t_c \rangle \cong \mathbb{Z}^2$ *if F is a pair-of-pants fragment with c and $a \cup b$ as boundary fibers.*

Proof. As is well-known (cf., Lemma 5.3.1) $\mathrm{Mod}(F) = \langle t_a, t_b, t_c \rangle \cong \mathbb{Z}^3$, where each of the boundary twists involved can be realised by a fiber-preserving map. Moreover, in $\mathrm{Mod}^s(F)$, the Dehn twists t_a and t_b can only be applied simultaneously, by Lemma 5.4.4, and any such a simultaneous twist can be realized by an element in $\mathrm{Mod}^s(F)$. □

5.5. **Exact sequence for adjacent fibration fragments.** We say that fragments $F_1 \to I_1$ and $F_2 \to I_2$ are *adjacent* if the intervals I_1 and I_2 intersect at one point, so that $F = F_1 \cup F_2$ is fibered over an interval $I = I_1 \cup I_2$.

5.5.1. **Lemma.** *For the union of adjacent fragments $F = F_1 \cup F_2$ intersecting along a connected curve $\alpha = F_1 \cap F_2$, we have the exact sequence*

$$0 \to \mathbb{Z} \to \mathrm{Mod}^s(F_1) \oplus \mathrm{Mod}^s(F_2) \xrightarrow{\theta} \mathrm{Mod}^s(F) \to 0$$

with the kernel $\mathbb{Z}$ generated by $t_{\alpha_1} \oplus t_{\alpha_2}^{-1}$, where α_i is a copy of α in F_i.

In the case of 2-component intersection $\alpha \cup \beta = F_1 \cap F_2$ of connected fragments F_1 and F_2 we have the exact sequence

$$0 \to \mathbb{Z} \to \mathrm{Mod}^s(F_1) \oplus \mathrm{Mod}^s(F_2) \xrightarrow{\theta} \mathrm{Mod}^s(F) \to \mathbb{Z}/2 \to 0,$$

where the kernel $\mathbb{Z}$ is generated by $s_1 \oplus s_2^{-1}$, $s_i = t_{\alpha_i} t_{\beta_i}$ (α_i, β_i being copies of α, β in F_i), and permutation of the components α and β by elements of $\mathrm{Mod}^s(F)$ defines the projection to $\mathbb{Z}/2 = \mathrm{Sym}(\alpha, \beta)$.

Proof. We prove the claim in the case of 2-component intersection (in the case of connected $F_1 \cap F_2$ the proof is similar and simpler).

Connectedness of F_1 and F_2 imples existence of sections λ_0 and λ_1 of F that intersect a and b respectively. Then $\langle \lambda_1 - \lambda_0 \rangle \in \mathrm{Mod}^s(F)$ permutes a and b, which gives surjectivity of $\mathrm{Mod}^s(F) \to \mathbb{Z}/2$.

For proving the exactness at $\mathrm{Mod}^s(F)$, it is sufficient to notice, first, that $Im(\theta)$ preserves the components α and β invariant, and second, that any diffeomorphism $g \in G(F)$ preserving α and β invariant can be made identical on these components by twisting via an isotopy in $G(F)$.

On the other hand, $\ker \theta \subset \mathrm{Ker}\{\mathrm{Mod}(F_1) \oplus \mathrm{Mod}(F_2) \to \mathrm{Mod}(F)\} = \mathbb{Z}^2 = \langle t_{\alpha_1} \oplus t_{\alpha_2}^{-1}, t_{\beta_1} \oplus t_{\beta_2}^{-1} \rangle$ (see, e.g., [FM, Theorem 3.18]) So, if $g_1 \oplus g_2 \in \mathrm{Ker}\, \theta$, then $g_i = t_{\alpha_i}^{k_i} t_{\beta_i}^{l_i}$, $i = 1, 2$, where $k_1 + k_2 = l_1 + l_2 = 0$, while, by Lemma 5.4.4, $k_i = l_i$. Also by Lemma 5.4.4 the elements $s_1 \oplus s_2^{-1} \in \mathrm{Mod}(F_1) \oplus \mathrm{Mod}(F_2)$ do belong to $\mathrm{Mod}^s(F_1) \oplus \mathrm{Mod}^s(F_2)$. □

5.6. **The elements $\Delta_i \in \mathrm{Mod}^s(N_i)$.** Pick a section $\lambda_0 : I_{N_i} \to N_i$ of $f_{N_i} : N_i \to I_{N_i} = [y_i, z_i]$ that forms a part of a fixed real line $L \subset X$ and equip the fibers of f_{N_i} with a group structure for which λ_0 is the null-section. With respect to this group structure the non-zero elements of order 2 form an oval and a segment, which represents a second section, $\lambda' : I_{N_i} \to N_i$, disjoint with λ_0.

Define another smooth section $\lambda : I_{N_i} \to N_i$ representing a *half of a Dehn twist about a fiber* (in accord with a fixed orientation of N_i) above each of two small

small intervals $[y_i, y_i + \varepsilon]$, $[z_i - \varepsilon, z_i]$ and coinciding with λ_0 (resp. λ') on ∂I_{N_I} (resp. $[y_i + \varepsilon, z_i - \varepsilon]$), see Fig. 15).

We fix also a pair-of pants decomposition of N_i along a 2-component fiber $a_i \cup b_i$ as in Section 5.3.

Fig. 15. Section λ representing $\Delta_i \in \mathrm{Mod}^s(N_i)$

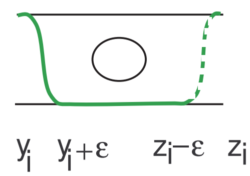

The upper segment depicts the section λ_0. The elements of order 2 form an oval and a segment at the bottom.

5.6.1. **Proposition.** *The section λ is well-defined up to isotopy fixed at the boundary, the corresponding to it element $\Delta_i = \langle \lambda - \lambda_0 \rangle \in \mathrm{Mod}^s(N_i)$ satisfies the following properties:*

(1) $t_{a_i}\Delta_i = \Delta_i t_{b_i}$, $t_{b_i}\Delta_i = \Delta_i t_{a_i}$,
(2) $\Delta_i^2 = t_{c_i} t_{c_{i+1}}$,

and it is the only element of $\mathrm{Mod}^s(N_i)$ satisfying these properties.

Proof. Note that for any element $\Delta \in \mathrm{Mod}^s(N_i)$ the relations (1) are equivalent to that Δ interchanges the curves a_i and b_i, which is obviously true for $\Delta = \Delta_i$. It follows also from the definition of λ that Δ_i^2 performs the Dehn twists t_{c_i} and t_{d_i} (*cf.* Fig. 13) on the intervals $[y_i, y_i + \varepsilon]$ and $[z_i - \varepsilon, z_i]$ respectively and the identity in $[y_i + \varepsilon, z_i - \varepsilon]$, so, (2) is also satisfied.

To show the required uniqueness of Δ_i, suppose that $\Delta \in \mathrm{Mod}^s(N_i)$ is another element satisfying (1) and (2). Then, the property (1) implies that Δ_i and Δ are both cross-sections of the epimomorphism $\mathrm{Mod}^s(N_i) \to \mathbb{Z}/2$ of Lemma 5.5.1. Thereon, by Lemma 5.5.1, we have $\Delta_i\Delta^{-1} = \theta(\delta_0 \oplus \delta_1)$, $\delta_j \in \mathrm{Mod}^s(F_j)$, where $N_i = F_0 \cup F_1$ is the pair-of-pants decomposition obtained by cutting N_i along the fiber $a_i \cup b_i$. Since $\delta_0 = s_i^{k_0} t_{c_i}^{m_0}$ and $\delta_1 = s_i^{k_1} t_{c_{i+1}}^{m_1}$ the relations (2) for Δ_i and Δ give

$$1 = \Delta_i^2 (\Delta^{-1})^2 = \delta_0^2 \delta_1^2 = s_i^{2k_0 + 2k_1} t_{c_i}^{2m_0} t_{c_{i+1}}^{2m_1}.$$

According to Lemma 5.4.5, this implies $m_0 = m_1 = k_0 + k_1 = 0$, which in its turns gives $\Delta_i \Delta^{-1} = 1$. □

5.6.2. **Corollary.** $\mathrm{Mod}^s(N_i) \cong \mathbb{Z}^3$ *with a basis* t_{c_i}, $s_i = t_{a_i} t_{b_i}$ *and* Δ_i.

Proof. Immediate consequence of Proposition 5.4.5 and Lemmas 5.5.1, 5.6.1. □

5.7. Computation of the group $\mathrm{Mod}^s(X_{\mathbb{R}})$.

5.7.1. **Proposition.** *If* $X_{\mathbb{R}} \cong \mathbb{K} \# p\mathbb{T}^2 \amalg q\mathbb{S}^2$, *then* $\mathrm{Mod}^s(X_{\mathbb{R}}) = \mathbb{Z}^{2p} + \mathbb{Z}/2$ *is generated by the elements* t_{c_1}, s_i, Δ_i, $1 \leqslant i \leqslant p$ *with the only relation*

$$t_{c_1}^{\epsilon} \prod_{1 \leqslant 2i+1 \leqslant p} \Delta_{2i+1}^2 = \prod_{1 \leqslant 2i \leqslant p} \Delta_{2i}^2 \qquad \text{where} \quad \epsilon = 1 + (-1)^p.$$

Proof. After we skip the eventual spherical components and cut the component $\mathbb{K}\#p\mathbb{T}^2$ in the same way as in Sec. 5.3, we obtain a surface N. From Lemma 5.5.1 and Corollary 5.6.2 it follows that $\mathrm{Mod}^s(N) \cong \mathbb{Z}^{2p+1}$ with a basis formed by t_{c_1} and s_i, Δ_i, $1 \leqslant i \leqslant p$. According to [S, Theorem 3.6] the group $\mathrm{Mod}^s(X_\mathbb{R})$ is obtained from $\mathrm{Mod}^s(N)$ by adding the relation

$$t_{c_{p+1}} = t_{c_1}^{-1}. \tag{5.7.1}$$

Finally, the relation required follows from (5.7.1) and Proposition 5.6.1(2).

□

In the remaining case, $X_\mathbb{R} = \mathbb{K} \amalg \mathbb{K}$, our elliptic fibration $f_\mathbb{R} : X_\mathbb{R} \to \mathbb{P}^1_\mathbb{R}$ cannot have critical points, so, it is a nonsingular fibration with a fiber $S^1 \amalg S^1$. The restriction of $f_\mathbb{R}$ to each copy of $\mathbb{K}$ admits a pair of disjoint sections, which we denote λ^1_1, λ^1_2 for one copy and λ^2_1, λ^2_2 for another.

FIG. 16

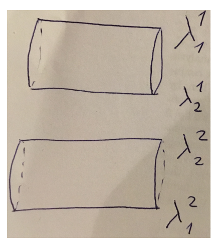

5.7.2. **Proposition.** *If* $X_\mathbb{R} = \mathbb{K} \amalg \mathbb{K}$, *then* $\mathrm{Mod}^s(X_\mathbb{R})$ *is isomorphic to* $\mathbb{Z}/2 \oplus \mathbb{Z}/2$ *and formed by the elements* $\{\langle \lambda^j_i - \lambda^1_1 \rangle\}_{i,j \in \{1,2\}}$.

Proof. Let us choose as λ^1_1 one of real lines and as $\lambda^1_2, \lambda^2_1, \lambda^2_2$ the 3 sections that form together with λ^1_1 the fixed point set of the fiberwise hyperelliptic involution determined by the choice of λ^1_1 as zero (see Fig. 16). They do form 4 disjoint sections, since in each fiber the fixed points are the points of period 2, and since the monodromy acts identically on the conj-invariant part of the period lattice of a fiber and as multiplication by -1 on its anti-invariant part, which provides pairwise distinction between the points of period 2. Under fiberwise addition these 4 sections form a group $\mathbb{Z}/2 \oplus \mathbb{Z}/2$. Thus, there remain to notice that any section of $X_\mathbb{R}$ is isotopic to one of the four λ^j_i, and to apply Proposition 5.4.3. □

5.8. **Elements of order 2 in the group $\mathrm{Mod}^s(X_\mathbb{R})$.** If $X_\mathbb{R} \cong \mathbb{K}\#p\mathbb{T}^2 \amalg q\mathbb{S}^2$, then to describe the unique element of order 2 in $\mathrm{Mod}^s(X_\mathbb{R})$ (see Proposition 5.7) we proceed as follows. For that, we consider a smooth section $\lambda_N : I_N \to N$ that is constantly an element of order 2 on the whole interval I_N except two small subintervals near the endpoints, where λ_N represents a half of a Dehn twist in positive direction on each of these two subintervals (see Fig. 17). Such a section self-matches at the boundary and, thus, factorizes to a smooth section $\lambda : \mathbb{P}^1_\mathbb{R} \to X_\mathbb{R}$ equal on $\mathbb{P}^1 \setminus I_N$ to the same element of order 2 as on ∂I_N. Due to relation (5.7.1), the element $\delta \in \mathrm{Mod}^s(X_\mathbb{R})$ defined by λ is of order 2.

FIG. 17. The section λ defining the element δ of order 2

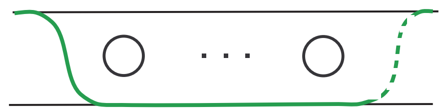

5.9. **Mordel-Weil group.** Recall that the Mordel-Weil group of an elliptic surface $f : X \to \mathbb{P}^1$ can be defined as a subgroup $\mathrm{MW}(X)$ of the automorphism group $\mathrm{Aut}(X)$ formed by those automorphisms that preserve the fibers of f and act as a translation in each nonsingular fiber. The Mordel-Weil group acts freely and transitively on the set of sections, so that the latter becomes a torsor over $\mathrm{MW}(X)$. This definition is applied to surfaces over any field. We keep notation $\mathrm{MW}(X)$ for the Mordel-Weil group of elliptic surfaces X defined over $\mathbb{C}$, while when X is a real elliptic surface, we notate by $\mathrm{MW}_{\mathbb{R}}(X)$ the subgroup of $\mathrm{MW}(X)$ formed by the elements $g \in \mathrm{MW}(X)$ preserving the real structure. In the latter case, it is the set of real lines in X that becomes a torsor over $\mathrm{MW}_{\mathbb{R}}(X)$.

Thus, if we fix a line $L \subset X$ (respectively, a real line $L \subset X$) then we can interpret $\mathrm{MW}(X)$ (respectively, $\mathrm{MW}_{\mathbb{R}}(X)$) as a group structure on the set of lines in X (respectively, the set of real lines in X) by associating with each line $L' \subset X$ (respectively, each real line $L' \subset X$) an element of $\mathrm{MW}(X)$ (respectively, of $\mathrm{MW}_{\mathbb{R}}(X)$) that transforms L into L', and which we denote by $\langle L' - L\rangle$.

Furthermore, by passing from lines to their homology classes and applying the natural correspondence $v \in E_8 = \langle K, L\rangle^\perp \mapsto L_v$ described in Proposition 5.1.1, one gets the next, well-known, result (see [SS]).

5.9.1. **Proposition.** *Assume that X is a rational relatively minimal elliptic surface with a fixed line $L \subset X$ and that f has only 1-nodal singular fibers. Then the compositions*

$$v \in E_8 \mapsto L_v \mapsto \langle L_v - L\rangle \in \mathrm{MW}(X)$$
$$v \in E_8 \cap \ker(1 + \mathrm{conj}_*) \mapsto L_v \mapsto \langle L_v - L\rangle \in \mathrm{MW}_{\mathbb{R}}(X) \quad \textit{if} \quad X \quad \textit{is real}$$

are group isomorphisms.

In particular, $\mathrm{MW}(X)$ *is a free abelian group naturally isomorphic to* E_8*, while* $\mathrm{MW}_{\mathbb{R}}(X)$ *is a free abelian group naturally isomorphic to* $\Lambda = E_8 \cap \ker(1+\mathrm{conj}_*)$. □

By definition each element of $\mathrm{MW}_{\mathbb{R}}(X)$ preserves the real fibers and act on them by translation. Thus, considering its restriction to $X_{\mathbb{R}}$ we get a well defined, natural, homomorphism to $\mathrm{Mod}^s(X)$, which we denote by $\Phi : \mathrm{MW}_{\mathbb{R}}(X) \to \mathrm{Mod}^s(X)$.

6. Proof of Theorem 1.3.3

Let us fix a real line $L \subset X$ and set $g_v = \Phi\langle L_v - L\rangle$, for every $v \in \Lambda = E_8 \cap \ker(1+\mathrm{conj}_*)$ (see Proposition 5.1.1). Recall our convention to use the canonical identification of $\Lambda \subset H_2(X)$ with the isomorphic to it $\Lambda \subset H_2(Y)$ (see Section 5.1) as identity, and, in particular, to treat (when it does not lead to a confusion) the oval- and bridge classes of Y as elements of both $\Lambda \subset H_2(Y)$ and $\Lambda \subset H_2(X)$.

6.1. **Preparation.**

6.1.1. **Proposition.** *The sections λ_0, λ on the fragments $F \to I_F$ of $f : X_{\mathbb{R}} \to \mathbb{P}^1_{\mathbb{R}}$ which are depicted on Fig. 18 represent the elements $g = \langle \lambda - \lambda_0 \rangle \in \mathrm{Mod}^s(F)$ indicated under the corresponding fragment.*

Fig. 18. Examples of [section/$\mathrm{Mod}^s(F)$-element] correspondence

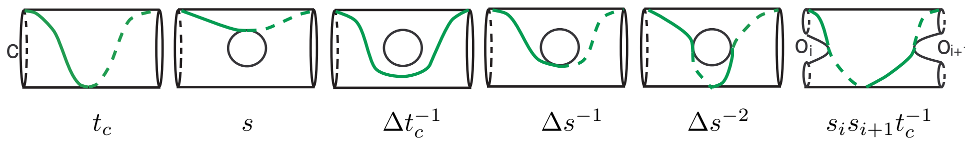

The upper segment depicts the section λ_0 while λ is drawn in green. By convention, the depicted fragments are equipped with an orientation induced from a fixed orientation of N and, on drawings, this is the right-hand orientation of the front side.

Proof. For each of the elements $g \in \mathrm{Mod}^s(F)$ pointed in the bottom of Fig. 18, the indicated shape of $g(\lambda_0)$ follows directly from the definitions of s, Δ, and t_c. Reciprocally, the isotopy class of $g(\lambda_0)$ determines g (see Lemma 5.4.3). □

6.1.2. **Lemma.** *If $X_{\mathbb{R}} \cong \mathbb{K}\#p\mathbb{T}^2 \amalg q\mathbb{S}^2$, the group $\mathrm{Mod}^s(X_{\mathbb{R}})$ contains the following elements g_e:*

1. *$g_e = \Delta_i s_i^{-2}$ for $e = O_i$, $i = 1, \dots p$.*
2. *$g_e = s_i s_{i+1} t_{c_{i+1}}^{-1}$ for $e = B_{i\,i+1}$, $i = 1, 2, p-1$.*
3. *$g_e = s_i$ for bridge-classes $e = B_i$ between the oval O_i and the J-component. Namely, it holds for $i = 1, 3$ if $p = 4$, $q = 0$ and for $i = 1, \dots, p$ if $p < 4$.*
4. *$g_e = t_{c_1}$ if $p = q = 0$ and e is any root of $\Lambda = 4A_1$.*

Proof. If $p = q = 0$, then $\mathrm{Mod}^s(X_{\mathbb{R}}) = \mathbb{Z}/2$, so to prove claim (4) it is sufficient to show that $g_e \neq 0$ for any root of $\Lambda = 4A_1$. In its turn, to show the non triviality of g_e it is sufficient to check that $L_{e\mathbb{R}}$ is not isotopic to $L_{\mathbb{R}}$ on $X_{\mathbb{R}}$, but the latter follows, for example, from Table 6 according to which, for any root e of $\Lambda = 4A_1$, the line L_e is a pull-back of a positive real tritangent on the del Pezzo surface obtained by contracting L_0.

Up to change of e by $-e$ (equivalently, up to replacement of g_e by g_e^{-1}), all the other three relations follow from Proposition 3.3.1 and the correspondence between sections and elements of $\mathrm{Mod}^s(F)$ described in Proposition 6.1.1 (see Fig.18). For each of these relations, correctness of the sign indicated in the statement is confirmed by the coincidence of the sign of $L_e \cdot O_i = -e \cdot O_i$ and the sign given by Corollary 2.8.2 according to that position of the line which corresponds to the element of $\mathrm{Mod}^s(F)$ indicated in the right-hand of the relation (and shown in Fig.18). □

6.1.3. **Lemma.** *Let $X_{\mathbb{R}} \cong \mathbb{K} \amalg \mathbb{K}$, and let $\{B_1, B_2, B_3, B_4\}$ be the bridge classes described in Lemma 4.3.1. Then, $\mathrm{Mod}^s(X_{\mathbb{R}})$ contains the following elements g_e:*

1. *g_e for each $e \in \{B_1, B_2, B_3, B_4\}$. These elements preserve invariant each of the two components of $X_{\mathbb{R}}$.*
2. *g_e with $e = -\frac{1}{2}(B_1 + B_2 + B_3 + B_4)$. This element interchanges the two components of $X_{\mathbb{R}}$.*

Proof. For $e, e' \in \{B_1, B_2, B_3, B_4\}$, the intersection number $L_e \cdot e' = -e \cdot e'$ is even, and therefore $L_{e\mathbb{R}}$ does not intersect the real loci of these four bridges. Thus,

$L_{e\mathbb{R}} = g_e(L_\mathbb{R})$ belongs to the same component of $X_\mathbb{R}$ as $L_\mathbb{R}$ and thus, g_e does not interchange the components of $X_\mathbb{R}$.

For $e = -\frac{1}{2}(B_1 + B_2 + B_3 + B_4)$ we have $L_e \cdot B_i = -e \cdot B_i = -1$ (for each $i = 1, \dots, 4$) which implies that $L_{e\mathbb{R}} = g_e(L_\mathbb{R})$ intersects the real locus of B_i and, thus, $L_{e\mathbb{R}}$ and $L_\mathbb{R}$ belong to different components of $X_\mathbb{R}$. □

6.2. **Case-by-case proof of Theorem 1.3.3.** Below, for any $h \in \mathrm{Mod}^s(X_\mathbb{R})$ we denote by $[h] \in \mathrm{Mod}^s(X_\mathbb{R})/\Phi(\mathrm{MW}_\mathbb{R})$ its coset.

6.2.1. **Proposition.** *If $X_\mathbb{R} = \mathbb{K}\#4\mathbb{T}^2$, then:*

(1) $\operatorname{Ker}\Phi = 0$ *and* $\operatorname{Im}\Phi \cong \mathbb{Z}^8$ *has index 2 in* $\mathrm{Mod}^s(X_\mathbb{R}) \cong \mathbb{Z}^8 \oplus \mathbb{Z}/2$.
(2) *The elements* $s_1, s_3, s_2^2, s_4^2, \Delta_i$, $i \in \{1, \dots, 4\}$, *belong to the group* $\operatorname{Im}\Phi$ *and generate it.*
(3) *The quotient* $\mathrm{Mod}^s(X_\mathbb{R})/\operatorname{Im}\Phi = \mathbb{Z}/2$ *is generated by the classes* $[s_2] = [s_4] = [t_{c_i}]$.

Proof. The relations (1) of Lemma 6.1.2 give $[\Delta_i] = [s_i]^2$. Relation (3) gives $[s_3] = 1$ and hence $[\Delta_3] = 1$. The relations (2) for $i = 1, 2, 3$ imply $[s_1][s_2] = [t_{c_2}]$, $[s_2] = [t_{c_3}]$, and $[s_4] = [t_{c_4}]$, which together with $[t_{c_i}][t_{c_{i+1}}] = [\Delta_i]^2$ (see Lemma 5.6.1) gives $[s_1][s_2]^2 = [t_{c_2}t_{c_3}] = [\Delta_2]^2 = [s_2]^4$, and thus, $[s_1] = [s_2]^2$. Similarly, $[s_2][s_4] = [t_{c_3}t_{c_4}] = [\Delta_3]^2 = 1$, $[t_{c_1}][s_1][s_2] = [t_{c_1}t_{c_2}] = [\Delta_1^2] = [s_1]^4$, and hence $[t_{c_1}] = [s_2]^5$.

In accordance with Proposition 5.7.1,this implies that $\mathrm{Mod}^s(X_\mathbb{R})/\Phi(\mathrm{MW}_\mathbb{R})$ is generated by $[s_2]$. Moreover, $[s_4]^4 = [\Delta_4]^2 = [t_{c_4}][t_{c_5}] = [s_4][t_{c_1}]^{-1} = [s_4][s_2]^{-5}$ implies that $[s_2]^{-5} = [s_4]^3 = [s_2]^{-3}$, and hence $[s_2]^2 = 1$.

Since $\mathrm{Mod}^s(X_\mathbb{R}) = \mathbb{Z}^8 + \mathbb{Z}/2$ requires > 8 generators contrary to $\mathrm{MW}_\mathbb{R} = \mathbb{Z}^8$, we conclude that $\mathrm{Mod}^s(X_\mathbb{R}) \neq \Phi(\mathrm{MW}_\mathbb{R})$ and, thus, due to above calculation, $\Phi(\mathrm{MW}_\mathbb{R})$ has index 2 in $\mathrm{Mod}^s(X_\mathbb{R})$. It then implies also that $[s_2] = [s_4]$ is a generator of $\mathrm{Mod}^s(X_\mathbb{R})/\Phi(\mathrm{MW}_\mathbb{R})$ and that $\operatorname{Ker}\Phi = 0$. □

6.2.2. **Proposition.** *If $X_\mathbb{R} = \mathbb{K}\#p\mathbb{T}^2$ with $0 \leqslant p \leqslant 3$, then $\Phi(\mathrm{MW}_\mathbb{R}) = \mathrm{Mod}^s(X_\mathbb{R})$ and $\operatorname{Ker}\Phi$ is isomorphic to $\mathbb{Z}^{4-p}$.*

Proof. Under the assumption $1 \leqslant p \leqslant 3$, the bridge classes B_i exist for every $i = 1, \dots, p$, see Figure 4. Applying Lemma 6.1.2 to g_e with $e = O_i$ and $e = B_i$, we get relations $[s_i] = 1$ and $[\Delta_i] = 1$ for every $i = 1, \dots, p$ (like in the case $p = 4$ for $i = 3$).

If $p = 2, 3$, we apply Lemma 6.1.2 to g_e with $e = B_{12}$ and get $[t_{c_2}] = [s_1][s_2] = 1$, which implies $[t_{c_1}] = [\Delta_1]^2[t_{c_2}]^{-1} = 1$. If $p = 1$, then we deduce $[t_{c_1}] = 1$ from $g_e = t_{c_1}$ for $e = B_{11}$ (see, for example, Table 6). If $p = 0$, then we deduce $[t_{c_1}] = 1$ from $g_e = t_{c_1}$ for any of the roots $e \in \Lambda = 4A_1$ (see Lemma 6.1.2).

According to Proposition 5.7.1 the above computation shows surjectivity of Φ. The latter implies $\operatorname{Ker}\Phi \cong \mathbb{Z}^{4-p}$, since $\mathrm{MW}_\mathbb{R}$ is a free abelian group of rank $4 + p$, while $\mathrm{Mod}^s(X_\mathbb{R}) = \mathbb{Z}^{2p} + \mathbb{Z}/2$. □

6.2.3. **Proposition.** *If $X_\mathbb{R} = \mathbb{K}\#\mathbb{T}^2 \amalg \mathbb{S}^2$, then:*

(1) $\Phi(MW_\mathbb{R})$ *is isomorphic to* $\mathbb{Z} + \mathbb{Z}/2$ *and generated by* s_1 *and* Δ_1, *while* $\mathrm{Mod}^s(X_\mathbb{R})/\Phi(\mathrm{MW}_\mathbb{R}) = \mathbb{Z}$ *is generated by* $[t_{c_1}]$.
(2) $\operatorname{Ker}\Phi$ *is isomorphic to* $\mathbb{Z}^3$.

Proof. Like in the case $X_\mathbb{R} = \mathbb{K}\#\mathbb{T}^2$ we obtain the relations $[s_1] = [\Delta_1] = 1$ by applying Lemma 6.1.2 to g_e with $e = O_1$ and $e = B_1$. Since in the case

$X_{\mathbb{R}}=\mathbb{K}\#\mathbb{T}^2\amalg\mathbb{S}^2$ the group $\mathrm{MW}_{\mathbb{R}}$ is generated by g_e with $e=O_1,B_1,B_1'$, and B_1'', to prove item (1) there remains to notice that $g_e=s_1$ for both B_1' and B_2', and to apply Proposition 5.7.1. Since the only remaining generator, $t_{c_1}\in\mathrm{Mod}^s(X_{\mathbb{R}})$ is not involved, its coset $[t_{c_1}]$ generates the quotient. Since $\mathrm{MW}_{\mathbb{R}}$ is a free abelian group of rank 4, from $\Phi(\mathrm{MW}_{\mathbb{R}})=\mathbb{Z}+\mathbb{Z}/2$ it follows that $\operatorname{Ker}\Phi$ is isomorphic to $\mathbb{Z}^3$. □

6.2.4. **Proposition.** *If $X_{\mathbb{R}}=\mathbb{K}\#\mathbb{K}$, then $\Phi(\mathrm{MW}_{\mathbb{R}})=\mathrm{Mod}^s(X_{\mathbb{R}})$ and $\operatorname{Ker}\Phi$ is isomorphic to $\mathbb{Z}^4$.*

Proof. Surjectivity of Φ follows from Proposition 5.7.2 and the possibility to realize the 4 disjoint sections involved by real lines (the latter follows, for example, from Proposition 4.3.2). Since $\mathrm{MW}_{\mathbb{R}}$ is a free abelian group of rank 4, from $\Phi(\mathrm{MW}_{\mathbb{R}})=\mathbb{Z}/2+\mathbb{Z}/2$ it follows that $\operatorname{Ker}\Phi$ is isomorphic to $\mathbb{Z}^4$. □

6.2.5. **Proposition.** *If $X_{\mathbb{R}}=\mathbb{K}\amalg q\mathbb{S}^2$ with $0<q<4$, then $\Phi(\mathrm{MW}_{\mathbb{R}})=\mathrm{Mod}^s(X_{\mathbb{R}})$ and $\operatorname{Ker}\Phi$ is isomorphic to $\mathbb{Z}^{4-q}$.*

Proof. By Proposition 5.7.1 $\mathrm{Mod}^s(X_{\mathbb{R}})=\mathbb{Z}/2$ with the only nontrivial element t_{c_1}. Thus, there remains to notice that $t_{c_1}=\langle L'-L\rangle$ for any pair of disjoint real lines $L,L'\subset X_{\mathbb{R}}$, and that $\mathrm{MW}_{\mathbb{R}}$ is a free abelian group of rank $4-q$. □

6.3. **Addendum: Lattice description of** $\operatorname{Ker}\Phi$**.** Our goal here is to give an explicit expression for $\operatorname{Ker}\Phi$ in terms of standard geometric generators of $\mathrm{MW}_{\mathbb{R}}=\Lambda=E_8\cap\ker(1+\mathrm{conj}_*)$, each generator being a root of Λ and represented either by an oval- or a bridge-classe (see Fig. 4). In the following theorem we consider *n-chains* formed by sequences of n roots in Λ that have pairwise intersection 1 if consecutive and 0 otherwise. The notation for roots is like in Sec. 2.5 and Lemma 4.3.1. For instance, in the case $X_{\mathbb{R}}=\mathbb{K}\#3\mathbb{T}^2$, for which $\Lambda=E_7$, we consider a 7-chain $B_1 — O_1 — B_{12} — O_2 — B_{23} — O_3 — B_3$ obtained from the 6-chain on the standard diagram of E_7 on Fig. 4 by adding the root B_3 (which, in fact, represents the so called *long root* of E_7, with respect to our choice of its standard root-generators). In the case $X_{\mathbb{R}}=\mathbb{K}\amalg\mathbb{K}$, for which $\Lambda=D_4$, we consider the 4 bridge-classes B_1,B_2,B_3,B_4 and their combination $B_0=-\frac{1}{2}(B_1+B_2+B_3+B_4)$ (see Lemma 4.3.1).

In the case $X_{\mathbb{R}}=\mathbb{K}\amalg q\mathbb{S}^2$, $0\leqslant r\leqslant 4$, we have $\Lambda=(4-q)A_1$, but have no oval- or bridge-classes in the sense of Section 2.5. However, for uniformity of notation we will denote by B_i, $0\leqslant i\leqslant 4-q$, the elements of a root basis of Λ (chosen arbitrarily).

6.3.1. **Theorem.** *If X satisfies Assumption* **A***, then $\operatorname{Ker}\Phi\subset\Lambda$ can be expressed as follows:*

(1) *If $X_{\mathbb{R}}=\mathbb{K}\#4\mathbb{T}^2$, then $\operatorname{Ker}\Phi=0$.*
(2) *If $X_{\mathbb{R}}=\mathbb{K}\#3\mathbb{T}^2$, then $\operatorname{Ker}\Phi=\{a(B_1+O_1+B_{12}+O_2+B_{23}+O_3+B_3)\mid a\in 2\mathbb{Z}\}$.*
(3) *If $X_{\mathbb{R}}=\mathbb{K}\#2\mathbb{T}^2$, then*

$$\operatorname{Ker}\Phi=\{a_1(B_1+O_1+B_{12}+O_2+B_2)+a_2(B_1+O_1+B_{12}+O_2+B_2')\mid a_1+a_2\in 2\mathbb{Z}\}.$$

(4) *If $X_{\mathbb{R}}=\mathbb{K}\#\mathbb{T}^2$, then*

$$\operatorname{Ker}\Phi=\{a_1(O_1+B_1+B_1')+a_2(O_1+B_1+B_1'')+a_3(O_1+B_1'+B_1'')\mid a_1+a_2+a_3\in 2\mathbb{Z}\}.$$

(5) *If $X_{\mathbb{R}}=\mathbb{K}\amalg q\mathbb{S}^2$, $0\leqslant q\leqslant 4$, then $\operatorname{Ker}\Phi=\{\sum_{i=1}^{4-q}a_iB_i\mid \sum_{i=1}^{4-q}a_i\in 2\mathbb{Z}\}$.*
(6) *If $X_{\mathbb{R}}=\mathbb{K}\amalg\mathbb{K}$, then $\operatorname{Ker}\Phi=\{\sum_{i=0}^{3}a_iB_i\mid a_0\in 2\mathbb{Z}$ and $\sum_{i=1}^{3}a_i\in 2\mathbb{Z}\}$.*

6.3.2. **Lemma.** *The order 2 element $\delta \in \mathrm{Mod}^s(X_{\mathbb{R}})$ in the cases $X_{\mathbb{R}} \cong \mathbb{K}\#p\mathbb{T}^2$, $0 \leqslant p \leqslant 3$, is as follows:*

- *If $p = 3$, then $\delta = \Delta_1\Delta_2^{-1}\Delta_3$ is represented as g_e, where e is a 7-chain root*
$$e = B_1 + O_1 + B_{12} + O_2 + B_{23} + O_3 + B_3 \in \Lambda = E_7.$$
- *If $p = 2$, then $\delta = \Delta_1\Delta_2^{-1}t_{c_1}^{-1}$ is represented as g_e, where e is a 5-chain root*
$$e = B_1 + O_1 + B_{12} + O_2 + B_2 \in \Lambda = D_6.$$
- *If $p = 1$, then $\delta = \Delta_1$ is represented as g_e, where e is a 3-chain root*
$$e = B_1 + O_1 + B_1' \in \Lambda = D_4 + A_1.$$
- *If $p = 0$, then $\delta = t_{c_1}$ is represented as g_e, where e is any root in $\Lambda = 4A_1$.*

Proof. The specified expressions for δ through the generators of $\mathrm{Mod}^s(X_{\mathbb{R}})$ follow directly from Proposition 5.7.1. In the case $p = 3$ we apply this expression, use Lemma 6.1.2 and Proposition 5.6.1(2), and get

$$g_e = g_{B_1}g_{O_1}g_{B_{12}}g_{O_2}g_{B_{23}}g_{O_3}g_{B_3} = s_1(\Delta_1 s_1^{-2})(s_1s_2t_{c_2}^{-1})(\Delta_2 s_2^{-2})(s_2s_3t_{c_3}^{-1})(\Delta_3 s_3^{-2})s_3 = \Delta_1\Delta_2\Delta_3 t_{c_2}^{-1}t_{c_3}^{-1} = \Delta_1\Delta_2\Delta_3\Delta_2^{-2} = \delta.$$

In the case $p = 2$, we get similarly

$$g_e = g_{B_1}g_{O_1}g_{B_{12}}g_{O_2}g_{B_2} = s_1(\Delta_1 s_1^{-2})(s_1s_2t_{c_2}^{-1})(\Delta_2 s_2^{-2})s_2 = \Delta_1\Delta_2 t_{c_2}^{-1} = \Delta_1\Delta_2^{-1}(t_{c_2}t_{c_3})t_{c_2}^{-1} = \Delta_1\Delta_2^{-1}t_{c_1}^{-1} = \delta.$$

In the case $p = 1$, we get

$$g_e = g_{B_1}g_{O_1}g_{B_1'} = s_1(\Delta_1 s_1^{-2})s_1 = \Delta_1 = \delta.$$

For $g_e = t_{c_1}$ in the case $p = 0$ see Lemma 6.1.2(4). □

6.3.3. **Lemma.** *Assume that $\mathcal{L} \subset E_8$ is a root lattice and $\mathcal{L}' \subset \mathcal{L}$ is generated by some pairwise orthogonal roots $e_1, \dots, e_n$, $n \leqslant 3$. Then $\mathcal{L}'$ is primitive in $\mathcal{L}$.*

Proof. Since $|\mathrm{discr}\mathcal{L}'| = 2^n$, and since, for any its extension $\mathcal{L} \supset \mathcal{M} \supset \mathcal{L}'$ of the same rank, we have $\frac{|\mathrm{discr}\mathcal{L}'|}{|\mathrm{discr}\mathcal{M}|} = [\mathcal{M} : \mathcal{L}']^2$, the only possibility for $\mathcal{M} \neq \mathcal{L}'$ is $[\mathcal{M} : \mathcal{L}'] = 2$, $n \geqslant 2$, and $|\mathrm{discr}\mathcal{M}| = 1, 2$. Since $\mathcal{M} \subset \mathcal{L} \subset E_8$, the lattice $\mathcal{M}$ is even and definite, but there are no such lattices of rank $n = 2, 3$ with $|\mathrm{discr}\mathcal{M}| = 1, 2$. □

Proof of Theorem 6.3.1. In the case $p = 3$, we have $\ker\Phi \cong \mathbb{Z}$ (see Proposition 6.2.2) and the result follows from Lemma 6.3.2 combined with Lemma 6.3.3.

In the case $p = 2$, in addition to the 5-chain e from Lemma 6.3.2, we have $\delta = g_e = g_{e'} \in \mathrm{Mod}^s(X_{\mathbb{R}})$ for another 5-chain e' (a subgraph of $\Lambda = D_6$) obtained by replacing B_2 by B_2'. It does give the same element of $\mathrm{Mod}^s(X_{\mathbb{R}})$, since, according to Lemma 6.1.2(3), $g_{B_2} = g_{B_2'}$. Thus, the combinations $a_1e + a_2e'$ with $a_1 + a_2 \in 2\mathbb{Z}$ give a subgroup $\mathbb{Z}^2$ of $\ker\Phi \cong \mathbb{Z}^2$ (see Proposition 6.2.2) and applying Lemma 6.3.3 we conclude that the kernel should coincide with this subgroup.

In the case $p = 1$, by Lemma 6.3.2 we have $\delta = g_e$, where e is presented by a 3-chain $B_1 + O_1 + B_1'$ (a subgraph of $\Lambda = D_4 + A_1$). For the same reasons as in the case $p = 2$, the element δ is presented by two other 3-chains in the summand D_4 of Λ. From here, the sublattice $\mathcal{K} \subset \Lambda$ formed by integer combinations of these three 3-chains with coefficients a_1, a_2, a_3 satisfying $a_1 + a_2 + a_3 \in 2\mathbb{Z}$ is contained in the $\ker\Phi$. Since the rank, 3, of $\mathcal{K}$ is the same as that of $\ker\Phi$ (see Proposition 6.2.2) and the lattice of all integer combinations of these three 3-chains is primitive due to Lemma 6.3.3, we conclude $\mathcal{K} = \ker \Phi$.

In the case $p = q = 0$, the proof follows the same lines, using Lemma 6.3.2 and Proposition 6.2.2 (in this case $\Lambda = 4A_1$ and the primitivity argument becomes trivial).

The case $X_{\mathbb{R}} = \mathbb{K} \amalg q\mathbb{S}^2$, $0 < q < 4$, is analogous to the case $p = q = 0$ and differs only in the rank of $\Lambda = (4-q)A_1$ and usage of Proposition 6.2.5 instead of Proposition 6.2.2.

In the cases $X_{\mathbb{R}} = (\mathbb{K} \# \mathbb{T}^2) \amalg \mathbb{S}^2$ and $X_{\mathbb{R}} = \mathbb{K} \amalg \mathbb{K}$ we make use of Propositions 6.2.3, 6.2.4 and provide matrices of the homomorphism $\Lambda \to \mathrm{Mod}^s(X_{\mathbb{R}})$ (see Tab. 9), which are calculated using Lemmas 6.1.2 and 6.1.3. The kernels claimed in Theorem 6.3.1 are then found from these matrices, (1) and (2) on Tab. 9. □

Tab. 9. Matrices of $\mathbb{Z}^4 = \Lambda \to \mathrm{Mod}^s(X_{\mathbb{R}})$, $v \mapsto g_v$

(1) $\Lambda = D_4 \to \mathrm{Mod}^s(\mathbb{K} \# \mathbb{T}^2 \amalg \Sigma^2) = \mathbb{Z}^2 + \mathbb{Z}/2$

	O_1	B_1	B_1'	B_1''
s_1	-2	1	1	1
Δ_1	1	0	0	0
t_{c_1}	0	0	0	0

(2) $\Lambda = D_4 \to \mathrm{Mod}^s(\mathbb{K} \amalg \mathbb{K}) = \mathbb{Z}/2 + \mathbb{Z}/2$

	B_0	B_1	B_2	B_3
$\langle \lambda_2^1 - \lambda_1^1 \rangle$	$*$	1	1	1
$\langle \lambda_1^2 - \lambda_1^1 \rangle$	1	0	0	0

In the second matrix $*$ stands for 0 or 1 depending on orientations chosen for B_1, B_2, B_3, B_4. By $\langle \lambda_2^1 - \lambda_1^1 \rangle \in \mathrm{Mod}^s(X_{\mathbb{R}})$ we denote an element preserving the components of $\mathbb{K} \amalg \mathbb{K}$, while $\langle \lambda_1^2 - \lambda_1^1 \rangle$ denotes an element which interchanges them (see Lemma 6.1.3).

7. Proof of Theorems 1.3.1, 1.3.2, 7.3.2, and 7.3.3

In this section we follow the setting and notation of Sections 5, 6. In particular, we fix a real line L on a real elliptic surface $f : X \to \mathbb{P}^1$ satisfying Assumption **A**.

7.1. **Proof of Theorem 1.3.1.** The topological types of $X_{\mathbb{R}}$ for the 11 deformation classes of real elliptic surfaces satisfying Assumption **A** are listed in Tab. 2, see Corollary 2.2.3.

If $X_{\mathbb{R}} \cong \mathbb{K} \# p\mathbb{T}^2$ with $p \geqslant 1$, then $s_1^n \in \Phi(\mathrm{MW}_{\mathbb{R}})$ for any $n \in \mathbb{Z}$ (see Proposition 6.2.2 if $1 \leqslant p \leqslant 3$ and Proposition 6.2.1 if $p = 4$). On the other hand, $g(L) \subset X$ is a real line, for any $g \in \mathrm{MW}_{\mathbb{R}}$. Since $L_{\mathbb{R}}$ intersects the fiber $a_1 \cup b_1$ at a point of a_1, the homology class $[s_1^n(L_{\mathbb{R}})] \in H_1(X_{\mathbb{R}})$ is $[L_{\mathbb{R}}] + n[a_1]$ and we obtain $\mathcal{N} = \infty$, since $[a_1] \in H_1(X_{\mathbb{R}})$ has infinite order.

If $X_{\mathbb{R}} \cong \mathbb{K} \# \mathbb{T}^2 \amalg \mathbb{S}^2$, the arguments are literally the same, except that we refer to Proposition 6.2.3(1) to justify that $s_1^n \in \Phi(\mathrm{MW}_{\mathbb{R}})$.

If $X_{\mathbb{R}} \cong \mathbb{K}$, then there exist only two classes in $H_1(X_{\mathbb{R}})$ realizable by sections: $[L_{\mathbb{R}}]$ and $[L_{\mathbb{R}}]+[c_1]$, where $[c_1]$ is the order 2 element of $H_1(X_{\mathbb{R}})$. The class $[L_{\mathbb{R}}]+[c_1]$ is realized by the line $t_{c_1}(L_{\mathbb{R}})$ (see Proposition 6.2.2 applied to $p = 0$), so $\mathcal{N} = 2$.

If $X_{\mathbb{R}} \cong \mathbb{K} \amalg q\mathbb{S}^2$ with $0 < q \leqslant 3$, we refer to Proposition 6.2.5, and the same arguments as for $X_{\mathbb{R}} = \mathbb{K}$ give $\mathcal{N} = 2$.

If $X_{\mathbb{R}} \cong \mathbb{K} \amalg 4\mathbb{S}^2$, then $\Lambda = 0$, which implies $\mathcal{N} = 1$ (see Proposition 5.1.1).

If $X_{\mathbb{R}} = \mathbb{K} \amalg \mathbb{K}$, then H_1 of each component contains only 2 classes realizable by sections. Finally, Proposition 6.2.4 and the same arguments as for $X_{\mathbb{R}} = \mathbb{K}$ imply that all 4 are realizable by real lines, which gives $\mathcal{N} = 4$. $\square$

7.2. **Proof of Theorem 1.3.2.**

7.2.1. **Lemma.** *Let $C \subset Q$ be a real nonsingular sextic $C \subset Q$ of type $\langle p \,|\, q\rangle$ with $p \geqslant 1$. Then, for any of the p positive ovals $o_i, 1 \leqslant i \leqslant p$, of $C_{\mathbb{R}}$, there exists a degeneration of C to a real 1-nodal sextic C_0 contracting o_i to a solitary real point. Furthermore, for any such degeneration there exists a real hyperplane section passing through the node of C_0 and tangent to C_0 at two other (not necessarily real) points.*

Proof. Due to deformation classification of real nonsingular sextics $C \subset Q$ (see Theorem 2.2.1), it is sufficient to construct a real 1-nodal sextic C_0 with one solitary node (that is a node without real branches), $p-1$ positive ovals and q negative ones, and to check existence of a section with enumerated properties. For doing that, we project C_0 from the node to $\mathbb{P}^2$ and observe that this reduces the problem to a construction of a real nonsingular quartic $A \subset \mathbb{P}^2$ of type $\langle p-1\rangle$ if $q = 0$ and of type $1\langle 1\rangle$ if $q = 1$, whose construction is well known. As to existence of a requested hyperplane section, it is provided by lifting of any of the real double tangents to A, and the existence of the latter ones is also well known. $\square$

Proof of Theorem 1.3.2. Due to stability of real vanishing classes under deformation and to deformation classification of real nonsingular relatively minimal rational elliptic surfaces containing a real line, it is sufficient to prove the statement on an example. Thus, we pick a real nonsingular sextic $C \subset Q$ like in Lemma 7.2.1, include it as $C_{\tau>0} = C$ in a generic, invariant under complex conjugation, one-parameter complex-analytic perturbation $C_\tau, 0 \leqslant |\tau| \leqslant \varepsilon, \tau \in \mathbb{C}$ of a real sextic C_0 obtained by contracting a positive oval o_i of $C_{\mathbb{R}}$, and consider the associated complex analytic family X'_τ of rational elliptic surfaces. The latter family inherits a complex conjugation such that X'_τ is real with $(X'_\tau)_{\mathbb{R}} = \mathbb{K}\#p\mathbb{T}^2 \amalg q\mathbb{S}^2$ for $\tau \in \mathbb{R}, \tau > 0$. Then, by a base change $\tau = t^2$ followed by Atiyah's smoothing construction (see [At]), we obtain a smooth complex analytic family of surfaces, X_t, such that $X_t = X'_{t^2}$ for $t \neq 0$ while X_0 is the minimal resolution of X'_0. Furthermore, since the nodal degeneration $X'_{\tau>0} \to X'_0$ is contracting a circle $o_i \subset (X'_\tau)_{\mathbb{R}}$ (case of signature 1 in terminology of [IKS]), the real structure on X_0 lifted from X'_0 and that real structure on $\{X_{t\neq 0}\}$ lifted from the real structure on $\{X'_{\tau\neq 0}\}$ for which $(X_t, \mathrm{conj}) = (X'_{t^2}, \mathrm{conj})$, they feat together and define a real structure on the total space of the Atiyah family $\{X_t\}$ (see [IKS] for details). In particular, this shows that $[o_i] \in H_1((X_{\sqrt{\tau}})_{\mathbb{R}})$ is a real vanishing class for any choice of orientation on o_i.

Next, due to stability of (-1)-curves (see [K]), any of two real lines $L' \subset X_0$ covering the hyperplane section provided by Lemma 7.2.1 extends, at least for small values of $t \in \mathbb{C}$, to an analytic family of lines $L'_t \subset X_t$. Due to unicity of this extension, and since $L'_0 = L'$ is real, the family $\{L'_t\}$ is also real, so that, for each small real t the line L'_t is also real. Having also a real family of zero sections $L_t \subset X_t$, we may reparametrize the family X_t via $g_t^n \in \mathrm{MW}(X_t)$, $n \in \mathbb{Z}$, $g_t = \langle L'_t - L_t\rangle$, and thus deduce that $g_\varepsilon^n(o_i)$ is a real vanishing cycle for any $n \in \mathbb{Z}$.

The intersection index of $L' = L'_0$, and hence of L'_t for any t, with the vanishing class $[O_i] \in H_2((X_{\sqrt{\tau}})_{\mathbb{R}}) = H_2((X'_\tau)_{\mathbb{R}}))$ is equal to ± 1. Thus, applying Corollary

2.8.2 and Proposition 6.1.1, we conclude that $\Phi(g_e)|_{N_i}$ is equal either to $(s_i)^{\pm 1}$ or $(\Delta_i s_i^{-1})^{\pm 1}$. Therefore, $\Phi(g_e^n|_{N_i})(o_i)$ reduces to iteration of Dehn twists and, as a result, is equal to $\pm(o_i \pm n(a_i - b_i))$ (with respect to orientations shown on Fig. 19), which gives us an infinite number of pairwise distinct real vanishing classes in $H_1((X_\varepsilon)_\mathbb{R}) = H_1((X'_{\tau>0})_\mathbb{R})$.

□

FIG. 19. Preferred orientations

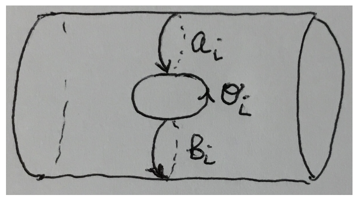

7.3. **Criterion for a section to be realizable by a line.** The fixed line $L \subset X$ determines (as any other line) a fiberwise involution $\beta_L : X \to X$ that preserves L. It is the lift of the Bertini involution $\beta : Y \to Y$, and its fixed point set is $L \cup C$ where we do not make difference between the sextic $C \subset Q$ and its lift to X.

If $X_\mathbb{R} = \mathbb{K}\#4\mathbb{T}^2$, then C considered as a sextic in Q is of type $\langle 4\,|\,0\rangle$. We numerate the ovals of $C_\mathbb{R}$ so that o_1, o_3 are lower ovals and o_2, o_4 are upper ones (see Subsection 2.6).

Considering a generic real smooth section $\lambda : \mathbb{P}^1_\mathbb{R} \to X_\mathbb{R}$ of f we let $l = \lambda(\mathbb{P}^1_\mathbb{R})$ and define subsets $S_{in}, S_{tan} \subset \{1,2,3,4\}$ associated with λ, extending our previous definition given in the case $L_\mathbb{R} \cap l = \varnothing$ (as it was given in the context of real tritangents to $C \subset Q$, see Section 3.3). Namely, we observe that $l \cup \beta_L(l)$ divides $X_\mathbb{R}$ into two singular domains with $l \cup \beta(l)$ as a common boundary, denote by $F_l \subset X_\mathbb{R}$ the domain containing $L_\mathbb{R}$ and set

$$S_{tan}(l) = \{i\,|\,o_i \circ l = 1 \mod 2\} \quad \text{and} \quad S_{in}(l) = \{i\,|\,o_i \subset F_l\}.$$

When working with the sets $S_{tan}(l), S_{in}(l)$ in concrete situations, we descend from X to Y and apply the terminology and encoding introduced in Sec. 4.5.

7.3.1. **Lemma.** *The residue* $r = |S_{in}(l) \smallsetminus S_{tan}(l)| + |S_{tan}(l) \cap \{1,3\}| + l \circ L_\mathbb{R} \mod 2$ *is preserved under replacement* l *by* $l' = g(l)$ *with* $g \in \mathrm{Mod}^s(X_\mathbb{R})$ *if and only if* g *belongs to* $\Phi(\mathrm{MW})$.

Proof. It is enough to check that for the generators of $\Phi(\mathrm{MW})$, $g \in \{s_1, s_3, s_2^2, s_4^2, \Delta_i\,|\,i = 1, \dots, 4\}$ (see Proposition 6.2.1(2)) the residue r does not change, while for $g = t_{c_i} \in \mathrm{Mod}^s(X_\mathbb{R})$ which represents the generator of $\mathrm{Mod}^s(X_\mathbb{R})/\Phi(\mathrm{MW}) = \mathbb{Z}/2$ (see Proposition 6.2.1(3)), the residue r changes.

Table 10 shows how varies r and each of its summands, $|S_{in}(l) \smallsetminus S_{tan}(l)|$, $|S_{tan}(l) \cap \{1,3\}|$, $l \circ L_\mathbb{R} \mod 2$, under the action of t_{c_i}, s_i and Δ_i.

For $g = t_{c_i}^{\pm 1}$, the sets S_{in} and S_{tan} are not affected, while $l \circ L_\mathbb{R}$ changes by 1, since the classes $[l'], [l] \in H_1(X_\mathbb{R})$ differ by the fiber-class. The action of s_i alternates the pairity of $l \circ o_i$, and, in particular, varies $|S_{in} \smallsetminus S_{tan}|$ if l is underpassing oval o_i, while the intersection index $l \circ L_\mathbb{R}$ alternates only if l is overpassing o_i. The action of Δ_i does not affect $l \circ o_i$, while alternates "overpasses" and "underpasses" of l over o_i. Fig. 20 shows how the action of Δ_i affects $l \circ L_\mathbb{R}$. □

Tab. 10. Variation of r and its summands

g	position of o_i and l	$\lvert S_{in} \setminus S_{tan}\rvert$	$\lvert S_{tan} \cap \{1,3\}\rvert$	$l \circ L_{\mathbb{R}} \mod 2$	r
$t_{c_i}^{\pm 1}$	in all positions	0	0	1	1
$s_1^{\pm 1}$ or $s_3^{\pm 1}$	$\overline{\bigcirc}$ or $\overline{\bigcirc}$	0	± 1	1	0
$s_1^{\pm 1}$ or $s_3^{\pm 1}$	$\underline{\bigcirc}$ or $\underline{\bigcirc}$	± 1	± 1	0	0
$s_2^{\pm 1}$ or $s_4^{\pm 1}$	$\overline{\bigcirc}$ or $\overline{\bigcirc}$	0	0	1	1
$s_2^{\pm 1}$ or $s_4^{\pm 1}$	$\underline{\bigcirc}$ or $\underline{\bigcirc}$	± 1	0	0	1
$\Delta_i^{\pm 1}$	$\overline{\bigcirc}$	0	0	0	0
$\Delta_i^{\pm 1}$	$\overline{\bigcirc}$	± 1	0	1	0
$\Delta_i^{\pm 1}$	$\underline{\bigcirc}$	0	0	0	0
$\Delta_i^{\pm 1}$	$\underline{\bigcirc}$	± 1	0	1	0

Fig. 20

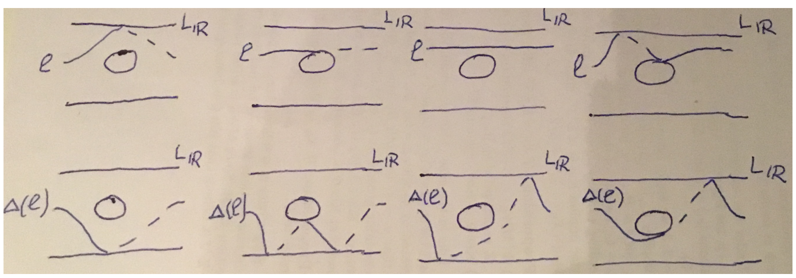

7.3.2. **Theorem.** *If X satisfying Assumption* **A** *is endowed with a fixed real line L and has $X_{\mathbb{R}} = \mathbb{K}\#4\mathbb{T}^2$, then a smooth section $l \subset X_{\mathbb{R}}$ is isotopic to the real locus of a real line if and only if the sets $S_{in}(l), S_{tan}(l) \subset \{1, \dots, 4\}$ defined by l satisfy*

$$|S_{in}(l) \setminus S_{tan}(l)| + |S_{tan}(l) \cap \{1,3\}| = l \circ L_{\mathbb{R}} + 1 \mod 2.$$

Proof. Due to Proposition 3.4.2, the statement holds for sections l represented by real lines disjoint from L. Thus, since by definition the mapping $g \in \mathrm{Mod}^s(X_{\mathbb{R}}) \mapsto l = g(L_{\mathbb{R}})$ establishes a bijection between $\mathrm{Mod}^s(X_{\mathbb{R}})$ and the set of isotopy classes of smooth sections $l \subset X_{\mathbb{R}}$ and restricts to a bijection between $\Phi(\mathrm{MW})$ and the isotopy classes of sections represented by real lines, the general result follows from Lemma 7.3.1. $\square$

The next theorem concerns the case $X_{\mathbb{R}} = \mathbb{K}\#\mathbb{T}^2 \amalg \mathbb{S}^2$. In this case the curve $C_{\mathbb{R}} \subset Q_{\mathbb{R}}$ has two ovals and we denote by o the positive one. On this oval the projection $f_{\mathbb{R}} : X_{\mathbb{R}} \to \mathbb{P}^1_{\mathbb{R}}$ has two critical points, $x, y \in o$ that we connect by a curve $\gamma \subset X_{\mathbb{R}}$ (see the leftmost sketch on Figure 21) with the following properties:

- γ is a section of $f_{\mathbb{R}}$ over the interval bounded by the critical values $f_{\mathbb{R}}(x)$, $f_{\mathbb{R}}(y)$ which is complementary to $f_{\mathbb{R}}(o)$ in $\mathbb{P}^1_{\mathbb{R}}$,
- γ does not intersect line $L_{\mathbb{R}}$ and the J-component of $C_{\mathbb{R}}$.

We choose arbitrarily a coorientation of γ, and note that the intersection index $\gamma \circ l \in \mathbb{Z}$ is well-defined for any smooth section $l \subset X_{\mathbb{R}}$ and depends only on the isotopy class of l.

Note that for the Bertini-partner $\gamma' = \beta_L(\gamma)$ of γ the same properties are satisfied and $\gamma \cup \gamma'$ form a simple closed curve since $\gamma \cap \gamma' = \{x, y\}$. Moreover, β_L induces a coorientation of γ' compatible with that of γ, so that $\gamma \cup \gamma'$ becomes a cooriented closed curve. Since in addition $\gamma \cup \gamma'$ bounds in $X_{\mathbb{R}}$, this implies that $\gamma \circ l = -\gamma' \circ l$ for any smooth section l.

Fig. 21

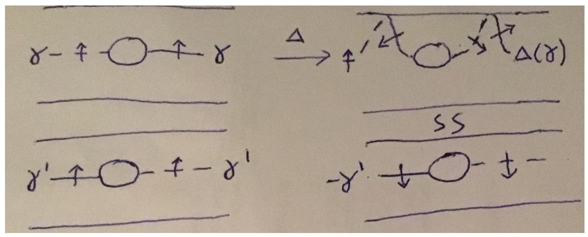

7.3.3. **Theorem.** *If X satisfying Assumption* **A** *is endowed with a fixed real line L and has $X_{\mathbb{R}} = \mathbb{K}\#\mathbb{T}^2 \amalg \mathbb{S}^2$, then a smooth section $l \subset X_{\mathbb{R}}$ is isotopic to the real locus of a real line if and only if $\gamma \circ l = 0$.*

Proof. Consider $g \in \mathrm{Mod}^s(X_{\mathbb{R}})$ such that l is isotopic to $g(L_{\mathbb{R}})$. Then $\gamma \circ l = g^{-1}(\gamma) \circ L_{\mathbb{R}}$. Clearly, $s \in \mathrm{Mod}^s(X_{\mathbb{R}})$ leaves γ invariant, while Δ sends γ to a curve isotopic to $\gamma' = \beta_L(\beta)$ with the opposite coorientation (see Fig. 21). By Proposition 5.7.1 g^{-1} can be presented in a form $\Delta_1^{\varkappa} s_1^n t_{c_1}^m$ where $n, m \in \mathbb{Z}$ and $\varkappa \in \{0, 1\}$. According to Proposition 6.2.3 it belongs to $\Phi(\mathrm{MW})$ if and only if $m = 0$. On the other hand,

$$g^{-1}(\gamma) \circ L_{\mathbb{R}} = \begin{cases} (\gamma + mc_1) \circ L_{\mathbb{R}} = m & \text{if } \varkappa = 0, \\ (-\gamma' + mc_1) \circ L_{\mathbb{R}} = m & \text{if } \varkappa = 1. \end{cases}$$

□

8. The action of $\mathrm{MW}_{\mathbb{R}}(X)$ in $H_1(X_{\mathbb{R}})$

8.1. **Decomposition of $H_1(X_{\mathbb{R}})$.** Let us fix a real line $L_{\mathbb{R}} \subset X_{\mathbb{R}} \cong \mathbb{K}^2\#p\mathbb{T}^2 \amalg q\mathbb{S}^2$ and choose a connected fiber $F_{\mathbb{R}} \subset X_{\mathbb{R}}$. Then, following Section 5.3, consider the subsurfaces N_i of the non-spherical component $\mathbb{K}^2\#p\mathbb{T}^2$ of $X_{\mathbb{R}}$ and their skeletons $a_i \cup o_i \cup b_i, 1 \leqslant i \leqslant p$, as on Fig. 13, where we assume in addition that o_i are positive ovals of the sextic C defined by L (see Sec. 7.3) and b_i are disjoint from $L_{\mathbb{R}}$. We orient $L_{\mathbb{R}}$ in accord with the orientation of $\mathbb{P}^1_{\mathbb{R}}$. To orient the circles o_i we notice that each of them splits into a pair of arcs connecting critical points of the projection $f_{\mathbb{R}} : X_{\mathbb{R}} \to \mathbb{P}^1_{\mathbb{R}}$: the *upper arc* intersecting a_i and the *lower arc* intersecting b_i. We orient o_i so that $f_{\mathbb{R}}$ preserves the orientation on the lower arc (and, thus, reverses on the upper one). For a_i, b_i, we fix an orientation of $X_{\mathbb{R}} \setminus F_{\mathbb{R}}$ and then orient a_i, b_i in a way to obtain the following local intersection indices

$$(8.1.1) \qquad o_i \circ a_i = b_i \circ o_i = 1, \quad \text{from where } a_i \circ [L_{\mathbb{R}}] = 1.$$

Finally, we notice that $[F_{\mathbb{R}}]$ represents the 2-torsion element of $H_1(X_{\mathbb{R}})$ and forms together with $[L_{\mathbb{R}}], o_i, b_i$ a basis of $H_1(X_{\mathbb{R}})$. This leads to a natural decomposition

$$(8.1.2) \qquad H_1(X_{\mathbb{R}}) = \langle [F_{\mathbb{R}}] \rangle \oplus \Big[\bigoplus_{i=1}^{p} \langle b_i, o_i \rangle \Big] \oplus \langle [L_{\mathbb{R}}] \rangle = \mathbb{Z}/2 \oplus \Big[\bigoplus_{i=1}^{p} (\mathbb{Z} \oplus \mathbb{Z}) \Big] \oplus \mathbb{Z}.$$

With respect to this basis, the class of any section has a coordinate expression

$$[L_{\mathbb R}]+\kappa[F_{\mathbb R}]+\sum_{i=1}^{p}(m_ib_i+\varkappa_i o_i),\quad \kappa\in\mathbb Z/2,\ m_i\in\mathbb Z,\ \varkappa_i\in\{0,1\}. \tag{8.1.3}$$

8.1.1. **Proposition.** *The decomposition 8.1.2 depends only on the isotopy class of $L_{\mathbb R}$ and the choice of $F_{\mathbb R}$. Moreover, the identification $\langle b_i,o_i\rangle=\mathbb Z\oplus\mathbb Z$ may be changed only by an automorphism $n\mapsto -n$ of the first $\mathbb Z$-summand, which happens if the orientation of N_i is changed by another choice of $F_{\mathbb R}$ or/and another choice of a fixed orientation of $X_{\mathbb R}\smallsetminus F_{\mathbb R}$.* □

8.2. **Matrix description of the action of** $\mathrm{Mod}^s(X_{\mathbb R})$ **in** $H_1(X_{\mathbb R})$**.** Here, in addition to $t_{c_i},s_i,\Delta_i\in \mathrm{Mod}^s(X_{\mathbb R})$ we consider auxilliary elements $\bar\Delta_i=\Delta_i t_{c_{i+1}}^{-1}$. If $p=1$ we use notation $a,b,c,o,s,\Delta,\bar\Delta,\dots$ instead of $a_1,b_1,c_1,o_1,s_1,\Delta_1,\bar\Delta_1,\dots$.

8.2.1. **Lemma.** *If $X_{\mathbb R}=\mathbb K\#\mathbb T^2$, then the matrices of the action of $\Delta,\bar\Delta,t_c,s\in$ $\mathrm{Mod}^s(X_{\mathbb R})$ in $H_1(X_{\mathbb R})$ with respect to the decomposition*

$$H_1(X_{\mathbb R})=\langle[F_{\mathbb R}]\rangle\oplus\langle b\rangle\oplus\langle o\rangle\oplus\langle[L_{\mathbb R}]\rangle\cong\mathbb Z/2\oplus\mathbb Z\oplus\mathbb Z\oplus\mathbb Z$$

are as follows (integers in brackets in the first rows stand for their $\mathbb Z/2$-residues)

$$M_\Delta=\begin{bmatrix}[1]&[1]&0&[1]\\0&-1&0&0\\0&0&-1&1\\0&0&0&1\end{bmatrix}\quad M_{\bar\Delta}=\begin{bmatrix}[1]&[1]&0&0\\0&-1&0&0\\0&0&-1&1\\0&0&0&1\end{bmatrix}\quad M_{t_c}=\begin{bmatrix}[1]&0&0&[1]\\0&1&0&0\\0&0&1&0\\0&0&0&1\end{bmatrix}\quad M_s=\begin{bmatrix}[1]&0&[1]&[1]\\0&1&2&-1\\0&0&1&0\\0&0&0&1\end{bmatrix}$$

Proof. The first column of all matrices contains $1,0,0,0$ because the order 2 element is invariant. The Dehn twist t_c acts trivially on $\langle b,o\rangle$ and sends the homology class $[L_{\mathbb R}]$ to $[L_{\mathbb R}]+[F_{\mathbb R}]$ which gives M_{t_c}. To obtains M_Δ we notice that Δ sends o to $-o$ and b to $a=[F_{\mathbb R}]-b$, whereas $[L_{\mathbb R}]$ is sent to $[L_{\mathbb R}]+o+[F_{\mathbb R}]$. The product $M_\Delta M_{t_c}^{-1}=M_\Delta M_{t_c}$ is the matrix of $\bar\Delta$.

To obtain M_s we notice that s preserves the class b, sends $[L_{\mathbb R}]$ to $[L_{\mathbb R}]+a=[L_{\mathbb R}]-b+[F_{\mathbb R}]$ and o to $t_at_b(o)=t_a(o+b)=o+b-a=o+2b-[F_{\mathbb R}]$, since our choice of orientations gives $b\cdot o=-a\cdot o=1$, $a+b=[F_{\mathbb R}]$. □

8.2.2. **Corollary.** $M_s^mM_{t_c}^n=\begin{bmatrix}[1]&0&[m]&[m+n]\\0&1&2m&-m\\0&0&1&0\\0&0&0&1\end{bmatrix}$ *and* $M_{\bar\Delta}M_s^mM_{t_c}^n=\begin{bmatrix}[1]&[1]&[3m]&[n]\\0&-1&-2m&m\\0&0&-1&1\\0&0&0&1\end{bmatrix}$.

In particular, for any $\varkappa\in\{0,1\}$, $n,m\in\mathbb Z$, and $g=\bar\Delta^{\varkappa}s^mt_c^n$, we have

$$[g(L)_{\mathbb R}]=[L_{\mathbb R}]+\kappa[F_{\mathbb R}]+(-1)^{1-\varkappa}mb+\varkappa o,\quad \kappa=[n+(1-\varkappa)m]\in\mathbb Z/2.\quad\square$$

8.3. **A special decomposition in** $\mathrm{Mod}^s(X_{\mathbb R})$**.**

8.3.1. **Proposition.** *If $X_{\mathbb R}\cong\mathbb K\#p\mathbb T^2\amalg q\mathbb S^2$, then every element $g\in\mathrm{Mod}^s(X_{\mathbb R})$ can be presented in a form*

$$g=\bar\Delta_1^{\varkappa_1}\dots\bar\Delta_p^{\varkappa_p}t_{c_1}^{n_1}\dots t_{c_p}^{n_p}s_1^{m_1}\dots s_p^{m_p},\quad \varkappa_i\in\{0,1\},n_i,m_i\in\mathbb Z, \tag{8.3.1}$$

and such presentation is unique.

With respect to this presentation, the class of $g(L)_{\mathbb R}$ in $H_1(X_{\mathbb R})$ is

$$[g(L)_{\mathbb R}]=[L_{\mathbb R}]+\kappa[F_{\mathbb R}]+(-1)^{1-\varkappa_1}m_1b_1+\varkappa_1o_1+\dots+(-1)^{1-\varkappa_p}m_pb_p+\varkappa_po_p$$

where $\kappa=n_1+\dots+n_p+m_1(1-\varkappa_1)+\dots+m_p(1-\varkappa_p)\bmod 2$.

Proof. Proposition 5.7.1 implies that $\bar\Delta_i$, s_i and t_{c_1} generate $\mathrm{Mod}^s(X_\mathbb{R})$ with only one relation $\bar\Delta_1^2\dots\bar\Delta_p^2=t_{c_1}^2$. Then a presentation $g=t_{c_1}^n\prod_{i=1}^p(\bar\Delta_i^{k_i}s_i^{m_i})$ is transformed to the form (8.3.1) using the relations $\bar\Delta_i^2=t_{c_{i+1}}t_{c_i}^{-1}$ and $t_{c_{p+1}}=t_{c_1}^{-1}$.

Since the relations in $\mathrm{Mod}^s(X_\mathbb{R})$ involve only even powers of $\bar\Delta_i$, an equality

$$\bar\Delta_1^{\varkappa_1}\dots\bar\Delta_p^{\varkappa_p}t_{c_1}^{n_1}\dots t_{c_p}^{n_p}s_1^{m_1}\dots s_p^{m_p}=\bar\Delta_1^{\varkappa_1'}\dots\bar\Delta_p^{\varkappa_p'}t_{c_1}^{n_1'}\dots t_{c_p}^{n_p'}s_1^{m_1'}\dots s_p^{m_p'}$$

may hold only if $\varkappa_i=\varkappa_i'$ for each $1\leqslant i\leqslant p$. So, to prove uniqueness of presentation in the form (8.3.1), it is left to notice that t_{c_i},s_i, $i=1,\dots,p$ generate a free subgroup in $\mathrm{Mod}^s(X_\mathbb{R})$, which follows from Lemma 5.3.1.

To evaluate the class $[g(L)_\mathbb{R}]\in H_1(X_\mathbb{R})$ we determine the contribution of each factor $\bar\Delta_i^{\varkappa_i}s_i^{m_i}t_{c_i}^{n_i}$ precisely like in Lemma 8.2.1 and Corollary 8.2.2. □

8.4. **Proof of Theorem 1.3.4.** By Proposition 8.3.1, each element $g\in\mathrm{Mod}^s(X_\mathbb{R})$, and, in particular, such that $L'=g(L)$, can be decomposed in the form of (8.3.1). This identifies the coordinate expression of $[L'_\mathbb{R}]$ with the last column of the matrix M. The first column of M is determined by the invariance of the $\mathbb{Z}/2$-generator, $[g(F)_\mathbb{R}]=[F_\mathbb{R}]$. The Dehn twists $t_{c_i}^{n_i}$ being supported in neighborhoods of the fibers c_i act only on $[F_\mathbb{R}]\in H_1(X_\mathbb{R})$, but not on $b_i,o_i\in H_1(N_i)$. The factor $\bar\Delta_j^{\varkappa_j}s_j^{m_j}$ of g acts identically on $b_i,o_i\in H_1(N_i)$, $j\neq i$, since the corresponding diffeomorphism is supported in N_j. Thus, the action of g on $b_i,o_i\in H_1(N_i)\subset H_1(X_\mathbb{R})$ is reduced to the action of $\bar\Delta_i^{\varkappa_i}s_i^{m_i}$, and its calculation is literally the same as in Lemma 8.2.1 and Corollary 8.2.2. □

8.5. **Proof of Theorem 1.3.5.** Immediate from multiplication of the matrix of g as given in Theorem 1.3.4 by the column of the coordinates of $[L''_\mathbb{R}]$, and an observation that $(-1)^{\varkappa_{1i}}m_{2i}-2m_{1i}\varkappa_{2i}+m_{1i}=(-1)^{\varkappa_{1i}}m_{2i}+(-1)^{\varkappa_{2i}}m_{1i}$. □

8.5.1. *Remark.* Theorem 1.3.5 gives a simple description of the group operation induced from $\mathrm{MW}_\mathbb{R}$ on the set $\mathcal{H}_\ell\subset H_1(X_\mathbb{R})/Tors$ of classes realized by real lines. Namely, for $X_\mathbb{R}=\mathbb{K}\#p\mathbb{T}^2\amalg q\mathbb{S}^2$, this set is contained in $L_\mathbb{R}+\left[\oplus_{i=1}^p(\mathbb{Z}b_i+\{0,1\}o_i)\right]$, the group operation on the direct sum $\oplus_{i=1}^p(\mathbb{Z}b_i+\{0,1\}o_i)$ is component-wise, and on each of the summands it turns into multiplication of triangular matrices $\pm\begin{bmatrix}1&n\\0&1\end{bmatrix}\in\mathrm{SL}(2,\mathbb{Z})$ via an identification

$$mb_i\mapsto\begin{bmatrix}1&-m\\0&1\end{bmatrix},\quad mb_i+o_i\mapsto\begin{bmatrix}-1&m\\0&-1\end{bmatrix}.$$

9. Concluding remarks

9.1. **Modulo 2 real MW-action.** Fixing a line L on a relatively minimal complex rational elliptic surface X leads to a direct sum decomposition

$$H_2(X)=\langle F\rangle\oplus W_L\oplus\langle L\rangle\cong\mathbb{Z}\oplus E_8\oplus\mathbb{Z},$$

where F stands for a fiber and $W_L=F^\perp\cap L^\perp\cong E_8$. The following proposition is well known.

9.1.1. **Proposition.** *If X has only one-nodal singular fibers, then any line in X can be decomposed as $kF+w+L$, where $w\in W$, $k=\frac{w^2}{2}\in\mathbb{Z}$, and this gives a 1–1 correspondence between the set of lines and E_8.*

The automorphism in $H_2(X)$ induced by the MW*-transform sending L to $L_w = kF+w+L$ has a block-matrix presentation (in the above derect-sum-decomposition)*

$$\begin{bmatrix}1 & w^* & k\\ 0 & I_V & w\\ 0 & 0 & 1\end{bmatrix}, \qquad \begin{bmatrix}m\\ v\\ n\end{bmatrix} \mapsto \begin{bmatrix}m+v\cdot w+kn\\ v+nw\\ n\end{bmatrix} \quad \begin{matrix}m,n\in\mathbb{Z},\ v\in W_L=E_8,\\ v\cdot w \text{ states for product in } E_8.\end{matrix}$$

In terms of $D = L_w - L = kF + w$, this action can be wriiten as

$$x \mapsto x - (Fx)D + ((Dx) - \frac{1}{2}D^2(Fx))F.$$

In particular, any other line, $L_{w'} = k'F + w' + L$, is sent to the line

$$L_{w+w'} = (k + w\cdot w' + k')F + (w + w') + L. \qquad \square$$

In the real setting, we fix a real line L and associate with it a decomposition

$$H_1(X_{\mathbb{R}};\mathbb{Z}/2) = \langle F_{\mathbb{R}}\rangle \oplus W_L^{\mathbb{R}} \oplus \langle L_{\mathbb{R}}\rangle = \mathbb{Z}/2 \oplus W_L^{\mathbb{R}} \oplus \mathbb{Z}/2, \quad W_L^{\mathbb{R}} = F_{\mathbb{R}}^{\perp} \cap L_{\mathbb{R}}^{\perp}$$

where we do not distinguish in notation the real loci $F_{\mathbb{R}}, L_{\mathbb{R}}$ and the classes realized by them in $H_1(X_{\mathbb{R}};\mathbb{Z}/2)$. The rule for the action of $MW(X)$ in $H_2(X)$ stated in Proposition 9.1.1 translates into a rule for the action of $MW_{\mathbb{R}}(X)$ in $H_1(X_{\mathbb{R}};\mathbb{Z}/2)$.

9.1.2. **Proposition.** *The automorphism in $H_1(X_{\mathbb{R}};\mathbb{Z}/2)$ induced by a real* MW*-transform sending L to $L_w = kF + w + L, w \in W_L, k = \frac{w^2}{2} \in \mathbb{Z}$, has a block-matrix form*

$$\begin{bmatrix}1 & w^* & k\\ 0 & I_V & w\\ 0 & 0 & 1\end{bmatrix}, \qquad \begin{bmatrix}\mu\\ v\\ \nu\end{bmatrix} \mapsto \begin{bmatrix}\mu+v\cdot w+k\nu\\ v+\nu w\\ \nu\end{bmatrix} \quad \begin{matrix}\mu,\nu\in\mathbb{Z}/2, v\in W_L^{\mathbb{R}}\\ \mu+v\cdot w+k\nu\in\mathbb{Z}/2\\ v+\nu w\in W_L^{\mathbb{R}}.\end{matrix}$$

or in terms of the class $D = L_{w\mathbb{R}} - L_{\mathbb{R}} \in H_1(X_{\mathbb{R}};\mathbb{Z}/2)$ this action on $x \in H_1(X_{\mathbb{R}};\mathbb{Z}/2)$ is

$$x \mapsto x + (F_{\mathbb{R}}\cdot x)D + ((D\cdot x) + k(F_{\mathbb{R}}\cdot x))F_{\mathbb{R}} \mod 2.$$

Proof. Direct application of the Viro homomorphism to Proposition 9.1.1. $\square$

The restriction $\Lambda_X \to W_L^{\mathbb{R}}$ of the Viro homomorphism $\Upsilon : H_2^-(X) \to H_1(X_{\mathbb{R}};\mathbb{Z}/2)$ (see [FK-1, Section 2.2]) factorizes through $V_X = \Lambda_X/2\Lambda_X$ to an isomorphism $V_X/R_X \to W_L^{\mathbb{R}}$ where $R_X = \{v \in V_X \mid v\cdot V_X = 0\}$. The pullback identification of Λ_X with $\Lambda = \Lambda_Y$ induces a natural identification of V_X, R_X with V, R studied in Section 3.1. In particular, the function $\mathfrak{q}_0 : V \to \mathbb{Z}/2$ introduced there descends to $W_L^{\mathbb{R}}$ if and only if $\mathfrak{q}_0$ vanishes on R. The latter happens if and only if $X_{\mathbb{R}}$ is $\mathbb{K}\#4\mathbb{T}^2$, or $\mathbb{K}\#\mathbb{T}^2\amalg\mathbb{S}^2$, or $\mathbb{K}\amalg\mathbb{K}$. When such a descend exists we keep for it the same notation, $\mathfrak{q}_0 : W_L^{\mathbb{R}} \to \mathbb{Z}/2$.

9.1.3. **Proposition.** *In the above real setting, assume that $X_{\mathbb{R}} = \mathbb{K}\#p\mathbb{T}^2\amalg q\mathbb{S}^2$ with a fixed real line $L \subset X$. Then any other real line $L' \subset X$ has a decomposition $L'_{\mathbb{R}} = \varkappa F_{\mathbb{R}} + v + L_{\mathbb{R}} \in H_1(X_{\mathbb{R}};\mathbb{Z}/2)$, $\varkappa \in \mathbb{Z}/2$, $v \in W_L^{\mathbb{R}}$. Conversely:*

(1) *If (p,q) is different from $(4,0)$ and $(1,1)$, a class $\varkappa F_{\mathbb{R}} + v + L_{\mathbb{R}}$ is realizable by a real line for any $\varkappa \in \mathbb{Z}/2$, $v \in W_L^{\mathbb{R}}$.*
(2) *If (p,q) is $(4,0)$ or $(1,1)$, then class $\varkappa F_{\mathbb{R}} + v + L_{\mathbb{R}}$ is realizable by a real line if and only if $\varkappa = \mathfrak{q}_0(v)$.*

Proof. The decomposition of the $\mathbb{Z}/2$-homology classes of real lines follows from that of $\mathbb{Z}$-homology classes of complex lines in Proposition 9.1.1 due to the Viro homomorphism, which sends $F, L \in H_2(X)$ to $F_\mathbb{R}, L_\mathbb{R} \in H_1(X_\mathbb{R}; \mathbb{Z}/2)$, and $\Lambda \subset H_2(X)$ onto $W_L^\mathbb{R} \subset H_1(X_\mathbb{R}; \mathbb{Z}/2)$.

By Proposition 5.1.1(3) the set of $\mathbb{Z}$-homology classes of real lines is

$$\{L' = L + \frac{w^2}{2}F + w \mid w \in \Lambda\} \subset H_2(X).$$

As we apply the Viro homomorphism, this gives $L'_\mathbb{R} = \varkappa F_\mathbb{R} + v + L_\mathbb{R} \in H_1(X_\mathbb{R}; \mathbb{Z}/2)$ with $v = \Upsilon(w)$ and $\varkappa = \frac{w^2}{2} \bmod 2$. The Viro homomorphism establishes an isomorphism between V/R and $W_L^\mathbb{R}$ preserving the intersection indices $\bmod 2$, and therefore there remains to notice that in the case of non vanishing $\mathfrak{q}_0|_R$ (in which $\mathfrak{q}_0$ does not descend to $W_L^\mathbb{R}$) we can get any $\varkappa \in \mathbb{Z}/2$ independently of $v \in W_L^\mathbb{R}$ by choosing an appropriate $w \in \Upsilon^{-1}(v)$.

□

9.1.4. *Remark.* A similar result holds for real del Pezzo surfaces Y of degree 1: *If $Y_\mathbb{R}$ is $\mathbb{RP}^2\#4\mathbb{T}^2$ or $\mathbb{RP}^2\#\mathbb{T}^2 \amalg \mathbb{S}^2$, and $K_\mathbb{R}$ is the real canonical class (dual to $w_1(Y_\mathbb{R})$), then a class $h \in H_1(Y_\mathbb{R}; \mathbb{Z}/2)$ is realized by a real line if and only if*

$$h \in K_\mathbb{R} + \{v \in K_\mathbb{R}^\perp \mid \mathfrak{q}_0(v) = 1.\}$$

This is a straightforward application of Propositions 2.3.2 and 3.1.4 by means of the Viro homomorphism.

9.2. **The obstruction for realizability of homology classes by real lines.** In Theorem 1.3.4 to simplify the formulation we omitted a description of the range for the coefficients $\kappa \in \mathbb{Z}/2$, $m_i \in \mathbb{Z}$, $\varkappa_i \in \{0, 1\}$ realizable by real lines L' in the decomposition

$$L'_\mathbb{R} = \kappa F_\mathbb{R} + \sum_{i=1}^4 m_i b_i + \sum_{i=1}^4 \varkappa_i o_i.$$

It can be deduced from Proposition 9.1.3 (cf. also Theorem 7.3.2) that for $X_\mathbb{R} = \mathbb{K}\#4\mathbb{T}^2$ the coefficients $m_i \in \mathbb{Z}$, $\varkappa_i \in \{0, 1\}$ can take any values, while

$$\kappa = m_1 + m_3 + \sum_{i=1}^4 m_i \varkappa_i + \sum_{i=1}^4 \varkappa_i \bmod 2.$$

In the case of $X_\mathbb{R} = \mathbb{K}\#\mathbb{T}^2 \amalg \mathbb{S}^2$ we have a relation

$$\kappa = m + m\varkappa + \varkappa = \begin{cases} m \bmod 2 & \text{if } \varkappa = 0 \\ 1 \bmod 2 & \text{if } \varkappa = 1 \end{cases}$$

whenever the homology class $\kappa F_\mathbb{R} + mb + \varkappa o \in H_1(X_\mathbb{R})$ is realizable by a real line.

9.3. **Application: Conics tangent to a pair of lines and a cubic.** Consider a pair $L_1, L_2 \subset \mathbb{P}^2$ of distinct real lines and a nonsingular real cubic $A \subset \mathbb{P}^2$ transversal to $L_1 \cup L_2$. Let us enumerate the set $\mathcal{B}$ of real nonsingular conics $B \subset \mathbb{P}^2$ tangent to both L_1, L_2 and tritangent to A. Consider for that the double covering $\pi : Q \to \mathbb{P}^2$ and observe that the real structure of $\mathbb{P}^2$ lifts to two real structures on Q that differ by composing with a deck transformation $s : Q \to Q$ of π. Furthermore, for each $B \in \mathcal{B}$, its preimage $\pi^{-1}(B)$ splits into a pair of distinct conic sections, l and $s(l)$, which are tritangent to C and real with respect to one, and only one, of the real structures. In the opposite direction we deal with an alternative. If for a tritangent $l \subset Q$, which is real with respect to one of the real structures, we have $l \neq s(l)$, then the pair $l, s(l)$ projects to a conic $B \in \mathcal{B}$. Otherwise, if $l = s(l)$ is real with respect to one real structure, then l is real with respect to the other real structure too and projects to a real line passing through one of the 6 intersection points of A with $L_1 \cup L_2$ and tangent to A at some other point. This leads to a formula $|\mathcal{B}| = \frac{1}{2}(|\mathcal{T}_1| + |\mathcal{T}_2|) - |\mathcal{R}|$ where $\mathcal{T}_1$ and $\mathcal{T}_2$ denote the sets of tritangents to C which are real with respect to the corresponding real structures on Q, while $\mathcal{R}$ is the set of real lines in $\mathbb{P}^2$ passing through one of the 6 intersection points of A with $L_1 \cup L_2$ and tangent to A at some other point. For

Fig. 22

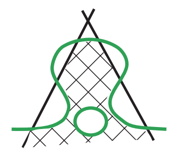

example, in the case of configuration L_1, L_2, A shown at Fig. 22 for one of the 2 covering real structures on Q the sextic is of type $\langle 4|0\rangle$, and of type $\langle 1|1\rangle$ for the other real structure, so that we obtain $|\mathcal{B}| = \frac{1}{2}(120 + 24) - 24 = 48$, with all conics from the set $\mathcal{B}$ lying in the shaded domain (because all $|\mathcal{T}_2| = 24$ tritangents to the sextic of type $\langle 1|1\rangle$ must be represented by the $|\mathcal{R}| = 24$ lines).

9.4. **Five types of real theta characteristics on real sextics lying on a quadric cone.** As is known, a nonsingular complete intersection of a quadric surface with a cubic surface in $\mathbb{P}^3$ is a canonically embedded curve of genus 4. Furthermore, every non-hyperelliptic genus 4 curve C arises as such a complete intersection sextic. The corresponding quadric, $Q \supset C$ is defined uniquely by sextic C and it is a quadratic cone if and only if C has a degenerate even theta-characteristic, θ_0. The latter is of dimension 2 and, thus, defines a map $\pi : C \to \mathbb{P}^1$ which can be identified with the central projection of $Q \to \mathbb{P}^1$ from the vertex $v \in Q$, where $\mathbb{P}^1$ is identified with the generating conic of Q.

Over the reals, θ_0 and π are real too. They allow us to distinguish the J-component of $C_{\mathbb{R}}$ from its ovals. Namely, the restriction $\pi|_{C_{\mathbb{R}}} : C_{\mathbb{R}} \to \mathbb{P}^1_{\mathbb{R}}$ is of degree 1 on the J-component and of degree 0 on the ovals.

On the other hand, the real tritangents to C are in 1-to-1 correspondence with the real odd theta-characteristics. Together with above property of π, we may distinguish 4 types of real odd theta-characteristics, equivalently 4 types of real tritangents, by counting the number τ of ovals on which a given characteristic has odd number of zeros, $0 \leqslant \tau \leqslant 3$. For $\tau \neq 0$, the corresponding tritangents are of type T_τ, while for $\tau = 0$ we have types T_0 and T_0^*.

It would be interesting to find how to distinguish in a language of theta-characteristics positive tritangents from negative, and elliptic ones from hyperbolic.

9.5. **Non rational elliptic surfaces.** In the case of non rational elliptic surfaces the Mordell-Weil group is no more stable under deformations in the class of elliptic surfaces even over $\mathbb{C}$. So, none of the questions treated in this paper makes sense beyond the rational case. However, it looks interesting to find how the *maximal* *rank* of the real Mordell-Weil group depends on the geometric genus of the elliptic surface. For instance, in the case of genus 1 (elliptic K3 surfaces) the maximal rank of the Mordell-Weill group is 18, both over $\mathbb{C}$ and over $\mathbb{R}$ (see [C] for $\mathbb{C}$; a similar application of strong Torelli can be adapted to $\mathbb{R}$). It seems to be unknown whether such a coincidence holds for genus > 1.

9.6. **10 real vanishing classes on del Pezzo surfaces.** The set of complex vanishing cycles on a del Pezzo surface Y is formed by the (-2)-roots in $K^\perp \subset H_2(Y)$. By analogy, one could think that for a real Y any -2-root in $\Lambda = K^\perp \cap \ker(1+\mathrm{conj}_*)$ gives a real vanishing class, but it is far from the truth. For example, if Y is a real del Pezzo surface of degree $K^2 = 1$ with $Y_\mathbb{R} = \mathbb{RP}^2 \# 4\mathbb{T}^2$, then $\Lambda = E_8$ has 120 pairs, $\pm e$, of roots, but among them only 10 pairs are real vanishing classes: the 4 pairs of oval-classes and 6 pairs of bridge-classes depicted on the rightmost diagram in the first row of Fig. 4.

Mysteriously, the same number 10 appears for real del Pezzo surfaces Y of other degrees $2 \leqslant d = K^2 \leqslant 5$, as we count pairs of real vanishing classes in the maximal case $Y_\mathbb{R} = \mathbb{RP}^2 \#(9-d)\mathbb{RP}^2$. On Fig. 23 we show the intersection graph of these real vanishing classes for $d = 1, \dots, 4$. Each vertex stands for a pair, $\pm e \in \Lambda$, of real vanishing classes, while edges indicate the intersection indexes ± 1. For $d = 1, 2$ the graphs are bipartite wherein the oval-classes and the bridge-classes are represented by circle- and cross-vertices, respectively.

Fig. 23

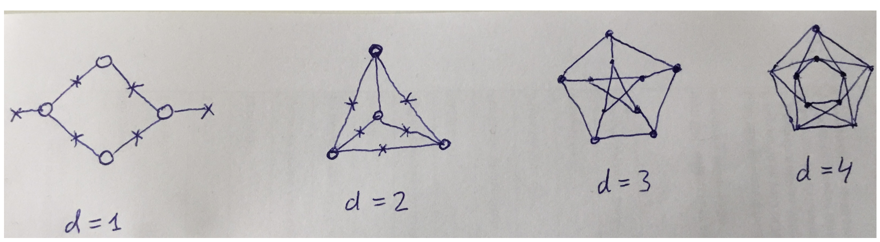

References

[At] M. Atiyah, *On analytic surfaces with double points.* Proc. Roy. Soc. London. Ser. A **247 (1958)**, 237 – 244.

[C] D. Cox, *Mordell-Weil Groups of Elliptic Curves over $\mathbb{C}(t)$ with $p_g = 0$ or* 1. Duke Math. Journal, vol. 49, No. 3 (1982), 677 – 689.

[DIK] A. Degtyarev, I. Itenberg, V. Kharlamov, *Real Enriques Surfaces.* Springer, Lecture Notes in Mathematics 1746, **2000**.

[DK] A.I. Degtyarev, V.M. Kharlamov, *Topological properties of real algebraic varieties: Rokhlin's way.* Russian Math. Surveys, **55:4 (2000)**, 735–814.

[FM] B. Farb, D. Margalit, *A Primer on Mapping Class Groups.* Princeton University Press, 2012.

[FK-1] S. Finashin, V. Kharlamov, *Two kinds of real lines on real del Pezzo surfaces of degree 1.* Selecta Math. (N.S.) **27 (2021)**, no. 5, Paper No. 83, 23 pp.

[FK-2] S. Finashin, V. Kharlamov, *Combined count of real rational curves of canonical degree 2 on real del Pezzo surfaces with $K^2 = 1$.* Journal of the Institute of Mathematics of Jussieu, 2022, First View , pp. 1 - 26.

[FK-3] S. Finashin, V. Kharlamov, *On wall-crossing invariance of certain sums of Welschinger numbers.* Sel. Math. New Ser. 29, 41 (2023), 31 pp.

[K] K. Kodaira, *On Stability of Compact Submanifolds of Complex Manifolds.* American Journal of Mathematics , Jan., 1963, Vol. 85, No. 1 (Jan., 1963), pp. 79 – 94.

[IKS] I. Itenberg, E. Shustin,V. Kharlamov, *Welschinger invariants of real del Pezzo surfaces of degree* $\geqslant 2$. International J. Math. **26** (2015), no. 6., 1550060, 63 pp.

[R] V.A. Rokhlin, Complex orientation of real algebraic curves.(Russian) Funkcional. Anal. i Prilozen. 8(1974), no.4, 71–75. English translation: Functional Analysis and Its Applications, 1974, Volume 8, Issue 4, Pages 331–334.

[SS] M. Schütt, T. Shioda *Mordell–Weil Lattices* Ergebnisse der Mathematik und ihrer Grenzgebiete. 3. Folge, 70, xvi+431 pp., Springer (2019).

[S] M. Stukow *Commensurability of geometric subgroups of mapping class groups* Geom. Dedicata (2009), 143: 117-142

[Z] V. I. Zvonilov, *Complex orientations of real algebraic curves with singularities.(Russian)* Dokl. Akad. Nauk SSSR, 268(1983), no.1, 22–26. English translation: Soviet Math. Dokl. 27 (1983), no. 1–6, 14–17.

Middle East Technical University, Department of Mathematics
Ankara 06531 Turkey

Université de Strasbourg et IRMA (CNRS)
7 rue René-Descartes 67084 Strasbourg Cedex, France